Syrian Arab Republic
Ministry of Higher Education and Scientific Research
Syrian Virtual University – SVU
Master In Bioinformatics – BIS

In silico identification of hub-genes in attributing the development, prognosis, and diagnosis of Pancreatic Ductal Adenocarcinoma using Weighted gene correlation network analysis of lncRNA and interactome analysis of their products.

Research submitted in partial fulfillment of the requirements for the degree of Master in Bioinformatics

Authored by

Abdul Rahman Albaba

Supervision of

Ph. D. Lama Youssef

August 2024

Abstract

Pancreatic Ductal Adenocarcinoma (PDAC) stands out as one of the most lethal forms of cancer, exhibiting a mere 11% 5-year survival rate when considering all stages collectively. The challenging prognosis is largely a result of delayed diagnosis owing to the highly aggressive nature of the tumor and the absence of early specific symptoms. Treatment of PDAC is further hindered by resistance to targeted therapies, immunotherapy, chemotherapy, and radiation, necessitating novel strategies to overcome this resistance. The present study endeavors to address these challenges by conducting an integrated bioinformatics analysis to elucidate the molecular mechanisms, identify diagnostic markers, and pinpoint therapeutic targets for PDAC. A considerable portion of the human genome is transcribed into long noncoding RNAs (lncRNAs) with the number of identified lncRNAs steadily increasing, although only a few have been functionally characterized. Notably, the functions of lncRNAs are closely linked to their subcellular localization, with cytoplasmic lncRNAs influencing mRNA stability, translation, and serving as miRNA sponges, while nuclear-retained lncRNAs have been implicated in transcriptional regulation, chromosome scaffolding, alternative splicing modulation, and chromatin remodeling. These diverse roles of lncRNAs play vital regulatory functions in both normal cellular processes and disease states. The analysis leveraged a normalized RNA-seq dataset from the GEO database, specifically the dataset with the accession number GSE133684 encompassing complete PDAC patient samples and full healthy controls. From this analysis, 451 differentially expressed genes (DEGs) were pinpointed. Subsequent Gene Ontology (GO) and Kyoto Encyclopedia of Genes and Genomes (KEGG) pathway analyses were executed to shed light on the biological processes and crucial pathways associated with PDAC. Following this, a protein-protein interaction (PPI) network was established, leading to the identification of 11 hub genes and five key modules. Notably, all identified hub genes, including SUZ12, EZH2, YWHAZ, CTNNA1, SMARCA5, H2AC6, H2BC11, H2BC12, H2BC21, H3-3B, and H3C12, exhibited overexpression in PDAC patients. The validation of these hub genes was carried out in-silico using expression profiles and reference datasets and published studies. Functional enrichment analysis

underscored the pivotal roles of these key genes in various biological processes, encompassing cytokine signaling in the immune system, cell cycle regulation, and apoptosis-related mechanisms such as DNA damage response and oxidative activities. Moreover, the study predicted and validated 6 lncRNA transcripts responsible for regulating 25 miRNAs and 7 key transcription factors known to govern a significant portion of the hub genes linked to PDAC. These lncRNAs are (ENST00000641741, ENST00000637240, ENST00000434887, ENST00000500800, ENST00000509873, ENST00000564694). This comprehensive bioinformatics analysis not only provides valuable insights into the pathogenesis of PDAC but also identifies potential biomarkers for clinical management and unveils novel drug targets. These findings advance our comprehension of PDAC and present promising prospects for further progress in diagnostics and therapeutic interventions.

Key words: Pancreatic Ductal Adenocarcinoma, lncRNA, DEG.

Table of Contents

List of Tables

List of Figures

List of Abbreviations

Abbreviation	Full Text
BP	Biological Processes
CC	Cellular Components
ceRNAs	competitive endogenous RNAs
CLC	Cancer LncRNA Census
DAVID	The Database for Annotation, Visualization and Integrated Discovery
DEGs	Differentially Expressed Genes
EMT	Epithelial-To-Mesenchymal Transition
FC	Fold Change
FDR	False Discovery Rate
FPKM	Fragments Per Kilobase of transcript per Million mapped reads
GEO	Gene Expression Omnibus Database
GO	Gene Ontology
GRN	Gene Regulatory Network
HPA	Human Protein Atlas
KEGG	Kyoto Encyclopedia of Genes and Genomes Pathways
lncRNA	Long non coding RNA
MCODE	Molecular Complex Detection
MF	Molecular Function
miRNAs	microRNAs
Nt	Nucleotides
PC	Pancreatic Cancer
PcG	Polycomb group
PDAC	Pancreatic Ductal Adenocarcinoma
PPI	Protein-Protein Interaction
RCI	Relative Concentration Index
STRING	Search Tool for Retrieval of Interacting Genes/Proteins
TCGA	The Cancer Genome Atlas
TFs	Transcription Factors
WGCNA	Weighted Gene Co-Expression Network Analysis

Introduction:

Pancreatic cancer (PC) is recognized as one of the most lethal malignancies in the medical realm, characterized by a notably grim prognosis that persists at alarmingly low levels, exemplified by a five-year net survival rate of less than 6% within the United States as highlighted in the study by (Kamisawa et al., 2016). Despite the notable strides made in the field of molecular diagnostics and therapeutic interventions within the realm of clinical medicine, there exists a prevailing sentiment that the advancements made in comprehending the mechanisms underlying PC carcinogenesis have not reached a level of sufficiency that aligns with the pressing need for deeper insights. The absence of reliable methods for detecting PC in its early stages and the lack of well-defined strategies tailored towards this end further exacerbate the grim outlook associated with this disease, resulting in a dire prognosis for affected individuals. Consequently, the urgent call for the identification and validation of specific prognostic biomarkers within the context of PC remains a critical imperative, carrying substantial weight in the realms of both early detection and the subsequent implementation of effective therapeutic interventions.

Long non-coding RNAs (lncRNAs) are RNA transcripts characterized by their length of more than 200 nucleotides (nt) and a lack of protein-coding capacity, as established by (Silva et al. 2015). The literature has documented multiple instances wherein lncRNAs play crucial roles in modulating various biological processes such as genomic imprinting, transcriptional regulation, cellular responses like death, growth, and differentiation, as well as in controlling vital functions like apoptosis, chromatin modification, and inflammatory responses, all of which are implicated in the intricate mechanisms underlying cancer development, as highlighted by (Bolha et al. 2017). Numerous research reports have underscored the differential expression patterns of lncRNAs across diverse tumor types, as evidenced by the studies conducted by (Yu et al. 2021), (J. Li et al. 2019), (Y. J. Lee et al. 2019), and (Kumar et al. 2019). Owing to their detectability and specificity in tissues and bodily fluids, lncRNAs have garnered attention as valuable biomarkers for diagnosing diseases, predicting prognoses, and potentially serving as targets for therapeutic interventions in various pathological conditions, as elucidated by (Thomas

et al. 2019), (Tamang et al. 2019), (C et al. 2019), and (Yin et al. 2019). Notably, lncRNAs have been extensively explored as diagnostic and prognostic indicators in a spectrum of cancers including prostate, breast, gastric, pancreatic, ovarian, bladder cancers, among others, thus underscoring their significance in oncology research and clinical practice, according to (Bolha et al. 2017). The collective evidence from these investigations underscores the utility of lncRNAs as non-invasive biomarkers with potential clinical applications in prostate cancer.

In the context of prostate cancer, the identification of a specific molecular biomarker assumes paramount importance in determining patient prognosis and facilitating timely intervention strategies. This current investigation endeavors to scrutinize the differential expression profiles of long non-coding RNAs (lncRNAs) between PC tissues and adjacent normal pancreas samples, with the objective of pinpointing potential lncRNA biomarkers utilizing data from The Cancer Genome Atlas (TCGA) database, which could potentially aid in prognostication for PC patients. Furthermore, the functional analyses of lncRNAs may yield critical insights into their impact on the biological pathways implicated in PC pathogenesis, thereby paving the way for a deeper understanding of the processes driving the initiation and progression of PC.

Identifying minimally invasive, reliable, and effective techniques for the early detection of pancreatic ductal adenocarcinoma represents a crucial clinical requirement that remains unaddressed within the medical field. This pressing necessity underscores the significance of exploring innovative approaches that can facilitate the timely identification of this aggressive form of cancer. Furthermore, within the context of this discourse, the focus is directed towards the intricate process of developing and subsequently validating a multi-biomarker signature specifically tailored for the purpose of detecting pancreatic ductal adenocarcinoma in its nascent stages. The complexity and intricacy of this endeavor are emphasized, as it involves a comprehensive examination of various immunoregulatory and cancer-associated biomarkers that collectively contribute to the diagnostic accuracy and reliability of the proposed signature. This targeted approach is intended to cater to individuals deemed to be at elevated risk for the development of pancreatic ductal adenocarcinoma, thereby highlighting the importance of precision and specificity in the identification of potential biomarkers.

The identification of long noncoding RNAs (lncRNAs) and the subsequent period—distinguished by investigations into their expression and functions (Ling et al., 2017)—has solidified the notion that they are considered as "valuable non-coding transcripts." lncRNAs exhibit numerous characteristics akin to messenger RNAs, including their transcription by RNA polymerase II, 5' capping, 3' polyadenylation, and splicing (Iyer et al., 2015). Furthermore, despite their classification as transcripts longer than 200 base pairs lacking a discernible open reading frame (ORF), the discovery of non-random ORFs, their potential to engage with ribosomes (Van Heesch et al., 2014), and their ability to produce micro-peptides (Wu et al., 2020) linked to tumorigenesis challenge their conventional definition. Extensive studies have identified over 50,000 lncRNAs, categorized based on their genomic location (intergenic and intronic), subcellular distribution (nuclear or cytoplasmic), transcriptional orientation (sense or antisense), target gene localization (cis or trans), and regulatory roles (transcriptional or posttranscriptional) (Fabbri et al., 2019). In particular, the subcellular localization of lncRNAs plays a crucial role in determining their functions. Nuclear lncRNAs, for instance, can impact epigenetic and transcriptional processes by recruiting regulatory molecules or indirectly influencing histone modifications, DNA methylation, m^6A methylation patterns, and the transcriptional machinery (Bridges et al., 2021). Conversely, cytoplasmic lncRNAs are commonly recognized as regulators of translation that can influence RNA stability and localization, as well as the activity of microRNAs by acting as competitive endogenous RNAs (ceRNAs). Therefore, alterations in their nuclear-to-cytoplasmic localization can significantly influence their physiological functions (Aprile et al., 2020).

Nevertheless, despite the expanding scope of our understanding regarding lncRNAs, the diverse nature of these molecules and the intricate mechanisms through which they operate continue to pose significant challenges to their utilization as biomarkers or therapeutic targets in clinical settings. This is particularly evident in their involvement in the regulation of fundamental cellular processes such as cell proliferation, apoptosis, angiogenesis, migration, and stemness, rendering them a focal point in cancer research. The distinct expression patterns of lncRNAs across various cancer types, along with their capacity to modulate crucial

oncogenes and tumor suppressors, have underscored their importance in genomic investigations related to cancer. Data stemming from resources like the Cancer Genome Atlas (TCGA), Cancer LncRNA Census (CLC) (Carlevaro-Fita et al., 2022), and The Atlas of non-coding RNA in Cancer (TANRIC) (J. Li et al., 2015) have significantly heightened the interest in lncRNAs for cancer diagnosis and prognosis. Alterations in the sequence or expression of lncRNAs have been identified as specific to certain types of cancer, further emphasizing their potential diagnostic value. Given their ability to influence a multitude of cancer-related processes, regulate pivotal cancer-associated genes, and exhibit either oncogenic, tumor-suppressive, or dual functions, the prospect of targeting lncRNAs for therapeutic purposes has been suggested (Y. Gao et al., 2019). Moreover, correlations between lncRNAs and clinical outcomes in cancer patients, as well as drug responsiveness, have prompted investigations into their viability as biomarkers for diagnosis and prognosis. This review focuses on oncogenic lncRNAs of clinical significance, elucidating their mechanisms of action and their potential utility as prognostic/diagnostic biomarkers or therapeutic targets.

Our comprehension of cancer has been significantly shaped by the discovery of long non-coding RNAs (lncRNAs). Utilizing data from The Cancer Genome Atlas (TCGA) and Cancer Cell Line Encyclopedia (CLC), research has paved the path for a thorough investigation of the genomic, epigenetic, and transcriptional characteristics unique to lncRNAs across various cancer types (Huarte, 2015). Nevertheless, only a small subset of these lncRNAs have been proven to play a causative role in cancer. In this context, we provide an accurate account—constrained by space—of the most impactful and well-defined lncRNAs exhibiting oncogenic properties (such as MALAT1, HOTAIR, PCA3, CCAT1, CCAT2, H19, HOTTIP, and UCA1; see Figure 1) that may hold significance for therapeutic interventions and/or the diagnosis and prognosis of cancer.

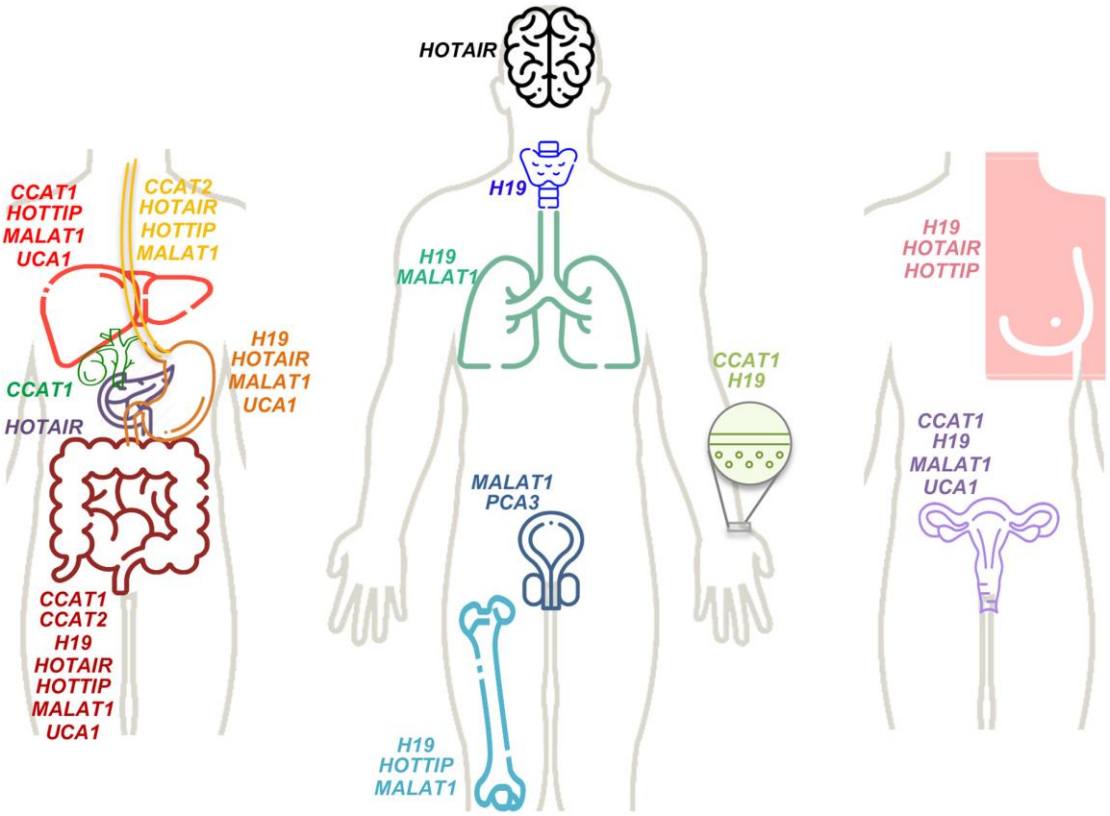

Figure 1: LncRNAs with diagnostic/prognostic relevance in different human solid tumors. Names of lncRNAs are depicted with colors corresponding to tissue/organ in which they have relevance as diagnostic and/or prognostic biomarkers. Tissues and organs pictures are only representative, anatomical localization/details should be not fully accurate. (Aprile et al., 2022)

The most significant of the several cancer-related biomarkers, which include DNA, RNA, and protein, are RNA-based biomarkers, which comprise coding and non-coding RNA expression levels (Zhang et al., 2019) and (Xi et al., 2017). Numerous investigations assess the possible function of single-strand ribonucleic acid molecules, or PDAC biomarkers, as protein-coding RNA.

Non-coding RNAs, including long non-coding RNAs (lncRNAs), microRNAs (miRNAs), piwi-interacting RNAs (piRNAs), and circular RNAs (circRNAs), have been shown in recent research to be potential prognostic cancer (Kishore & Karunagaran, 2022) and diagnostic biomarkers, Figure 2. One of the most significant indicators linked to cancer is miRNAs, which are short noncoding RNAs (18–24 nt) (W. Zhang et al., 2021), (Mahmoudi et al., 2021). Over the past ten years, miRNA has been identified as a potential biomarker for the start, progression, and prognosis of PDAC (Xing et al., 2020). MiRNAs play a major regulatory role in proliferation,

survival, metastasis, and angiogenesis and can function as oncogenes or suppressors under different circumstances (Peng et al., 2016). System biology techniques enable researchers to discover new and promising biomarkers for cancer diagnosis, prognosis, and therapy response by methodically mining high-throughput data, such as microarray data (Smith et al., 2021). As a novel approach to system biology, the weighted gene co-expression network analysis (WGCNA) method provides a systems-level perspective and can be used to identify clusters of highly related genes. Moreover, therapeutic targets and significant and useful biomarkers may be found using this approach (Liao et al., 2020), (Zhong et al., 2022).

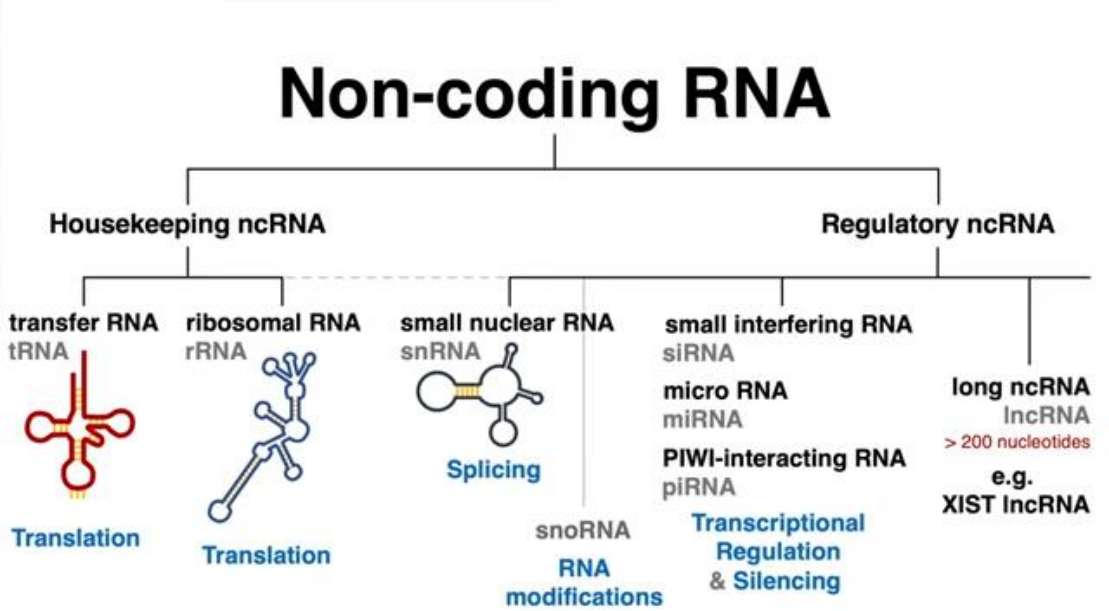

Figure 2: Classification of RNA molecules

Depending on location, sequence, morphology, structure, and function features, lncRNA can be categorized into different groups.

1- Due to lncRNA allostery effect for interacting with different ligand proteins. As per Figure 3

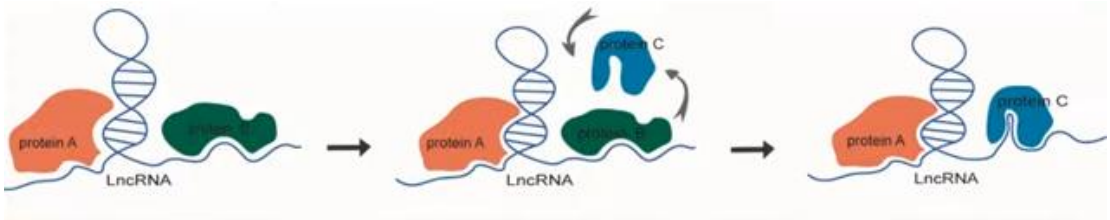

Figure 3: Allosteric effect of lncRNA

2- LncRNA acting as molecular scaffold to recruit and combine with multiple regulatory proteins, as per Figure 4

Figure 4: Mechanism of lncRNA molecular scaffold

3- LncRNA mediating histone modification by the functional region repeat elements, as per Figure 5

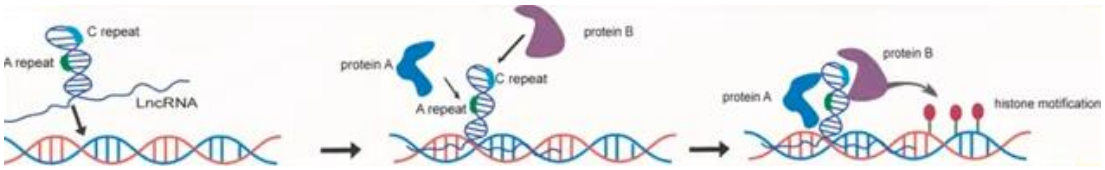

Figure 5: LncRNA mediating histone modification

Because Circulating RNAs (cRNAs) cannot encode proteins, it was previously thought that they would not have a significant effect on the beginning and progression of tumors. On the other hand, new data has brought attention to ncRNAs' crucial regulatory roles. ncRNAs actively take part in a variety of tumorigenic processes, including as epithelial-to-mesenchymal transition EMT, autophagy, and apoptosis, in addition to their ability to alter the expression of genes and proteins (Takahashi et al., 2021), (Donati et al., 2022) and (M. Zhang et al., 2022). NcRNAs fall into two primary categories according to their lengths: long noncoding RNAs (lncRNAs) and small noncoding RNAs (sncRNAs), which have lengths greater than or equal to 200 nucleotides (Huynh et al., 2016), (Aurilia et al., 2021).

The most common trend of WCGNA was to use the sncRNAs. Whereas, in recent years, the important regulatory roles that RNA molecules with a circular structure, or circRNAs, have been acknowledged in the development of diseases as well as in the regulation of gene expression, cell proliferation, and proliferation. Micro-RNAs (miRNAs), small nucleolar RNAs, small nuclear RNAs, piwi-interacting RNAs, and tRNA-derived small RNAs are among the several subtypes of sncRNAs (Smolkova et al., 2022).

Of them, miRNAs are the ones that have been investigated in cancer research the most. Genes are influenced by miRNAs; thousands of miRNAs regulate about 60% of all genes. Their main job is to attach to recognition sites in the 3' untranslated region, which decreases the stability of mRNA and suppresses the expression of genes (Zandieh et al., 2023).

LncRNAs regulate the expression levels and functions of miRNA and proteins, and they also help to remodel the chromatin (Zandieh et al., 2023). Since they mediate several processes involved in the growth of tumor cells, some lncRNAs are thought to be effective biomarkers for PDAC and can be used in liquid biopsy (Takahashi et al., 2021).

In pancreatic cancer (PC), Kirsten rat sarcoma virus oncogene homolog (KRAS) mutations are the most common genetic modification. They are thought to be an early driving element in PDAC and are found in more than 90% of patients (Heredia-Soto et al., 2021). KRAS mutations in plasma DNA were shown by Castells et al. (Castells et al., 1999) to be a highly specific molecular diagnostic for PDAC diagnosis and prognosis.

KRAS mutations are unquestionably one of the most important markers for assessing PDAC, and several PC studies have focused primarily on their significance (Table 1). Overall, additional approaches are still needed to fully evaluate the use of ctDNA and mutation analysis in PDAC.

Table 1 Genes previously identified by recent studies

	Testing method	Markers	# of patients	Stages	Year of report	Ref
Diagnosis	ddPCR	KRAS	105	All stages PDAC	2022	(R. Wang et al., 2022a)
	Methylation-specific PCR	ADAMTS1, BNC1	39	All stages PDAC	2019	(Eissa et al., 2019c)
	Methylation-specific PCR	BMP3, RASSF1A, BNC1, MESTv2, TEPI2, APC, SFRP1	95	All stages PDAC	2016	(Henriksen et al., 2016)

	Testing method	Markers	# of patients	Stages	Year of report	Ref
		and SFRP2				
Prognosis	ddPCR	KRAS	108	All stages PDAC	2023	(Nitschke et al., 2023)
	NGS	TP53, KRAS	145	All stages PDAC	2022	(Watanabe et al., 2022)
	BEAMing	KRAS	61	Metastatic PDAC	2020	(Toledano-Fonseca et al., 2020)
	ddPCR	KRAS	104	metastatic PDAC	2019	(Bernard et al., 2019)
Treatment	ddPCR	KRAS	70	Metastatic PDAC	2022	(Kirchweger et al., 2022)
	dPCR	KRAS	47	Metastatic PDAC	2019	(Sugimori et al., 2019)
	PCR based SafeSeqS assays	KRAS	112	Resectable PDAC	2019	(Lee et al., 2019)
	ddPCR	KRAS	78	Localized, metastatic, and recurrent PDAC	2019	(F. Watanabe et al., 2019)

In recent studies several genes have been identified in PDAC that contributed to cancer proliferation, development, diagnosis, prognosis and treatment. According to (Hussain et al., 2023) lncRNA offers hope as a possible diagnostic biomarker which also supports the finding of (Feng. Y et al, 2020)

According to (Huang et al., 2017) suggested that lncRNA can be a crucial modulator of the onset and development of pancreatic cancer through AsPC-1, BxPC-3, PANC-1, SW1990. On the other hand, machine learning algorithm were used by (L. Huang et al., 2023) to construct an ML model to identify genes related to PDAC and TP53 (17p13.1), TUBGCP6

(22q13.33), DNAH9 (17p12), SHANK1 (19q13.33), NUP214 (9q34.13), ZNF678 (1q42.13), UNC13C (15q21.3), NALCN (13q32.3-q33.1), MALT1 (18q21.32), and DYNC2H1 (11q22.3)) were significantly different between states of relapse and first-timer patients. Another ML work (J. Huang et al., 2023) found that ANO1, AHNAK2, and ADAM9 are of great significance as biomarkers in pancreatic cancer. Using molecular biology methods (Hu et al., 2023) were able to identify Urothelial carcinoma antigen 1(UCA1) as oncogene for pancreatic cancer through partially regulating miR-582-5p/BRCC3. Whereas, (Chirravuri-Venkata et al., 2023) found that MUC16 control in association with TP53 family tumor-stromal heterogeneity in pancreatic ductal adenocarcinoma.

The regulation of miRNAs' expression levels by lncRNAs in human cancers is an intriguing phenomenon. PVT1 has been identified to exhibit oncogenic properties in pancreatic cancer by enhancing HIF1A expression through the sequestration of MIR143, consequently promoting gemcitabine resistance in pancreatic cancer cells (Y. Liu et al., 2021). Similarly, LINC01207, another long non-coding RNA, has been found to promote tumorigenesis in pancreatic cancer by downregulating MIR143–5p expression, leading to the upregulation of AGR2 (anterior gradient 2, protein disulfide isomerase family member). This upregulation of AGR2 inhibits apoptosis and autophagy, thereby facilitating carcinogenesis (C. Liu et al., 2019).

In this research, a comprehensive bioinformatics strategy was utilized to examine lncRNA RNA-Seq data from individuals with PDAC obtained from the GEO database. The main aims included the identification of key genes, clarification of molecular pathways, discovery of possible diagnostic markers, and revelation of therapeutic targets for PDAC. The analysis effectively pinpointed DEGs, specifically emphasizing 11 central genes. To gain a deeper understanding, enrichment analyses of GO and KEGG pathways were carried out. Additionally, the research anticipated and validated the regulatory network involving miRNAs and important TFs linked to PDAC and their impact on the central genes. In summary, this bioinformatics investigation offers valuable insights into the development of PDAC, potential markers for clinical intervention.

Method and Materials:

1. Data source and descriptions:

Collection of gene expression profiles as raw data (case/control) Publicly accessible gene expression profiles dataset with accession number GSE133684 (Yu et al., 2019c) was downloaded from the National Center of Biotechnology Information (NCBI) Gene Expression Omnibus (GEO) database (https://www.ncbi.nlm.nih.gov/geo/). The total number of samples in this data set is 501 sample. Human blood samples from pancreatic ductal adenocarcinoma (PDAC), chronic pancreatitis (CP) and healthy individuals were drawn, and samples were treated for blood extracellular vesicle long RNA profiles of human plasma by deep sequencing using Illumina Hiseq using bulk RNA-Seq strategy.

The dataset was used to Expression profiling by high throughput sequencing Non-coding RNA profiling by high throughput sequencing. (Yu et al., 2019b).

2. Identification of Differentially Expressed Genes (DEGs):

DEGs were determined using GEO2R (https://www.ncbi.nlm.nih.gov/geo/geo2r/) an online analytical tool available at GEO that uses the GEO query and limma R packages from the Bioconductor project. The GEO query R package is utilized to extract GEO data and convert it into R data structures, allowing for further analysis using other R packages. Among these packages, limma (Linear Models for Microarray Analysis) has gained popularity as a powerful statistical tool for identifying genes that are differentially expressed. (Barrett et al., 2013) The analysis was made based on the following parameters; multiple testing correction is the Benjamini and Hochberg False Discovery Rate (FDR), Significance level cut-off $P < 0.05$, and $|\text{Log2 Fold Change (FC)}| > 0.2$. Various plots such as PCA plot, Heatmap, and Volcano plot were generated to depict the gene expression results.

3. Functional Annotation of DEGs by GO and KEGG Pathway Enrichment Analysis:

Functional annotation of genes that exhibit differential expression is an essential and crucial step in analyzing microarray data. The **D**atabase for **A**nnotation, **V**isualization and **I**ntegrated **D**iscovery **DAVID** (https://david.ncifcrf.gov/home.jsp) was used to functionally categorize the significant DEGs, as the functionality provided by DAVID accelerates the analysis of genome-scale datasets by facilitating the transition from data collection to biological meaning. Gene Ontology (GO) covers three main aspects of biology: Biological Process (BP), Cellular Component (CC), and Molecular Function (MF), while Kyoto Encyclopedia of Genes and Genomes (KEGG) is used to understand the relevant signaling pathways.

In order to obtain GO and KEGG enrichment analysis of the significant DEGs, DAVID was used with P-value>0.05.

4. PPI Network Construction & Analysis

STRING **S**earch **T**ool for **R**etrieval of **I**nteracting **G**enes/Proteins (https://string-db.org/) is a comprehensive database that provides predicted functional associations between proteins used to explore protein interactions, pathways, and functional relationships (von Mering et al., 2003). PPI network was first plotted using the online Search Tool for the Acquisition of Interacting Genes (STRING) (https:// string- db. org/). It was further displayed and interpreted through Cytoscape software (version 3.10.2).

The PPI network of the identified DEGs was built by considering only interactions with a minimum required interaction score of 0.9, indicating the highest level of confidence in the interactions included in the network.

5. PPI Network Module Analysis & Hub Genes Selection

The analysis results of the PPI network were loaded into **Cytoscape** software (version 3.10.2) for visual adjustment. Cytoscape, an open-source software project, facilitates the integration of biomolecular interaction networks with high-throughput expression data and other molecular states, providing a unified conceptual framework.

The Cytoscape plugin **CytoHubba Version 0.1** (**https://apps.cytoscape.org/apps/cytohubba - CytoHubba: identifying hub objects and sub-networks from complex interactome**) was used to calculate the connectivity scores and identify the intersections among the first 30 genes. Since a single algorithm sometimes produces false positives, a four-fold algorithm was adopted, combining two local-based algorithms (MCC and Degree) and two global-based algorithms (Stress and Radiality).

To identify the central hub genes, a Venn diagram was generated using Venny 2.1, (https://bioinfogp.cnb.csic.es/tools/venny/) (Collazos, n.d.-b), overlapping the first 25 genes obtained from the four aforementioned methods.

Then, the **M**olecular **Co**mplex **De**tection (**MCODE**) plug-in within Cytoscape, which enables the clustering of a given network based on topology to discover densely connected regions, was applied for further analysis.

6. Verification and Survivability Assessment of Hub Genes.

The GEPIA2 database (GEPIA2: an enhanced web server for large-scale expression profiling and interactive analysis, (Tang et al., 2019) - http://gepia2.cancer-pku.cn/#index) was selected to evaluate the impact of hub gene biomarkers on PDAC patient survival rates. It depicts the analysis of normal and tumor sample data, which were collected from TCGA and GTEx. The genes found significantly ($p < 0.05$) in the formats were chosen for further investigation. The biomarkers were translated into expression profiles for selected hub genes in normal as well as PDAC samples and further visualized and evaluated using GEPIA2.
In addition, for protein expression in the Human Protein Atlas, a web interface (http://www.proteinatlas.org) (Uhlén et al., 2015) has been utilized to assess the role of genes in normal as well as PDAC samples. Subsequently, another interface, UALCAN (http://ualcan.path.uab.edu/) (Chandrashekar et al., 2017b), (Chandrashekar et al., 2022c), was used for the examination of relationships between different stages of cancer for mRNA expression of the genes of interest using the TCGA set of data.

7. Immune infiltration.

TIMER is a cancer-targeted web-accessible immune infiltration database, which is a robust and efficient database that analyzes the immune cell infiltration (TIMER 2.0) (http://timer.cistrome.org/) (T. Li et al., 2017b), (T. Li et al., 2020c), and (B. Li et al., 2016b), by utilizing data from TCGA from 32 different cancers40. The tumor-infiltrating immune cells (TIICs) comprise CD4+ T cells, macrophages, CD8+ T cells, B cells, macrophage, and neutrophil cells. TIMER was used for the correlation of gene expression between immune cells and hub genes.

8. Hub Genes Functional Enrichment Analysis:

At first, the STRING database was used to visualize the PPI of the hub genes. The first analysis was performed by Metascape (http://metascape.org/), a gene function annotation tool used to apply bioinformatics methods to batch analysis of genes and proteins. It was used to conduct the functional and pathway enrichment analysis of the selected hub genes (Y. Zhou et al., 2019).

9. Identification & Validation of hub genes lncRNAs:

In order to effectively identify the transcription variants resulting the activity of hub genes of interest, the LNCipedia database was used. LNCipedia (Version 5.2) (https://lncipedia.org/) (Volders et al., 2018) is a public database for long non-coding RNA (lncRNA) sequence and annotation. The current release contains 127,802 transcripts and 56,946 genes. In addition, currently LNCipedia offers 2,482 manually curated lncRNA articles.

Moreover, the list of resulting lncRNAs was uploaded to lncATLAS (https://lncatlas.crg.eu/#tab-6270-1) (Mas-Ponte et al., 2017c), an open access online database for subcellular localization of long noncoding RNAs. This localization is expressed in units of Relative Concentration Index (RCI) - a comparison of the concentration of a gene, per unit mass of RNA, between two cellular compartments.

10. Prediction and Validation of Target miRNA:

The prediction of miRNAs targeting the hub genes was performed using **miRNet** (https://www.mirnet.ca/), an open-source online platform created to help understanding microRNA (miRNA) functions by integrating users' data with existing knowledge through network-based visual analytics (Chang et al., 2020).

In addition, the initial hit list of target miRNAs was verified through using DIANA-LncBase v3 (https://diana.e-ce.uth.gr/lncbasev3/home) (Paraskevopoulou et al., 2018), (Karagkouni et al., 2019), which is a reference repository with experimentally supported miRNA targets on non-coding transcripts. It catalogues approximately ~500,000 entries, corresponding to ~240,000 unique tissue and cell-type specific miRNA-lncRNA interactions. The incorporated interactions are defined by 15 distinct low-/high-throughput methodologies, corresponding to 243 distinct cell types/tissues and 162 experimental conditions.

Results:

1. Identification of Differentially Expressed Genes (DEGs):

The analysis was conducted using specific parameters, including the Benjamini and Hochberg False Discovery Rate (FDR) for multiple testing correction, a significance level cut-off of $P < 0.05$, and a threshold of $|\text{Log2 Fold Change (FC)}| > 0.2$. As a result, a total of 500 genes were identified as differentially expressed genes (DEGs), with 451 genes being upregulated and 49 genes being downregulated in the control group compared to the PDAC group. For better visualization of the data, a heatmap was created Figure 6.

2. Dispersion Plot and Volcano Plot:

A mean dispersion plot was constructed to visualize the dispersion values on the y-axis and the mean of normalized counts on the x-axis for an RNA-seq experiment, as demonstrated in Figure 7. A volcano plot, on the other hand, is a type of scatterplot that illustrates the relationship between statistical significance (p-value) and the magnitude of change (fold change) Figure 8. Another commonly used comparison between two treatment conditions involves plotting the adjusted P-value against the log

fold change. In our analysis, we have identified and presented the top ten upregulated genes in Table 2 and the top ten downregulated genes in Table 3.

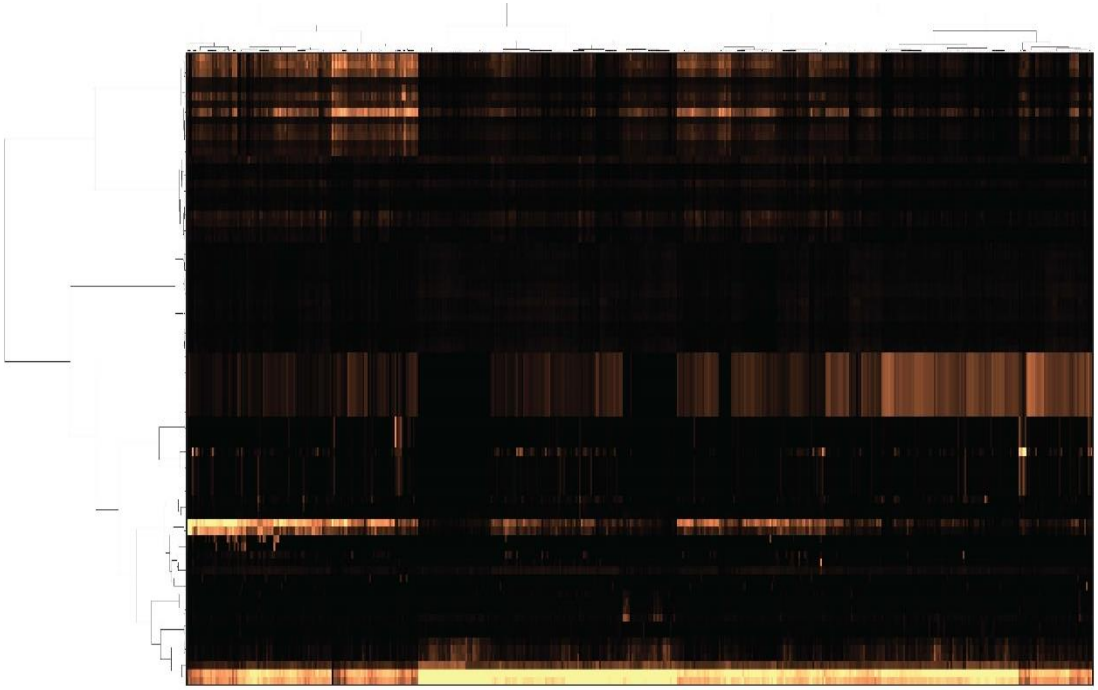

Figure 6: The heatmap of DElncRNA expression in the dataset pancreatic cancer.
Black to yellow indicates low to high expression. DElncRNAs, differentially expressed long non-coding RNAs

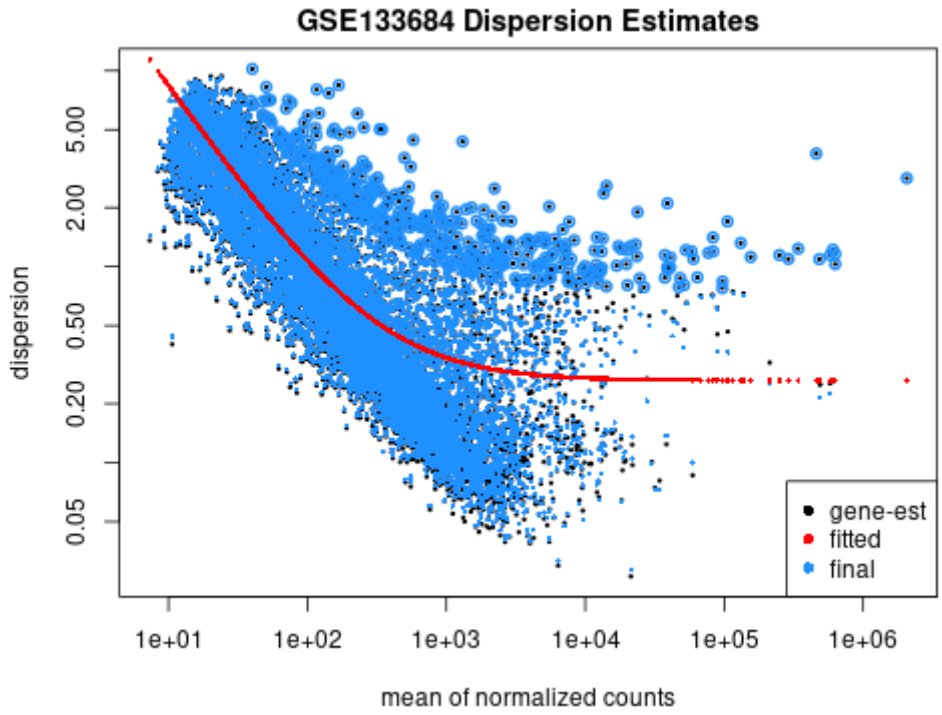

Figure 7: Dispersion plot describes genes which are expressed based on p-value

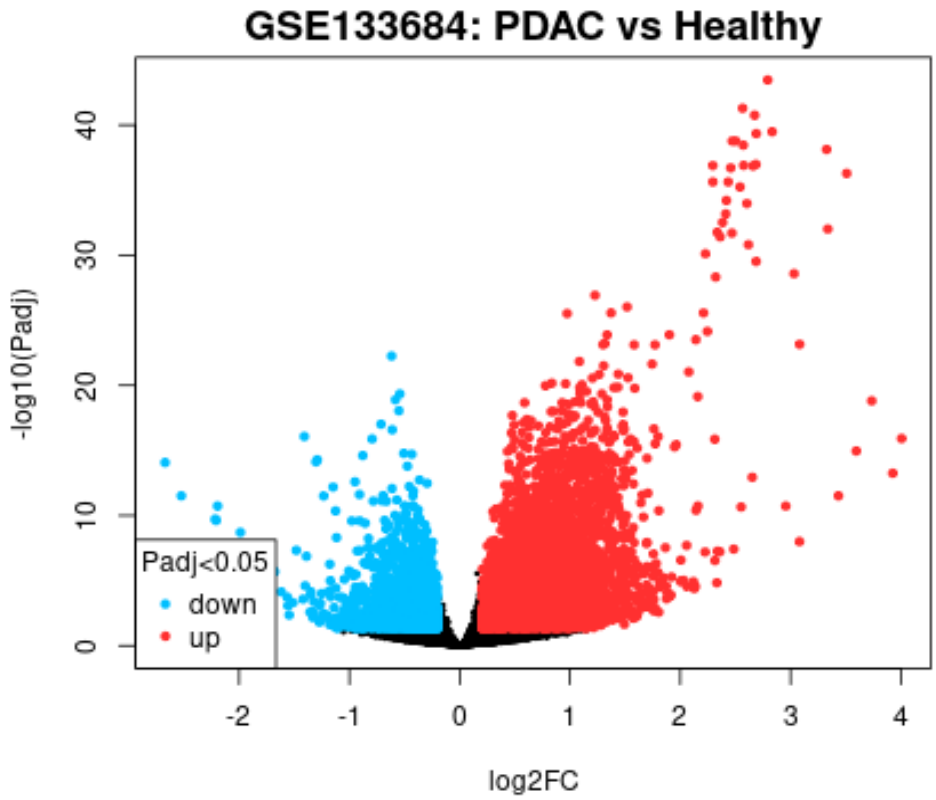

Figure 8: Volcano Plot generated using a DESeq2 dataset,
with base-10 log and base 2-fold change and P-value threshold of 0.05. In the plot the genes are colored if they pass thresholds for FDR and log fold change red indicates the upregulated genes and blue color indicates the downregulated genes, below the central line white color indicates non-significant genes

Table 2:Top 10 Upregulated genes identified the significantly DEGs using the parameters: FDR corrected P-value < 0.05 and fold change > 0

Symbol	padj	pvalue	lfcSE	stat	log2FoldChange	baseMean
TRNT	3.43E-44	2.30E-48	0.1911	14.6136798	2.79335245	18131.15
CYTB	5.20E-42	6.97E-46	0.1804	14.2191318	2.56472176	289664.03
TRNR	1.77E-41	3.56E-45	0.1896	14.1046388	2.67409878	11674.27
TRNF	3.30E-40	8.85E-44	0.2042	13.8760275	2.8332532	5111.66
TRNM	4.57E-40	1.53E-43	0.1944	13.8366691	2.6894044	17351.38
COX3	1.68E-39	7.40E-43	0.1824	13.7229561	2.5025009	155243.43
ND5	1.68E-39	7.90E-43	0.1802	13.7181656	2.47157869	484294.67
TRNG	3.48E-39	1.86E-42	0.1883	13.6558029	2.57142451	13097.77
TRNN	7.52E-39	4.54E-42	0.2448	13.5908938	3.32654329	2589.21

Table 3: Top 10 Downregulated genes Identified the significantly DEGs using the parameters: FDR corrected P-value < 0.05 and fold change < 0

Symbol	padj	pvalue	lfcSE	stat	log2FoldChange	baseMean
AHNAK	5.60E-23	1.73E-25	0.0592	-10.4344017	-0.6176414	13108.5
CD44	4.55E-20	2.01E-22	0.0557	-9.7411245	-0.54293269	2677.09
HLA-DRA	1.28E-19	5.84E-22	0.0605	-9.6323842	-0.58289333	2874.76
TRIM66	8.90E-19	4.89E-21	0.0585	-9.41153	-0.55093378	1032.49
FBXO7	9.62E-18	6.51E-20	0.0781	-9.1354509	-0.71326764	3928.19
ITGA4	2.58E-17	2.00E-19	0.0678	-9.0130437	-0.61120632	1059.86
RMRP	8.43E-17	7.40E-19	0.1589	-8.8687068	-1.40884028	1145.43
OGT	1.30E-16	1.20E-18	0.0901	-8.8147264	-0.7939878	603.14
BTG1	1.70E-15	2.01E-17	0.0597	-8.4930105	-0.50680125	1929.29
TXNIP	1.94E-15	2.40E-17	0.0513	-8.4723596	-0.43424634	10738.88

3. Gene Regulatory Network (GRN) of DEGs & Enrichment

DAVID was employed to conduct GO and KEGG enrichment analysis of the significant DEGs with a significance threshold of P-value<0.05.

The k-mean absolute clustering analysis resulted in determination of 31 clusters mainly regarding Respiratory chain complex, Respiratory electron transport, ATP synthesis by chemiosmotic coupling, and heat production by uncoupling proteins, NADH dehydrogenase (ubiquinone) activity, Nucleosome, and Histone methyltransferase complex, Structural constituent of chromatin, and Histone H3-K4 methylation, **Table 4**.

The analysis also showed that these DEGs were mainly involved in many **biologic processes** associated with mRNA maturation and Transcription including; Electron transport coupled proton transport, Actin filament fragmentation, Cell-cell adhesion mediated by integrin, Mitochondrial electron transport, ubiquinol to cytochrome c, Mitochondrial electron transport, NADH to ubiquinone, Polyamine biosynthetic process, Proton motive force-driven mitochondrial ATP synthesis, Aerobic electron transport chain, Actin filament depolymerization, Mitochondrial ATP synthesis coupled electron transport, Respiratory electron transport chain, Mitochondrial respiratory chain complex I assembly, Oxidative phosphorylation, ATP biosynthetic process, Negative regulation of DNA-templated transcription, elongation, Barbed-end actin filament capping, Aerobic respiration, Nucleoside triphosphate biosynthetic process, Cellular respiration, Electron transport chain, Actin filament polymerization, Actin polymerization or depolymerization, Platelet aggregation, Lamellipodium assembly, Lamellipodium organization, Substantia nigra development, Energy derivation by oxidation of organic compounds, ATP metabolic process, Cortical cytoskeleton organization, Regulation of reactive oxygen species biosynthetic process, **Table 5**.

With regards to **molecular functions**, the DEGs were enriched in Oxidoreduction-driven active transmembrane transporter activity, Electron transfer activity, NADH dehydrogenase (ubiquinone) activity, Cytoskeletal protein binding, Primary active transmembrane transporter activity, Actin binding, Oxidoreductase activity, acting on NAD(P)H, Protein-containing complex binding, Cell adhesion molecule binding,

Binding, Cadherin binding, Enzyme binding, lncRNA binding, GTPase activity, Protein domain specific binding, Kinase binding, Protein heterodimerization activity, Active transmembrane transporter activity, Oxidoreductase activity, Nucleoside-triphosphatase activity, Protein kinase binding, Pyrophosphatase activity, GTP binding, Myosin binding, Actin filament binding, Structural molecule activity, Myosin V binding, Structural constituent of muscle, Structural constituent of chromatin, Carbohydrate derivative binding, Nucleotide binding, Purine ribonucleotide binding, G protein activity, **Table 6**.

The screened DEGs were mainly located in nucleus, nucleoplasm, cytosol, cytoplasm, intracellular membrane-bounded organelle, nucleolus, endoplasmic reticulum, and Golgi apparatus, **Table 7**.

On the other hand, the analysis of **KEGG pathways** indicated that the pathways associated with DEGs were Parkinson disease, Oxidative phosphorylation, Thermogenesis, Alzheimer disease, Amyotrophic lateral sclerosis, Prion disease, Huntington disease, Non-alcoholic fatty liver disease, Retrograde endocannabinoid signaling, Cardiac muscle contraction, Shigellosis, Regulation of actin cytoskeleton, Bacterial invasion of epithelial cells, Leukocyte transendothelial migration, Tight junction, Platelet activation, Viral carcinogenesis, Salmonella infection, Alcoholism, Endocytosis, Systemic lupus erythematosus, Pathogenic Escherichia coli infection, Metabolic pathways, Axon guidance, Adherens junction, Human cytomegalovirus infection, Dilated cardiomyopathy, Focal adhesion, Yersinia infection, Hippo signaling pathway, Vascular smooth muscle contraction, Vasopressin-regulated water reabsorption, Cell adhesion molecules, Neurotrophin signaling pathway, Hypertrophic cardiomyopathy, Hematopoietic cell lineage, Fc gamma R-mediated phagocytosis, **Table 8**.

Finally, the analysis of **disease-gene interaction** stated that the DEGs contribute in Parkinson disease, Oxidative phosphorylation, Thermogenesis, Alzheimer disease, Amyotrophic lateral sclerosis, Prion disease, Huntington disease, Non-alcoholic fatty liver disease, Retrograde endocannabinoid signaling, Cardiac muscle contraction, Shigellosis, Regulation of actin cytoskeleton, Bacterial invasion of epithelial cells, Leukocyte transendothelial migration, Tight junction, Platelet activation, Viral carcinogenesis, Salmonella infection, Alcoholism, Endocytosis,

Systemic lupus erythematosus, Pathogenic Escherichia coli infection, Metabolic pathways, Axon guidance, Adherens junction, Human cytomegalovirus infection, Dilated cardiomyopathy, Focal adhesion, Yersinia infection, Hippo signaling pathway, Vascular smooth muscle contraction, Vasopressin-regulated water reabsorption, Cell adhesion molecules, Neurotrophin signaling pathway, Hypertrophic cardiomyopathy, Hematopoietic cell lineage, Fc gamma R-mediated phagocytosis, **Table 9**.

4. PPI Network Construction:

With defining the minimum required interaction score as the highest confidence 0.9, a gene network that contains; 420 nodes, 370 edges, 1.76 as average node degree, 0.337 as average local clustering coefficient, and < 1.0e-16 as PPI enrichment P-values was built by **STRING**.

The expected number of edges is 154. However, the constructed network has more interactions than expected which means that the screened proteins have more interactions among themselves than what would be expected for a random set of proteins of the same size and degree distribution drawn from the genome. This indicated that the proteins are at least partially biologically connected as a group **Figure 9**.

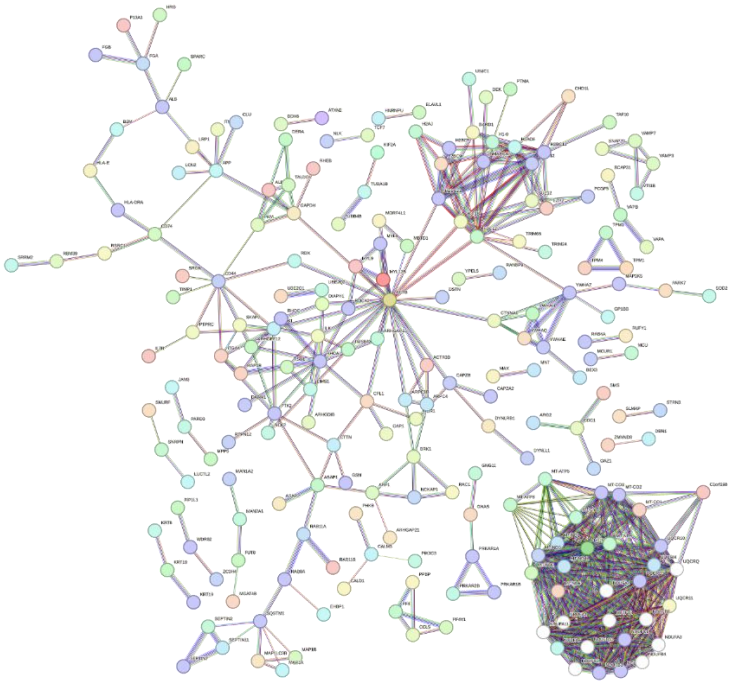

Figure 9: The DEGs Protein-Protein Interaction (PPI) Network by STRING Database

Table 4: Cluster Analysis of DEGs Associated with PDAC.

#	#Term ID	Term Description (Clusters)	Strength	Matching Proteins In Your Network (Labels)
1.	CL:11077	Respiratory chain complex	1.26	NDUFB4,NDUFB11,NDUFC2,UQCRH,UQCR10,NDUFA4,NDUFV3,MT-CO1,MT-CYB,MT-ND6,MT-ND1,MT-ND4L,MT-ND5,MT-CO2,MT-ND4,MT-CO3,MT-ND2,MT-ND3,NDUFA1,UQCRQ,NDUFB6,NDUFA11,NDUFA3,NDUFB2,UQCRB,NDUFC1,UQCR11,NDUFA6,NDUFB1
2.	CL:11068	Respiratory electron transport, ATP synthesis by chemiosmotic coupling, and heat production by uncoupling proteins., and Proton-transporting ATP synthase complex	1.06	NDUFB4,NDUFB11,NDUFC2,UQCRH,UQCR10,NDUFA4,NDUFV3,MT-CO1,MT-CYB,MT-ATP6,MT-ND6,MT-ND1,MT-ND4L,MT-ND5,MT-CO2,MT-ND4,MT-CO3,MT-ND2,MT-ND3,MT-ATP8,C1orf198,NDUFA1,UQCRQ,NDUFB6,NDUFA11,NDUFA3,NDUFB2,UQCRB,NDUFC1,UQCR11,NDUFA6,NDUFB1
3.	CL:11069	Respiratory electron transport, ATP synthesis by chemiosmotic coupling, and heat production by uncoupling proteins.	1.06	NDUFB4,NDUFB11,NDUFC2,UQCRH,UQCR10,NDUFA4,NDUFV3,MT-CO1,MT-CYB,MT-ATP6,MT-ND6,MT-ND1,MT-ND4L,MT-ND5,MT-CO2,MT-ND4,MT-CO3,MT-ND2,MT-ND3,MT-ATP8,NDUFA1,UQCRQ,NDUFB6,NDUFA11,NDUFA3,NDUFB2,UQCRB,NDUFC1,UQCR11,NDUFA6,NDUFB1
4.	CL:11079	NADH dehydrogenase (ubiquinone) activity	1.31	NDUFB4,NDUFB11,NDUFC2,NDUFV3,MT-ND6,MT-ND1,MT-ND4L,MT-ND5,MT-ND4,MT-ND2,MT-ND3,NDUFA1,NDUFB6,NDUFA11,NDUFA3,NDUFB2,NDUFC1,NDUFA6,NDUFB1
5.	CL:17810	Mixed, incl. Actin filament organization, and CDC42 GTPase cycle	0.85	ARHGDIB,NCK2,PLEK,DSTN,PTPN12,ACTR3B,RHOC,ROCK2,LIMS1,RAC1,NCKAP1,CDC42BPB,GSN,CTTN,RSU1,TMSB4X,DIAPH1,DBN1,ILK,ARPC4-TTLL3,ARHGEF12,PSTPIP2,ARPC4,ARPC1B,CORO1C,RHOA,WDR1,BRK1,CFL1,ACTB
6.	CL:17811	Mixed, incl. Regulation of actin dynamics for phagocytic cup formation, and CDC42 GTPase cycle	0.86	ARHGDIB,NCK2,PLEK,DSTN,ACTR3B,RHOC,ROCK2,RAC1,NCKAP1,CDC42BPB,GSN,CTTN,TMSB4X,DIAPH1,DBN1,ARPC4-TTLL3,ARHGEF12,ARPC4,ARPC1B,CORO1C,RHOA,WDR1,BRK1,CFL1,ACTB
7.	CL:11080	NADH dehydrogenase (ubiquinone) activity	1.25	NDUFB4,NDUFB11,NDUFC2,NDUFV3,MT-ND5,MT-ND4,NDUFA1,NDUFB6,NDUFA11,NDUFA3,NDUFB2,NDUFC1,NDUFA6,NDUFB1
8.	CL:17814	Mixed, incl. RHO GTPases Activate WASPs and WAVEs, and ADF-	1.03	NCK2,DSTN,ACTR3B,NCKAP1,GSN,CTTN,TMSB4X,DBN1,ARPC4-TTLL3,ARPC4,ARPC1B,WDR1,BRK1,ACTB

#	#Term ID	Term Description (Clusters)	Strength	Matching Proteins In Your Network (Labels)
		H/Gelsolin-like domain superfamily		
9.	CL:17813	Mixed, incl. RHO GTPases Activate WASPs and WAVEs, and Actin nucleation	0.96	NCK2,DSTN,ACTR3B,NCKAP1,GSN,CTTN,TMSB4X,DIAPH1,DBN1,ARPC4-TTLL3,ARPC4,ARPC1B,WDR1,BRK1,ACTB
10.	CL:11166	Cytochrome complex	1.24	UQCRH,UQCR10,NDUFA4,MT-CO1,MT-CYB,MT-CO2,MT-CO3,UQCRQ,UQCRB,UQCR11
11.	CL:17883	Mixed, incl. Actin-depolymerising factor homology domain, and Sequestering of actin monomers	1.2	DSTN,GSN,CTTN,TMSB4X,DBN1,WDR1,ACTB
12.	CL:11151	Ubiquinone	1.58	MT-ND6,MT-ND1,MT-ND4L,MT-ND2,MT-ND3
13.	CL:11167	Respiratory chain complex III, and Cytochrome-c oxidase activity	1.32	UQCRH,UQCR10,MT-CYB,UQCRQ,UQCRB,UQCR11
14.	CL:11082	NADH dehydrogenase (ubiquinone) activity	1.12	NDUFB11,NDUFC2,MT-ND5,MT-ND4,NDUFB6,NDUFA11,NDUFA6
15.	CL:4766	Structural constituent of chromatin	0.78	H3-3B,H2BC5,EZH2,H1-0,H2BC12,H3C12,H2BC21,H2AC6,H2AJ,H2BC11,H2BC9
16.	CL:17973	Mixed, incl. Sema4D in semaphorin signaling, and ARHGEF1-like, PH domain	1.01	ARHGDIB,PLEK,RHOC,ROCK2,ARHGEF12,RHOA,CFL1
17.	CL:17971	Mixed, incl. Rho protein signal transduction, and P21-Rho-binding domain	0.82	ARHGDIB,PLEK,RHOC,ROCK2,RAC1,CDC42BPB,ARHGEF12,RHOA,CFL1
18.	CL:17815	RHO GTPases Activate WASPs and WAVEs, and Arp2/3 complex-mediated actin nucleation	0.97	NCK2,ACTR3B,NCKAP1,ARPC4-TTLL3,ARPC4,ARPC1B,BRK1
19.	CL:4859	RNA Polymerase I Promoter Opening	1.56	H2BC5,H2AC6,H2AJ,H2BC9

#	#Term ID	Term Description (Clusters)	Strength	Matching Proteins In Your Network (Labels)
20.	CL:17972	Mixed, incl. Rho protein signal transduction, and p21 activated kinase binding domain	0.83	ARHGDIB,PLEK,RHOC,ROCK2,RAC1,ARHGEF12,RHOA,CFL1
21.	CL:4759	Nucleosome, and Histone methyltransferase complex	0.57	H3-3B,SRCAP,H2BC5,WDR82,EZH2,H1-0,H2BC12,H3C12,H2BC21,H2AC6,H2AJ,MBTD1,H2BC11,H2BC9
22.	CL:4760	Structural constituent of chromatin, and Histone H3-K4 methylation	0.63	H3-3B,H2BC5,WDR82,EZH2,H1-0,H2BC12,H3C12,H2BC21,H2AC6,H2AJ,H2BC11,H2BC9
23.	CL:18732	Mixed, incl. COVID-19, thrombosis and anticoagulation, and Scavenging of heme from plasma	1.02	HRG,LRP1,F13A1,ALB,FGB,FGA
24.	CL:11170	Respiratory chain complex III	1.41	UQCRH,UQCR10,UQCRQ,UQCR11
25.	CL:17976	Mixed, incl. ARHGEF1-like, PH domain, and Rho protein GDP-dissociation inhibitor	1.12	ARHGDIB,PLEK,RHOC,ARHGEF12,RHOA
26.	CL:18733	Mixed, incl. COVID-19, thrombosis and anticoagulation, and Inter-alpha-trypsin inhibitor heavy chain C-terminus	1.03	HRG,F13A1,ALB,FGB,FGA
27.	CL:18734	COVID-19, thrombosis and anticoagulation, and Negative regulation of fibrinolysis	1.22	HRG,F13A1,FGB,FGA
28.	CL:11193	Mitochondrial electron transport, cytochrome c to oxygen	1.18	NDUFA4,MT-CO1,MT-CO2,MT-CO3
29.	CL:17886	Mixed, incl. Sequestering of actin monomers, and Baraitser-Winter syndrome	1.18	GSN,CTTN,TMSB4X,ACTB
30.	CL:1975	Polyamine biosynthetic process	1.18	ODC1,SMS,OAZ1,SMOX

#	#Term ID	Term Description (Clusters)	Strength	Matching Proteins In Your Network (Labels)
31.	CL:18595	14-3-3 domain, and M-phase inducer phosphatase	1.14	YWHAH,YWHAE,YWHAQ,YWHAZ

Table 5: Ontology Analysis of DEGs Associated with PDAC - (Biological Process - BP).

#	#Term ID	Term Description (Biological Process – BP) – Top 30	Strength	Matching Proteins In Your Network (Labels)
1.	GO:0015990	Electron transport coupled proton transport	1.53	MT-CO1,MT-ND5,MT-ND4
2.	GO:0030043	Actin filament fragmentation	1.53	DSTN,WDR1,CFL1
3.	GO:0033631	Cell-cell adhesion mediated by integrin	1.35	ITGB1,ITGA4,ADAM9
4.	GO:0006122	Mitochondrial electron transport, ubiquinol to cytochrome c	1.32	UQCRH,UQCR10,MT-CYB,UQCRQ,UQCRB,UQCR11
5.	GO:0006120	Mitochondrial electron transport, NADH to ubiquinone	1.25	NDUFB4,NDUFC2,NDUFA4,NDUFV3,MT-ND6,MT-ND1,MT-ND4L,MT-ND5,MT-ND4,MT-ND2,MT-ND3,NDUFA1,NDUFB6,NDUFA3,NDUFB2,NDUFC1,NDUFA6,NDUFB1
6.	GO:0006596	Polyamine biosynthetic process	1.18	ODC1,SMS,OAZ1,SMOX
7.	GO:0042776	Proton motive force-driven mitochondrial ATP synthesis	1.17	NDUFB4,NDUFB11,NDUFC2,NDUFV3,MT-ATP6,MT-ND6,MT-ND1,MT-ND4L,MT-ND5,MT-ND4,MT-ND2,MT-ND3,MT-ATP8,NDUFA1,NDUFB6,NDUFA11,NDUFA3,NDUFB2,NDUFC1,NDUFA6,NDUFB1
8.	GO:0019646	Aerobic electron transport chain	1.15	NDUFB4,NDUFC2,UQCRH,UQCR10,NDUFA4,NDUFV3,MT-CO1,MT-CYB,MT-ND6,MT-ND1,MT-ND4L,MT-ND5,MT-CO2,MT-ND4,MT-CO3,MT-ND2,MT-ND3,NDUFA1,UQCRQ,NDUFB6,NDUFA3,NDUFB2,UQCRB,NDUFC1,UQCR11,NDUFA6,NDUFB1
9.	GO:0030042	Actin filament depolymerization	1.14	DSTN,GSN,WDR1,CFL1

#	#Term ID	Term Description (Biological Process – BP) – Top 30	Strength	Matching Proteins In Your Network (Labels)
10.	GO:0042775	Mitochondrial ATP synthesis coupled electron transport	1.12	NDUFB4,NDUFC2,UQCRH,UQCR10,NDUFA4,NDUFV3,MT-CO1,MT-CYB,MT-ND6,MT-ND1,MT-ND4L,MT-ND5,MT-CO2,MT-ND4,MT-CO3,MT-ND2,MT-ND3,NDUFA1,UQCRQ,NDUFB6,NDUFA3,NDUFB2,UQCRB,NDUFC1,UQCR11,NDUFA6,NDUFB1
11.	GO:0022904	Respiratory electron transport chain	1.08	NDUFB4,NDUFC2,UQCRH,UQCR10,PUM2,NDUFA4,NDUFV3,MT-CO1,MT-CYB,MT-ND6,MT-ND1,MT-ND4L,MT-ND5,MT-CO2,MT-ND4,MT-CO3,MT-ND2,MT-ND3,NDUFA1,UQCRQ,NDUFB6,NDUFA3,NDUFB2,UQCRB,NDUFC1,SOD2,ETFA,UQCR11,NDUFA6,NDUFB1
12.	GO:0032981	Mitochondrial respiratory chain complex I assembly	1.07	NDUFB4,NDUFB11,NDUFC2,MT-ND6,MT-ND1,MT-ND5,MT-ND4,MT-ND2,NDUFA1,NDUFB6,NDUFA11,NDUFA3,NDUFB2,NDUFC1,NDUFA6,NDUFB1
13.	GO:0006119	Oxidative phosphorylation	1.06	NDUFB4,NDUFB11,NDUFC2,UQCRH,UQCR10,NDUFA4,NDUFV3,MT-CO1,MT-CYB,MT-ATP6,MT-ND6,MT-ND1,MT-ND4L,MT-ND5,MT-CO2,MT-ND4,MT-CO3,MT-ND2,MT-ND3,MT-ATP8,NDUFA1,UQCRQ,NDUFB6,NDUFA11,NDUFA3,NDUFB2,UQCRB,NDUFC1,UQCR11,NDUFA6,NDUFB1
14.	GO:0006754	ATP biosynthetic process	1.06	NDUFB4,NDUFB11,NDUFC2,NDUFV3,MT-ATP6,MT-ND6,MT-ND1,MT-ND4L,MT-ND5,MT-ND4,MT-ND2,MT-ND3,MT-ATP8,NDUFA1,NDUFB6,NDUFA11,NDUFA3,NDUFB2,NDUFC1,NDUFA6,NDUFB1,ALDOA
15.	GO:0032785	Negative regulation of DNA-templated transcription, elongation	1.03	ZC3H4,WDR82,EZH2,SIRT6,HNRNPU
16.	GO:0051016	Barbed-end actin filament capping	0.99	NCK2,CAPZA2,GSN,CAPZB,RDX
17.	GO:0009060	Aerobic respiration	0.95	NDUFB4,NDUFB11,NDUFC2,UQCRH,UQCR10,NDUFA4,NDUFV3,MT-CO1,MT-CYB,MT-ATP6,MT-ND6,MT-ND1,MT-ND4L,MT-ND5,MT-CO2,MT-ND4,MT-CO3,MT-ND2,MT-ND3,MT-ATP8,NDUFA1,MTFR1L,UQCRQ,NDUFB6,NDUFA11,NDUFA3,NDUFB2,UQCRB,NDUFC1,UQCR11,NDUFA6,NDUFB1

#	#Term ID	Term Description (Biological Process – BP) – Top 30	Strength	Matching Proteins In Your Network (Labels)
18.	GO:0009142	Nucleoside triphosphate biosynthetic process	0.95	NDUFB4,NDUFB11,NDUFC2,NDUFV3,MT-ATP6,MT-ND6,MT-ND1,MT-ND4L,MT-ND5,MT-ND4,MT-ND2,MT-ND3,MT-ATP8,NDUFA1,CMPK1,NDUFB6,NDUFA11,NDUFA3,NDUFB2,NDUFC1,NDUFA6,NDUFB1,ALDOA
19.	GO:0045333	Cellular respiration	0.92	NDUFB4,NDUFB11,NDUFC2,UQCRH,UQCR10,PUM2,NDUFA4,NDUFV3,MT-CO1,MT-CYB,MT-ATP6,MT-ND6,MT-ND1,MT-ND4L,MT-ND5,MT-CO2,MT-ND4,MT-CO3,MT-ND2,MT-ND3,MT-ATP8,NDUFA1,MTFR1L,UQCRQ,NDUFB6,NDUFA11,NDUFA3,NDUFB2,UQCRB,NDUFC1,SOD2,ETFA,UQCR11,NDUFA6,NDUFB1
20.	GO:0022900	Electron transport chain	0.92	NDUFB4,NDUFC2,UQCRH,UQCR10,PUM2,NDUFA4,NDUFV3,MT-CO1,MT-CYB,MT-ND6,MT-ND1,MT-ND4L,MT-ND5,MT-CO2,MT-ND4,MT-CO3,MT-ND2,MT-ND3,NDUFA1,UQCRQ,ASPH,NDUFB6,NDUFA3,NDUFB2,UQCRB,NDUFC1,SOD2,ETFA,UQCR11,NDUFA6,NDUFB1
21.	GO:0030041	Actin filament polymerization	0.91	RAC1,GSN,CTTN,DIAPH1,ARPC4-TTLL3,PSTPIP2,ARPC4
22.	GO:0008154	Actin polymerization or depolymerization	0.88	DSTN,RAC1,GSN,CTTN,DIAPH1,ARPC4-TTLL3,PSTPIP2,ARPC4,CAPZB,WDR1,CFL1
23.	GO:0070527	Platelet aggregation	0.87	PLEK,MYL9,FGB,GNAS,ILK,ACTB,FGA
24.	GO:0030032	Lamellipodium assembly	0.87	NCK2,RAC1,ITGB1,CAPZB,ABLIM3,FGD4
25.	GO:0097581	Lamellipodium organization	0.84	NCK2,RAC1,CTTN,ITGB1,CAPZB,ABLIM3,FGD4
26.	GO:0021762	Substantia nigra development	0.83	YWHAH,YWHAE,CALM3,YWHAQ,DYNLL1,RHOA,ACTB
27.	GO:0015980	Energy derivation by oxidation of organic compounds	0.82	NDUFB4,PYGL,NDUFB11,NDUFC2,UQCRH,PHKB,UQCR10,PUM2,NDUFA4,NDUFV3,MT-CO1,MT-CYB,MT-ATP6,MT-ND6,MT-ND1,MT-ND4L,MT-ND5,MT-CO2,MT-ND4,MT-CO3,MT-ND2,MT-ND3,MT-

#	#Term ID	Term Description (Biological Process – BP) – Top 30	Strength	Matching Proteins In Your Network (Labels)
				ATP8,NDUFA1,MTFR1L,UQCRQ,NDUFB6,IL6ST,NDUFA11,NDUFA3,NDUFB2,UQCRB,NDUFC1,SOD2,ETFA,UQCR11,NDUFA6,NDUFB1
28.	GO:0046034	ATP metabolic process	0.82	NDUFB4,NDUFB11,NDUFC2,PKM,NDUFV3,MT-ATP6,MT-ND6,MT-ND1,MT-ND4L,MT-ND5,MT-ND4,MT-ND2,MT-ND3,MT-ATP8,NDUFA1,NDUFB6,GAPDH,NDUFA11,NDUFA3,NDUFB2,NDUFC1,NDUFA6,NDUFB1,ALDOA
29.	GO:0030865	Cortical cytoskeleton organization	0.82	PLEK,RHOC,ROCK2,RHOBTB1,RAC1,NCKAP1,RHOBTB3,RHOA,WDR1
30.	GO:1903426	Regulation of reactive oxygen species biosynthetic process	0.81	ARG2,NDUFC2,PARK7,MT-CO2,RHOA,SOD2

Table 6: Ontology Analysis of DEGs Associated with PDAC - (Molecular Function - MF)

#	#Term ID	Term Description (Molecular Function – MF)	Strength	Matching Proteins In Your Network (Labels)
1.	GO:0005515	Protein binding	0.22	CD74,RANBP9,VAMP3,MNT,EIF2AK1,PYGL,PGRMC1,TIMP1,NUTF2,CDC37,TAX1BP3,PF4V1,IL10RA,ARHGDIB,HRG,NCK2,ODC1,PLEK,CCDC92,LRP1,IL9R,DSTN,GNG11,PTPN12,YWHAH,SNAP23,RBM39,H3-3B,ACTR3B,BTG1,NOTCH2,AKIRIN2,BARD1,MAN2A1,MPP5,CDK2AP1,RAB11A,SMAD2,DNAJB6,RHEB,SRCAP,VAMP7,SLA2,YWHAE,CEP70,PRKAR2B,FBXO7,PRUNE1,FTH1,RASA1,LAMTOR1,ESAM,MYL9,SCLT1,UXS1,APP,RAB6B,RHOC,H2BC5,FCER1G,NPTN,AMFR,CALM3,ALB,PPBP,PF4,MAP1B,JAM3,TAF10,MAP1A,MAPRE2,RAB8A,SRRM2,FRMD3,CTNNA1,CAVIN2,HOOK3,FGB,RAB6A,DAB2,PHKB,CLU,SUZ12,ROCK2,EZH2,PKM,TMC8,RUFY1,PTTG1IP,MORF4L1,RAB11B,NEXN,BCL9L,ATF4,TUBA1B,SIRT6,LIMS1,RHOBTB1,LRRFIP2,GRAP2,PARK7,SSX2IP,TCF7,TRIM24,PTK2,TUBB4B,PTMA,GFI1B,HMGB1,VAPA,ANP32B,GPX4,SVIP,PDGFA,NRDC,LUC7L2,OPHN1,STK39,RAC1,H2BC12,DYNLRB1,STRN3,TPM1,MAX,MAP3K5,H3C12,AGBL5,FUT8,UBAP2,KIFAP3,MINDY1,CALD1,CAPZA2,MT-ND2,CDC42BPB,RAB32,TAGLN2,ARHGAP18,HDGF,LMNA,PBXIP1,RGS10,H2BC21,SHOC2,

#	#Term ID	Term Description (Molecular Function – MF)	Strength	Matching Proteins In Your Network (Labels)
				MPP1,SH3BGRL2,CETN2,GADD45A,GNAS,PDLIM1,BEX3,CAP1,LCN2,MCU,SH3BGRL,GSN,TMEFF1,CTTN,HLA-E,LZIC,H2AC6,AHNAK,PCYT1B,DNAJC2,ASPH,RHOBTB3,KATNAL1,TMSB4X,CNTLN,IL6ST,ASAH1,YWHAQ,KRT18,DIAPH1,SQSTM1,DYNLL1,PRKAR1A,DBN1,DAAM1,HLA-DRA,EGFL8,YWHAZ,ITGB1,ILK,GAPDH,ITGA4,ARPC4-TTLL3,ARHGEF12,PPME1,GP1BB,MIER1,LRRC32,ZFPM2,NLK,KIF2A,ELAVL1,PRKAR1B,LTBP1,PSTPIP2,ARPC4,ITPRID2,ARPC1B,MITF,BCAP31,DAP,CORO1C,BEST1,RHOA,CAPZB,AP2M1,ICA1,ANO6,PTPRC,SEPTIN7,VAPB,ADAM9,UIMC1,NEK1,ABLIM3,WDR1,STAU2,ASAP1,BRK1,CFL1,FGD4,NUCB2,H2AJ,MTRNR2L8,ZMYND8,ARF1,SOD2,ATXN2,KRT8,VTI1B,STON2,UBE2J1,CD226,TXNIP,SNURF,MYL12B,MBTD1,DNAJC3,CCL5,H2BC11,NAP1L1,DDX6,H2BC9,SEPTIN2,ZCCHC17,PCSK6,SCYL2,HNRNPU,TPM4,ACTB,ALDOA,RDX,TCEAL9,PCMT1,B2M,FGA,MAP1LC3B,TPM3,DEK,FHL1,SLMAP
2.	GO:0015453	Oxidoreduction-driven active transmembrane transporter activity	1.18	NDUFB4,NDUFC2,UQCRH,UQCR10,NDUFA4,NDUFV3,MT-CO1,MT-CYB,MT-ND6,MT-ND1,MT-ND4L,MT-ND5,MT-CO2,MT-ND4,MT-CO3,MT-ND2,MT-ND3,NDUFA1,NDUFB6,NDUFA3,NDUFB2,NDUFC1,NDUFA6,NDUFB1
3.	GO:0009055	Electron transfer activity	1	NDUFB4,NDUFC2,UQCRH,UQCR10,NDUFA4,NDUFV3,MT-CO1,MT-CYB,MT-ND6,MT-ND1,MT-ND4L,MT-ND5,MT-CO2,MT-ND4,MT-CO3,MT-ND2,MT-ND3,NDUFA1,ASPH,NDUFB6,NDUFA3,NDUFB2,NDUFC1,ETFA,UQCR11,NDUFA6,NDUFB1
4.	GO:0008137	NADH dehydrogenase (ubiquinone) activity	1.3	NDUFB4,NDUFC2,NDUFA4,NDUFV3,MT-ND6,MT-ND1,MT-ND4L,MT-ND5,MT-ND4,MT-ND2,MT-ND3,NDUFA1,NDUFB6,NDUFA3,NDUFB2,NDUFC1,NDUFA6,NDUFB1
5.	GO:0008092	Cytoskeletal protein binding	0.49	NCK2,DSTN,YWHAH,ACTR3B,RAB11A,SMAD2,CEP70,PRUNE1,MYL9,RAB6B,CALM3,MAP1B,MAP1A,MAPRE2,RAB8A,FRMD3,CTNNA1,HOOK3,RAB6A,CLU,ROCK2,RAB11B,NEXN,PTK2,VAPA,OPHN1,TPM1,AGBL5,KIFAP3,CALD1,CAPZA2,HDGF,CETN2,PDLIM1,CAP1,GSN,CTTN,KATNAL1,TMSB4X,DIAPH1,DBN1,DAAM1,ITGB1,GAPDH,ARPC4-TTLL3,KIF2A,PSTPIP2,ARPC4,ITPRID2,ARPC1B,CORO1C,RHOA,CAPZB,PTPRC,VAPB,ABLIM3,WDR1,STAU2,CFL1,FGD4,MYL12B,HNRNPU,TPM4,ACTB,ALDOA,RDX,MAP1LC3B,TPM3

#	#Term ID	Term Description (Molecular Function – MF)	Strength	Matching Proteins In Your Network (Labels)
6.	GO:0015399	Primary active transmembrane transporter activity	0.84	NDUFB4,NDUFC2,UQCRH,UQCR10,NDUFA4,NDUFV3,MT-CO1,MT-CYB,MT-ND6,MT-ND1,MT-ND4L,MT-ND5,MT-CO2,MT-ND4,MT-CO3,MT-ND2,MT-ND3,NDUFA1,NDUFB6,ATP8A1,NDUFA3,NDUFB2,NDUFC1,NDUFA6,NDUFB1,ABCC4
7.	GO:0003779	Actin binding	0.6	NCK2,DSTN,YWHAH,ACTR3B,MAP1B,MAP1A,CTNNA1,NEXN,PTK2,OPHN1,TPM1,CALD1,CAPZA2,HDGF,PDLIM1,CAP1,GSN,CTTN,TMSB4X,DIAPH1,DBN1,DAAM1,ITGB1,ARPC4-TTLL3,PSTPIP2,ARPC4,ITPRID2,ARPC1B,CORO1C,CAPZB,ABLIM3,WDR1,CFL1,FGD4,HNRNPU,TPM4,ALDOA,RDX,TPM3
8.	GO:0016651	Oxidoreductase activity, acting on NAD(P)H	0.98	NDUFB4,NDUFC2,NDUFA4,NDUFV3,CYB5R3,MT-ND6,MT-ND1,MT-ND4L,MT-ND5,MT-ND4,MT-ND2,MT-ND3,NDUFA1,NDUFB6,NDUFA3,NDUFB2,NDUFC1,NDUFA6,NDUFB1
9.	GO:0044877	Protein-containing complex binding	0.37	CD74,SPARC,HRG,NCK2,LRP1,DSTN,RAP1B,H3-3B,YWHAE,SMARCA5,APP,FCER1G,AMFR,MAP1B,JAM3,CTNNA1,CLU,EZH2,PKM,NEXN,SIRT6,NDUFA4,PARK7,PTK2,H1-0,HMGB1,PDGFA,RAC1,STRN3,TPM1,MAX,KIFAP3,CAPZA2,CDC42BPB,RAB32,CETN2,GNAS,GSN,CTTN,HLA-E,DNAJC2,SQSTM1,DBN1,HLA-DRA,ITGB1,ITGA4,PSTPIP2,ITPRID2,ARPC1B,BCAP31,CORO1C,CD44,CAPZB,PTPRC,ADAM9,EIF1,ABLIM3,WDR1,STAU2,BRK1,CFL1,CD226,HNRNPU,TPM4,B2M,TPM3
10.	GO:0050839	Cell adhesion molecule binding	0.49	YWHAE,ESAM,APP,NPTN,JAM3,CTNNA1,PKM,RAB11B,NEXN,PARK7,PTK2,HMGB1,VAPA,H3C12,UBAP2,CALD1,TAGLN2,ARHGAP18,PDLIM1,CTTN,AHNAK,KRT18,DBN1,YWHAZ,ITGB1,ITGA4,PPME1,CAPZB,SEPTIN7,VAPB,ADAM9,ASAP1,CD226,DDX6,SEPTIN2,ALDOA,RDX,PCMT1
11.	GO:0005488	Binding	0.08	CD74,RANBP9,VAMP3,MNT,EIF2AK1,PYGL,PGRMC1,TIMP1,NUTF2,CDC37,TAX1BP3,PF4V1,IL10RA,ARHGDIB,SPARC,HRG,NEK4,NCK2,ODC1,PLEK,CCDC92,LRP1,SRSF6,IL9R,DSTN,GNG11,PTPN12,YWHAH,SNAP23,RAP1B,ZC3H4,RBM39,H3-3B,ACTR3B,BTG1,NOTCH2,AKIRIN2,BARD1,MAN2A1,MPP5,CDK2AP1,ARG2,RAB11A,PIK3C3,SMAD2,DNAJB6,RHEB,SRCAP,VAMP7,SLA2,YWHAE,F13A1,CEP70,PRKAR2B,FBXO7,UBE2Q2,PRUNE1,FTH1,RASA1,LAMTOR1,ESAM,MYL9,SCLT1,ASAP2,SMARCA5,UXS1,APP,RAB6B,CA2,RHOC,H2BC5,FCER1G,NPTN,AMFR,CALM3,UBE2Q1,ALB,PPBP,PF4,WDR82,MAP1B,JAM3,TAF10,MAP1A,MAPRE2,RAB8A,SRRM2,FRMD3,HIPK3,CTNNA1,CAVIN2,HOOK3,F

#	#Term ID	Term Description (Molecular Function – MF)	Strength	Matching Proteins In Your Network (Labels)
				GB,IL7R,CAMTA1,APLF,RAB6A,DAB2,PHKB,CLU,SUZ12,ROCK2,EZH2,PKM,TALDO1,LARP1B,HADHB,TMC8,RUFY1,PTTG1IP,MORF4L1,RAB11B,NEXN,BCL9L,FIP1L1,ATF4,TUBA1B,SIRT6,PCGF5,LIMS1,PUM2,MGAT4B,RHOBTB1,LRRFIP2,GRAP2,NDUFA4,PARK7,SSX2IP,TCF7,TRIM24,PTK2,TUBB4B,DYRK2,H1-0,PTMA,GFI1B,HMGB1,VAPA,ANP32B,GPX4,SVIP,NDUFV3,PDGFA,NRDC,LUC7L2,OPHN1,MLH3,STK39,RAC1,MAN1A2,H2BC12,DYNLRB1,REPS2,STRN3,TPM1,MAX,MAP3K5,H3C12,AGBL5,FUT8,UBAP2,CYB5R3,MT-CO1,MT-CYB,KIFAP3,MINDY1,CALD1,MT-CO2,CAPZA2,MT-ND4,MT-ND2,CDC42BPB,RAB4A,RAB32,TAGLN2,ARHGAP18,HDGF,LMNA,PBXIP1,GTF3C6,RGS10,H2BC21,CHD1L,SHOC2,MPP1,SH3BGRL2,CETN2,GADD45A,GNAS,PDLIM1,CMPK1,BEX3,CAP1,LCN2,MCU,SH3BGRL,OGT,GSN,SUSD1,PARD3,TMEFF1,CTTN,HLA-E,LZIC,H2AC6,AHNAK,PCYT1B,DNAJC2,ASPH,YPEL5,RHOBTB3,SLTM,KATNAL1,TMSB4X,CNTLN,ADAMTS6,IL6ST,ATP8A1,ASAH1,YWHAQ,KRT18,DIAPH1,SQSTM1,DYNLL1,RAB37,PRKAR1A,DBN1,PAIP2,DAAM1,HLA-DRA,EGFL8,YWHAZ,ITGB1,ILK,GAPDH,ITGA4,ARPC4-TTLL3,ARHGEF12,PPME1,EIF4G3,GP1BB,MIER1,LRRC32,RBM33,ZFPM2,NLK,KIF2A,ELAVL1,PRKAR1B,PHF14,LTBP1,PSTPIP2,RAB6C,ARPC4,ITPRID2,ARPC1B,MITF,BCAP31,DAP,CORO1C,CHD9,CD44,TNIK,BEST1,RHOA,CAPZB,TNRC6B,AP2M1,ICA1,LIMS4,ANO6,TLK1,PTPRC,SEPTIN7,VAPB,ADAM9,EIF1,UIMC1,SEPTIN11,MCTP1,NEK1,ABLIM3,WDR1,STAU2,VDAC3,ASAP1,BRK1,CFL1,FGD4,NUCB2,CALU,H2AJ,MTRNR2L8,ZMYND8,ARF1,SOD2,ATXN2,MYL6,KRT8,VTI1B,STON2,UBE2J1,ETFA,RAB31,CD226,TXNIP,SNURF,MYL12B,MBTD1,DNAJC3,CCL5,H2BC11,NAP1L1,UBE2F,DDX6,H2BC9,SEPTIN2,ZCCHC17,PCSK6,SCYL2,HNRNPU,TPM4,ABCC4,ACTB,SNRPN,TRIM66,ALDOA,RDX,TCEAL9,ITM2B,PCMT1,B2M,FGA,POLR3G,MAP1LC3B,TPM3,DEK,FHL1,BIN2,SLMAP
12.	GO:0045296	Cadherin binding	0.58	YWHAE,CTNNA1,PKM,RAB11B,PARK7,VAPA,H3C12,UBAP2,CALD1,TAGLN2,ARHGAP18,PDLIM1,CTTN,AHNAK,KRT18,DBN1,YWHAZ,ITGB1,PPME1,CAPZB,SEPTIN7,VAPB,ASAP1,DDX6,SEPTIN2,ALDOA,RDX,PCMT1
13.	GO:0019899	Enzyme binding	0.28	CD74,RANBP9,TIMP1,NUTF2,CDC37,ARHGDIB,NCK2,PLEK,YWHAH,BTG1,NOTCH2,AKIRIN2,BARD1,CDK2AP1,SMAD2,RHEB,YWHAE,PRKAR2B,FBXO7,RASA1,LAMTOR1,APP,RHOC,A

#	#Term ID	Term Description (Molecular Function – MF)	Strength	Matching Proteins In Your Network (Labels)
				MFR,CALM3,TAF10,MAPRE2,RAB8A,CAVIN2,CLU,ROCK2,ATF4,TUBA1B,LIMS1,RHOBTB1,PARK7,PTK2,HMGB1,ANP32B,SVIP,LUC7L2,STK39,RAC1,STRN3,MAP3K5,KIFAP3,MT-ND2,CDC42BPB,SHOC2,GADD45A,CAP1,GSN,RHOBTB3,TMSB4X,CNTLN,DIAPH1,SQSTM1,PRKAR1A,DAAM1,YWHAZ,ITGB1,ILK,PPME1,MIER1,NLK,ELAVL1,PRKAR1B,ARPC4,CORO1C,RHOA,PTPRC,VAPB,ADAM9,STAU2,FGD4,SOD2,UBE2J1,CD226,TXNIP,SNURF,DNAJC3,H2BC9,HNRNPU,ACTB,RDX,MAP1LC3B,SLMAP
14.	GO:0106222	lncRNA binding	1.6	EZH2,HADHB,SIRT6,PUM2,PPME1,ELAVL1,HNRNPU
15.	GO:0003924	GTPase activity	0.57	ARHGDIB,GNG11,RAP1B,RAB11A,RHEB,RASA1,RAB6B,RHOC,RAB8A,RAB6A,RAB11B,RHOBTB1,RAC1,RAB4A,RAB32,RGS10,GNAS,RHOBTB3,RAB37,RAB6C,RHOA,SEPTIN7,SEPTIN11,ARF1,RAB31,SEPTIN2
16.	GO:0019904	Protein domain specific binding	0.41	PTPN12,YWHAH,RBM39,MPP5,SMAD2,YWHAE,PRKAR2B,APP,CALM3,SRRM2,RAB6A,RUFY1,ATF4,LRRFIP2,SSX2IP,PTK2,VAPA,STRN3,MAP3K5,FUT8,SH3BGRL2,SH3BGRL,CNTLN,YWHAQ,SQSTM1,PRKAR1A,YWHAZ,GAPDH,NLK,DAP,RHOA,AP2M1,ICA1,VAPB,ADAM9,ZMYND8,ARF1,DDX6,TCEAL9
17.	GO:0019900	Kinase binding	0.37	CDC37,NCK2,PLEK,BTG1,BARD1,RHEB,PRKAR2B,FBXO7,RHOC,CALM3,MAPRE2,RAB8A,CAVIN2,ATF4,LIMS1,RHOBTB1,PARK7,PTK2,STK39,RAC1,MAP3K5,MT-ND2,GADD45A,GSN,RHOBTB3,CNTLN,SQSTM1,PRKAR1A,YWHAZ,ITGB1,ILK,PPME1,ELAVL1,PRKAR1B,RHOA,PTPRC,ADAM9,STAU2,CD226,DNAJC3,ACTB
18.	GO:0046982	Protein heterodimerization activity	0.49	YWHAH,H3-3B,BARD1,YWHAE,FBXO7,APP,H2BC5,JAM3,CLU,ATF4,VAPA,PDGFA,H2BC12,TPM1,MAX,H3C12,H2BC21,GADD45A,H2AC6,ITGB1,VAPB,H2AJ,H2BC11,H2BC9,TPM4
19.	GO:0022804	Active transmembrane transporter activity	0.46	NDUFB4,NDUFC2,UQCRH,UQCR10,NDUFA4,NDUFV3,MT-CO1,MT-CYB,MT-ND6,MT-ND1,MT-ND4L,MT-ND5,MT-CO2,MT-ND4,MT-CO3,MT-ND2,MT-ND3,NDUFA1,MCU,NDUFB6,ATP8A1,NDUFA3,NDUFB2,NDUFC1,NDUFA6,NDUFB1,ABCC4
20.	GO:0016491	Oxidoreductase activity	0.37	NDUFB4,YWHAH,FTH1,NDUFC2,UQCRH,HADHB,UQCR10,NDUFA4,PARK7,GPX4,NDUFV3,CYB5R3,MT-CO1,MT-CYB,MT-ND6,MT-ND1,MT-ND4L,MT-ND5,MT-CO2,MT-ND4,MT-CO3,MT-ND2,MT-

#	#Term ID	Term Description (Molecular Function – MF)	Strength	Matching Proteins In Your Network (Labels)
				ND3,NDUFA1,ASPH,NDUFB6,YWHAZ,GAPDH,NDUFA3,NDUFB2,NDUFC1,SOD2,ETFA,UQCR11,SMOX,NDUFA6,NDUFB1,ABCC4
21.	GO:0017111	Nucleoside-triphosphatase activity	0.39	ARHGDIB,GNG11,RAP1B,RAB11A,RHEB,SRCAP,RASA1,SMARCA5,RAB6B,RHOC,RAB8A,RAB6A,RAB11B,RHOBTB1,MLH3,RAC1,RAB4A,RAB32,RGS10,CHD1L,GNAS,RHOBTB3,KATNAL1,ATP8A1,RAB37,KIF2A,RAB6C,CHD9,RHOA,SEPTIN7,SEPTIN11,ARF1,RAB31,DDX6,SEPTIN2
22.	GO:0019901	Protein kinase binding	0.37	CDC37,NCK2,PLEK,RHEB,PRKAR2B,FBXO7,RHOC,CALM3,MAPRE2,RAB8A,CAVIN2,ATF4,LIMS1,RHOBTB1,PTK2,STK39,RAC1,MAP3K5,MT-ND2,RHOBTB3,CNTLN,SQSTM1,PRKAR1A,YWHAZ,ITGB1,ILK,PPME1,ELAVL1,PRKAR1B,RHOA,PTPRC,ADAM9,STAU2,CD226,DNAJC3,ACTB
23.	GO:0016462	Pyrophosphatase activity	0.36	ARHGDIB,GNG11,RAP1B,RAB11A,RHEB,SRCAP,PRUNE1,RASA1,SMARCA5,RAB6B,RHOC,RAB8A,RAB6A,RAB11B,RHOBTB1,MLH3,RAC1,RAB4A,RAB32,RGS10,CHD1L,GNAS,RHOBTB3,KATNAL1,ATP8A1,RAB37,KIF2A,RAB6C,CHD9,RHOA,SEPTIN7,SEPTIN11,ARF1,RAB31,DDX6,SEPTIN2
24.	GO:0005525	GTP binding	0.46	RAP1B,RAB11A,RHEB,RAB6B,RHOC,RAB8A,RAB6A,RAB11B,TUBA1B,RHOBTB1,TUBB4B,RAC1,RAB4A,RAB32,GNAS,RHOBTB3,RAB37,RAB6C,RHOA,SEPTIN7,SEPTIN11,ARF1,RAB31,SEPTIN2
25.	GO:0017022	Myosin binding	0.79	RAB11A,MYL9,RAB6B,RAB8A,RAB6A,RAB11B,CALD1,GSN,RHOA,MYL12B
26.	GO:0051015	Actin filament binding	0.56	DSTN,CTNNA1,NEXN,TPM1,CAPZA2,GSN,CTTN,DBN1,PSTPIP2,ITPRID2,CORO1C,CAPZB,ABLIM3,WDR1,CFL1,TPM4,TPM3
27.	GO:0005198	Structural molecule activity	0.32	NUTF2,H3-3B,MYL9,H2BC5,MAP1B,MAP1A,CTNNA1,FGB,ROCK2,KRT7,NEXN,TUBA1B,TUBB4B,H1-0,H2BC12,TPM1,H3C12,KRT19,LMNA,H2BC21,H2AC6,AHNAK,ASPH,KRT18,LTBP1,ARPC4,ARPC1B,SEPTIN7,H2AJ,MYL6,KRT8,H2BC11,H2BC9,TPM4,ACTB,FGA
28.	GO:0031489	Myosin V binding	1.15	RAB11A,RAB6B,RAB8A,RAB6A,RAB11B

#	#Term ID	Term Description (Molecular Function – MF)	Strength	Matching Proteins In Your Network (Labels)
29.	GO:0008307	Structural constituent of muscle	0.86	MYL9,NEXN,TPM1,KRT19,ASPH,MYL6,TPM4
30.	GO:0030527	Structural constituent of chromatin	0.65	H3-3B,H2BC5,H1-0,H2BC12,H3C12,H2BC21,H2AC6,H2AJ,H2BC11,H2BC9
31.	GO:0097367	Carbohydrate derivative binding	0.18	EIF2AK1,PYGL,PF4V1,HRG,NEK4,LRP1,RAP1B,ACTR3B,MPP5,RAB11A,PIK3C3,RHEB,SRCAP,PRKAR2B,UBE2Q2,SMARCA5,APP,RAB6B,RHOC,UBE2Q1,PF4,RAB8A,HIPK3,RAB6A,ROCK2,PKM,RAB11B,TUBA1B,RHOBTB1,PTK2,TUBB4B,DYRK2,HMGB1,MLH3,STK39,RAC1,MAP3K5,CDC42BPB,RAB4A,RAB32,HDGF,CHD1L,GNAS,CMPK1,RHOBTB3,KATNAL1,ATP8A1,RAB37,PRKAR1A,ILK,NLK,KIF2A,PRKAR1B,RAB6C,CHD9,CD44,TNIK,RHOA,TLK1,PTPRC,SEPTIN7,SEPTIN11,NEK1,ARF1,UBE2J1,RAB31,H2BC11,UBE2F,DDX6,SEPTIN2,PCSK6,SCYL2,HNRNPU,ABCC4,ACTB,ITM2B
32.	GO:0000166	Nucleotide binding	0.18	EIF2AK1,PYGL,NEK4,RAP1B,ACTR3B,MPP5,RAB11A,PIK3C3,RHEB,SRCAP,PRKAR2B,UBE2Q2,SMARCA5,UXS1,RAB6B,RHOC,UBE2Q1,RAB8A,HIPK3,APLF,RAB6A,ROCK2,PKM,RAB11B,TUBA1B,SIRT6,RHOBTB1,PTK2,TUBB4B,DYRK2,MLH3,STK39,RAC1,MAP3K5,CYB5R3,CDC42BPB,RAB4A,RAB32,HDGF,CHD1L,GNAS,CMPK1,RHOBTB3,KATNAL1,ATP8A1,RAB37,PRKAR1A,ILK,GAPDH,NLK,KIF2A,PRKAR1B,RAB6C,CHD9,TNIK,RHOA,TLK1,SEPTIN7,SEPTIN11,NEK1,VDAC3,ARF1,UBE2J1,ETFA,RAB31,UBE2F,DDX6,SEPTIN2,SCYL2,HNRNPU,ABCC4,ACTB,ITM2B
33.	GO:0032555	Purine ribonucleotide binding	0.19	EIF2AK1,PYGL,NEK4,RAP1B,ACTR3B,MPP5,RAB11A,PIK3C3,RHEB,SRCAP,PRKAR2B,UBE2Q2,SMARCA5,RAB6B,RHOC,UBE2Q1,RAB8A,HIPK3,RAB6A,ROCK2,PKM,RAB11B,TUBA1B,RHOBTB1,PTK2,TUBB4B,DYRK2,MLH3,STK39,RAC1,MAP3K5,CDC42BPB,RAB4A,RAB32,CHD1L,GNAS,CMPK1,RHOBTB3,KATNAL1,ATP8A1,RAB37,PRKAR1A,ILK,NLK,KIF2A,PRKAR1B,RAB6C,CHD9,TNIK,RHOA,TLK1,SEPTIN7,SEPTIN11,NEK1,ARF1,UBE2J1,RAB31,UBE2F,DDX6,SEPTIN2,SCYL2,HNRNPU,ABCC4,ACTB,ITM2B
34.	GO:0003925	G protein activity	0.83	RAP1B,RAB11A,RAB11B,RAC1,RAB4A,RHOA

Table 7: Ontology Analysis of DEGs Associated with PDAC - (Cellular Components - CC).

#	#Term ID	Term Description (Cellular Components – CC) – Top 30	Strength	Matching Proteins In Your Network (Labels)
1.	GO:0035692	Macrophage migration inhibitory factor receptor complex	1.66	CD74,CD44
2.	GO:0005862	Muscle thin filament tropomyosin	1.53	TPM1,TPM4,TPM3
3.	GO:0005750	Mitochondrial respiratory chain complex III	1.39	UQCRH,UQCR10,MT-CO1,MT-CYB,UQCRQ,UQCRB,UQCR11
4.	GO:0097413	Lewy body	1.29	FBXO7,ATF4,SQSTM1
5.	GO:0005747	Mitochondrial respiratory chain complex I	1.26	NDUFB4,NDUFB11,NDUFC2,NDUFA4,NDUFV3,MT-ND6,MT-ND1,MT-ND4L,MT-ND5,MT-ND4,MT-ND2,MT-ND3,NDUFA1,NDUFB6,NDUFA11,NDUFA3,NDUFB2,NDUFC1,NDUFA6,NDUFB1
6.	GO:0098803	Respiratory chain complex	1.16	NDUFB4,NDUFB11,NDUFC2,UQCRH,UQCR10,NDUFA4,NDUFV3,MT-CO1,MT-CYB,MT-ND6,MT-ND1,MT-ND4L,MT-ND5,MT-CO2,MT-ND4,MT-CO3,MT-ND2,MT-ND3,NDUFA1,UQCRQ,NDUFB6,NDUFA11,NDUFA3,NDUFB2,UQCRB,NDUFC1,UQCR11,NDUFA6,NDUFB1
7.	GO:0005746	Mitochondrial respirasome	1.15	NDUFB4,NDUFB11,NDUFC2,UQCRH,UQCR10,NDUFA4,NDUFV3,MT-CO1,MT-CYB,MT-ND6,MT-ND1,MT-ND4L,MT-ND5,MT-CO2,MT-ND4,MT-CO3,MT-ND2,MT-ND3,NDUFA1,UQCRQ,NDUFB6,NDUFA11,NDUFA3,NDUFB2,UQCRB,NDUFC1,UQCR11,NDUFA6,NDUFB1
8.	GO:0005952	cAMP-dependent protein kinase complex	1.13	PRKAR2B,PRKAR1A,PRKAR1B
9.	GO:0005885	Arp2/3 protein complex	1.09	ARPC4-TTLL3,ARPC4,ARPC1B
10.	GO:0070069	Cytochrome complex	1.05	UQCRH,UQCR10,NDUFA4,MT-CO1,MT-CYB,MT-CO2,MT-CO3,UQCRQ,UQCRB,UQCR11

#	#Term ID	Term Description (Cellular Components – CC) – Top 30	Strength	Matching Proteins In Your Network (Labels)
11.	GO:1990204	Oxidoreductase complex	1.04	NDUFB4,NDUFB11,NDUFC2,UQCRH,UQCR10,NDUFA4,NDUFV3,RAC1,CYB5R3,MT-CO1,MT-CYB,MT-ND6,MT-ND1,MT-ND4L,MT-ND5,MT-ND4,MT-ND2,MT-ND3,NDUFA1,UQCRQ,NDUFB6,NDUFA11,NDUFA3,NDUFB2,UQCRB,NDUFC1,ETFA,UQCR11,NDUFA6,NDUFB1
12.	GO:0031093	Platelet alpha granule lumen	1.04	TIMP1,SPARC,HRG,SRGN,F13A1,APP,ALB,PPBP,PF4,FGB,CLU,PDGFA,TMSB4X,VTI1B,ALDOA,FGA
13.	GO:0002102	Podosome	1.01	PTPN12,GSN,CTTN,WDR1,ASAP1,TPM4,BIN2
14.	GO:0098800	Inner mitochondrial membrane protein complex	0.96	NDUFB4,NDUFB11,NDUFC2,UQCRH,UQCR10,NDUFA4,NDUFV3,MT-CO1,MT-CYB,MT-ATP6,MT-ND6,MT-ND1,MT-ND4L,MT-ND5,MT-CO2,MT-ND4,MT-CO3,MT-ND2,MT-ND3,MT-ATP8,NDUFA1,MCU,UQCRQ,NDUFB6,NDUFA11,NDUFA3,NDUFB2,UQCRB,NDUFC1,UQCR11,NDUFA6,NDUFB1
15.	GO:0031091	Platelet alpha granule	0.94	TIMP1,SPARC,HRG,SRGN,VAMP7,F13A1,APP,ALB,PPBP,PF4,FGB,CLU,PDGFA,TMSB4X,VTI1B,ALDOA,FGA
16.	GO:0042641	Actomyosin	0.91	MYL9,PTK2,TPM1,CDC42BPB,PDLIM1,DBN1,DAAM1,SEPTIN7,SEPTIN11,ABLIM3,MYL12B,TPM4,TPM3
17.	GO:0001725	Stress fiber	0.88	MYL9,PTK2,TPM1,PDLIM1,DAAM1,SEPTIN7,SEPTIN11,ABLIM3,MYL12B,TPM4,TPM3
18.	GO:0005790	Smooth endoplasmic reticulum	0.88	PGRMC1,APP,SVIP,DNAJC3,SLMAP
19.	GO:0005751	Mitochondrial respiratory chain complex IV	0.88	NDUFA4,MT-CO1,MT-CO2,MT-CO3
20.	GO:0042611	MHC protein complex	0.88	CD74,HLA-E,HLA-DRA,B2M
21.	GO:0030863	Cortical cytoskeleton	0.82	DSTN,MYZAP,CALD1,CAPZA2,KRT19,MPP1,CAP1,GSN,CTTN,DBN1,CAPZB,WDR1,TPM4,ACTB,RDX

#	#Term ID	Term Description (Cellular Components – CC) – Top 30	Strength	Matching Proteins In Your Network (Labels)
22.	GO:0030670	Phagocytic vesicle membrane	0.82	VAMP3,SNAP23,PIK3C3,VAMP7,PIP4P2,RAB8A,RAB11B,RAB32,HLA-E,RAB31,B2M
23.	GO:0030864	Cortical actin cytoskeleton	0.79	DSTN,MYZAP,CALD1,KRT19,CAP1,GSN,CTTN,DBN1,WDR1,RDX
24.	GO:0032154	Cleavage furrow	0.79	RAB11A,RHOC,ITGB1,RHOA,SEPTIN7,SEPTIN2,RDX
25.	GO:0035577	Azurophil granule membrane	0.75	RAP1B,VAMP7,LAMTOR1,NDUFC2,VAPA,ATP8A1,RAB37
26.	GO:0032153	Cell division site	0.71	RAB11A,RHOC,ITGB1,RHOA,SEPTIN7,SEPTIN11,SEPTIN2,RDX
27.	GO:0098798	Mitochondrial protein-containing complex	0.7	NDUFB4,NDUFB11,NDUFC2,UQCRH,HADHB,UQCR10,NDUFA4,NDUFV3,MT-CO1,MT-CYB,MT-ATP6,MT-ND6,MT-ND1,MT-ND4L,MT-ND5,MT-CO2,MT-ND4,MT-CO3,MT-ND2,MT-ND3,MT-ATP8,NDUFA1,MCU,UQCRQ,NDUFB6,NDUFA11,NDUFA3,NDUFB2,UQCRB,NDUFC1,UQCR11,NDUFA6,NDUFB1
28.	GO:1904724	Tertiary granule lumen	0.69	FTH1,PPBP,YPEL5,ASAH1,ALDOA,B2M
29.	GO:0000786	Nucleosome	0.68	H3-3B,SRCAP,H2BC5,MORF4L1,H1-0,H2BC12,H3C12,H2BC21,H2AC6,H2AJ,MBTD1,H2BC11,H2BC9,ACTB
30.	GO:0035692	Macrophage migration inhibitory factor receptor complex	1.66	CD74,CD44

Table 8: KEGG Pathways Analysis of DEGs Associated with PDAC.

#	#term ID	term description (KEGG Pathway)	Strength	matching proteins in your network (labels)
1.	hsa05012	Parkinson disease	0.89	NDUFB4,NDUFC2,CALM3,UQCRH,UQCR10,ATF4,TUBA1B,NDUFA4,PARK7,TUBB4B,NDUFV3,MAP3K5,MT-CO1,MT-CYB,MT-ATP6,MT-ND6,MT-ND1,MT-ND4L,MT-ND5,MT-CO2,MT-ND4,MT-CO3,MT-ND2,MT-ND3,MT-

#	#term ID	term description (KEGG Pathway)	Strength	matching proteins in your network (labels)
				ATP8,GNAS,NDUFA1,MCU,UQCRQ,NDUFB6,NDUFA11,NDUFA3,NDUFB2,VDAC3,UQCRB,NDUFC1,UBE2J1,UQCR11,NDUFA6,NDUFB1
2.	hsa00190	Oxidative phosphorylation	1.03	NDUFB4,NDUFC2,UQCRH,UQCR10,NDUFA4,NDUFV3,MT-CO1,MT-CYB,MT-ATP6,MT-ND6,MT-ND1,MT-ND4L,MT-ND5,MT-CO2,MT-ND4,MT-CO3,MT-ND2,MT-ND3,MT-ATP8,NDUFA1,UQCRQ,NDUFB6,NDUFA11,NDUFA3,NDUFB2,UQCRB,NDUFC1,UQCR11,NDUFA6,NDUFB1
3.	hsa04714	Thermogenesis	0.85	NDUFB4,RHEB,NDUFC2,UQCRH,UQCR10,SIRT6,NDUFA4,NDUFV3,MAP3K5,MT-CO1,MT-CYB,MT-ATP6,MT-ND6,MT-ND1,MT-ND4L,MT-ND5,MT-CO2,MT-ND4,MT-CO3,MT-ND2,MT-ND3,MT-ATP8,GNAS,NDUFA1,UQCRQ,NDUFB6,NDUFA11,NDUFA3,NDUFB2,UQCRB,NDUFC1,UQCR11,NDUFA6,NDUFB1,ACTB
4.	hsa05010	Alzheimer disease	0.72	NDUFB4,LRP1,PIK3C3,NDUFC2,APP,CALM3,UQCRH,UQCR10,ATF4,TUBA1B,NDUFA4,TUBB4B,NDUFV3,MAP3K5,MT-CO1,MT-CYB,MT-ATP6,MT-ND6,MT-ND1,MT-ND4L,MT-ND5,MT-CO2,MT-ND4,MT-CO3,MT-ND2,MT-ND3,MT-ATP8,NDUFA1,MCU,UQCRQ,NDUFB6,GAPDH,NDUFA11,NDUFA3,NDUFB2,VDAC3,UQCRB,NDUFC1,UQCR11,NDUFA6,NDUFB1
5.	hsa05014	Amyotrophic lateral sclerosis	0.72	NDUFB4,PIK3C3,NDUFC2,RAB8A,UQCRH,UQCR10,ATF4,TUBA1B,NDUFA4,TUBB4B,NDUFV3,MAP3K5,MT-CO1,MT-CYB,MT-ATP6,MT-ND6,MT-ND1,MT-ND4L,MT-ND5,MT-CO2,MT-ND4,MT-CO3,MT-ND2,MT-ND3,MT-ATP8,NDUFA1,MCU,UQCRQ,NDUFB6,SQSTM1,NDUFA11,VAPB,NDUFA3,NDUFB2,UQCRB,NDUFC1,ATXN2,UQCR11,NDUFA6,NDUFB1,ACTB
6.	hsa05020	Prion disease	0.79	NDUFB4,NDUFC2,UQCRH,UQCR10,ATF4,TUBA1B,NDUFA4,TUBB4B,NDUFV3,MT-CO1,MT-CYB,MT-ATP6,MT-ND6,MT-ND1,MT-ND4L,MT-ND5,MT-CO2,MT-ND4,MT-CO3,MT-ND2,MT-ND3,MT-ATP8,NDUFA1,MCU,UQCRQ,NDUFB6,NDUFA11,NDUFA3,NDUFB2,VDAC3,UQCRB,NDUFC1,UQCR11,CCL5,NDUFA6,NDUFB1
7.	hsa05016	Huntington disease	0.74	NDUFB4,PIK3C3,NDUFC2,UQCRH,UQCR10,TUBA1B,NDUFA4,TUBB4B,NDUFV3,MAP3K5,MT-CO1,MT-CYB,MT-ATP6,MT-ND6,MT-ND1,MT-ND4L,MT-ND5,MT-CO2,MT-ND4,MT-CO3,MT-ND2,MT-ND3,MT-

#	#term ID	term description (KEGG Pathway)	Strength	matching proteins in your network (labels)
				ATP8,NDUFA1,UQCRQ,NDUFB6,NDUFA11,NDUFA3,NDUFB2,VDAC3,UQCRB,NDUFC1,SOD2,UQCR11,NDUFA6,NDUFB1
8.	hsa04932	Non-alcoholic fatty liver disease	0.85	NDUFB4,NDUFC2,UQCRH,UQCR10,ATF4,NDUFA4,NDUFV3,MAP3K5,MT-CO1,MT-CYB,MT-CO2,MT-CO3,NDUFA1,UQCRQ,NDUFB6,NDUFA11,NDUFA3,NDUFB2,UQCRB,NDUFC1,UQCR11,NDUFA6,NDUFB1
9.	hsa04723	Retrograde endocannabinoid signaling	0.8	NDUFB4,GNG11,NDUFC2,NDUFA4,NDUFV3,MT-ND6,MT-ND1,MT-ND4L,MT-ND5,MT-ND4,MT-ND2,MT-ND3,NDUFA1,NDUFB6,NDUFA11,NDUFA3,NDUFB2,NDUFC1,NDUFA6,NDUFB1
10.	hsa04260	Cardiac muscle contraction	0.83	UQCRH,UQCR10,TPM1,MT-CO1,MT-CYB,MT-CO2,MT-CO3,UQCRQ,ASPH,UQCRB,UQCR11,TPM4,TPM3
11.	hsa05131	Shigellosis	0.62	H3-3B,PIK3C3,MYL9,ROCK2,PTK2,H3C12,DIAPH1,SQSTM1,ITGB1,ILK,ARPC4,ARPC1B,CD44,RHOA,SEPTIN11,ARF1,MYL12B,CCL5,SEPTIN2,ACTB
12.	hsa04810	Regulation of actin cytoskeleton	0.61	MYL9,ROCK2,PTK2,PDGFA,NCKAP1,GSN,TMSB4X,DIAPH1,ITGB1,ITGA4,ARHGEF12,ARPC4,ARPC1B,RHOA,BRK1,CFL1,MYL12B,ACTB,RDX
13.	hsa05100	Bacterial invasion of epithelial cells	0.85	CTNNA1,ARHGAP10,PTK2,ITGB1,ILK,ARPC4,ARPC1B,RHOA,SEPTIN11,SEPTIN2,ACTB
14.	hsa04670	Leukocyte transendothelial migration	0.72	RAP1B,ESAM,MYL9,JAM3,CTNNA1,ROCK2,PTK2,CD99,ITGB1,ITGA4,RHOA,MYL12B,ACTB
15.	hsa04530	Tight junction	0.64	ACTR3B,MPP5,MYL9,JAM3,RAB8A,ROCK2,TUBA1B,MAP3K5,PARD3,ITGB1,RHOA,MYL6,MYL12B,ACTB,RDX
16.	hsa04611	Platelet activation	0.68	SNAP23,RAP1B,FCER1G,FGB,ROCK2,GNAS,ITGB1,ARHGEF12,GP1BB,RHOA,MYL12B,ACTB,FGA
17.	hsa05203	Viral carcinogenesis	0.6	YWHAH,YWHAE,H2BC5,PKM,ATF4,H2BC12,H2BC21,GSN,HLA-E,IL6ST,YWHAQ,YWHAZ,RHOA,VDAC3,H2BC11,H2BC9
18.	hsa05132	Salmonella infection	0.57	PIK3C3,MYL9,ROCK2,TCF7,DYNLRB1,NCKAP1,AHNAK,DYNLL1,GAPDH,ARPC4,ARPC1B,RHOA,PTPRC,BRK1,ARF1,MYL12B,ACTB

#	#term ID	term description (KEGG Pathway)	Strength	matching proteins in your network (labels)
19.	hsa05034	Alcoholism	0.61	GNG11,H3-3B,H2BC5,CALM3,ATF4,H2BC12,H3C12,H2BC21,GNAS,H2AC6,H2AJ,H2BC11,H2BC9
20.	hsa04144	Endocytosis	0.5	RAB11A,SMAD2,ASAP2,RAB8A,DAB2,RUFY1,RAB11B,CAPZA2,RAB4A,PARD3,HLA-E,ARPC4,ARPC1B,RHOA,ASAP1,ARF1,RAB31
21.	hsa05322	Systemic lupus erythematosus	0.68	H3-3B,H2BC5,H2BC12,H3C12,H2BC21,H2AC6,HLA-DRA,H2AJ,H2BC11,H2BC9
22.	hsa05130	Pathogenic Escherichia coli infection	0.53	NCK2,ROCK2,TUBA1B,TUBB4B,NCKAP1,ITGB1,GAPDH,ARHGEF12,ARPC4,ARPC1B,RHOA,BRK1,ARF1,ACTB
23.	hsa01100	Metabolic pathways	0.22	NDUFB4,PYGL,ODC1,MAN2A1,ARG2,PIK3C3,PRUNE1,NDUFC2,UXS1,CA2,UQCRH,EZH2,PKM,TALDO1,HADHB,UQCR10,SIRT6,MGAT4B,NDUFA4,GPX4,NDUFV3,MAN1A2,FUT8,MT-CO1,MT-CYB,MT-ATP6,MT-ND6,MT-ND1,MT-ND4L,MT-ND5,MT-CO2,MT-ND4,MT-CO3,MT-ND2,MT-ND3,MT-ATP8,NDUFA1,UQCRQ,PCYT1B,ASAH1,AGPAT1,GAPDH,SMS,NDUFA11,DERA,NDUFA3,NDUFB2,UQCRB,NDUFC1,UQCR11,NDUFA6,NDUFB1,ALDOA
24.	hsa04360	Axon guidance	0.52	NCK2,RASA1,MYL9,ROCK2,PTK2,PARD3,ITGB1,ILK,ARHGEF12,RHOA,ABLIM3,CFL1,MYL12B
25.	hsa04520	Adherens junction	0.66	CTNNA1,SSX2IP,TCF7,PARD3,NLK,RHOA,ACTB
26.	hsa05163	Human cytomegalovirus infection	0.43	IL10RA,GNG11,RHEB,CALM3,ROCK2,ATF4,PTK2,GNAS,HLA-E,ARHGEF12,RHOA,CCL5,B2M
27.	hsa05414	Dilated cardiomyopathy	0.59	TPM1,LMNA,GNAS,ITGB1,ITGA4,TPM4,ACTB,TPM3
28.	hsa04510	Focal adhesion	0.45	RAP1B,MYL9,ROCK2,PTK2,PDGFA,DIAPH1,ITGB1,ILK,ITGA4,RHOA,MYL12B,ACTB
29.	hsa05135	Yersinia infection	0.52	SKAP2,ACTR3B,ROCK2,PTK2,ITGB1,ITGA4,ARHGEF12,RHOA,ACTB
30.	hsa04390	Hippo signaling pathway	0.47	YWHAH,MPP5,SMAD2,YWHAE,CTNNA1,TCF7,PARD3,YWHAQ,YWHAZ,ACTB
31.	hsa04270	Vascular smooth muscle contraction	0.49	MYL9,CALM3,PPP1R14A,ROCK2,CALD1,GNAS,ARHGEF12,RHOA,MYL6
32.	hsa04962	Vasopressin-regulated water reabsorption	0.72	ARHGDIB,RAB11A,RAB11B,GNAS,DYNLL1
33.	hsa04514	Cell adhesion molecules	0.47	ESAM,JAM3,HLA-E,CD99,HLA-DRA,ITGB1,ITGA4,PTPRC,CD226
34.	hsa04722	Neurotrophin signaling pathway	0.51	ARHGDIB,RAP1B,YWHAE,CALM3,ATF4,MAP3K5,BEX3,RHOA
35.	hsa05410	Hypertrophic cardiomyopathy	0.56	TPM1,LMNA,ITGB1,ITGA4,TPM4,ACTB,TPM3
36.	hsa04640	Hematopoietic cell lineage	0.55	IL9R,IL7R,CD37,HLA-DRA,ITGA4,GP1BB,CD44

#	#term ID	term description (KEGG Pathway)	Strength	matching proteins in your network (labels)
37.	hsa04666	Fc gamma R-mediated phagocytosis	0.55	ASAP2,GSN,ARPC4,ARPC1B,PTPRC,ASAP1,CFL1

Table 9: Disease-Gene Analysis of DEGs Associated with PDAC.

#	#term ID	Term Description (Disease-Gene association)	Strength	matching proteins in your network (labels)
1.	DOID:705	Leber hereditary optic neuropathy	1.58	MT-CO1,MT-CYB,MT-ATP6,MT-ND6,MT-ND1,MT-ND4L,MT-ND5,MT-ND4,MT-CO3,MT-ND2
2.	DOID:0060536	Mitochondrial complex I deficiency	1.05	NDUFB11,NDUFV3,MT-ND6,MT-ND1,MT-ND4L,MT-ND5,MT-ND4,MT-ND2,MT-ND3,NDUFA1,NDUFA11
3.	DOID:700	Mitochondrial metabolism disease	0.67	NDUFB11,NDUFA4,NDUFV3,MT-CO1,MT-CYB,MT-ATP6,MT-ND6,MT-ND1,MT-ND4L,MT-ND5,MT-CO2,MT-ND4,MT-CO3,MT-ND2,MT-ND3,NDUFA1,MTFR1L,UQCRQ,NDUFA11,UQCRB
4.	DOID:3652	Leigh disease	0.88	NDUFA4,MT-ATP6,MT-ND6,MT-ND1,MT-ND5,MT-ND4,MT-CO3,MT-ND2,MT-ND3,NDUFA1,UQCRQ,NDUFA11
5.	DOID:162	Cancer	0.35	H3-3B,BARD1,EHBP1,YWHAE,CEP70,RASA1,NPTN,ALB,RAB8A,CTNNA1,CAMTA1,DAB2,SUZ12,EZH2,KRT7,RAB11B,FIP1L1,SIRT6,TTC33,PARK7,TRIM24,GFI1B,RAC1,H3C12,CALD1,KRT19,GNAS,CD99,KRT18,SQSTM1,PRKAR1A,GAPDH,ARHGEF12,ANKRD28,MITF,TSC22D1,RHOA,MTRNR2L8,KRT8,TXNIP,DDX6,SEPTIN2,TPM4,ACTB,TRIM66,B2M,TPM3,DEK
6.	DOID:9120	Amyloidosis	0.82	APP,ALB,CLU,MT-ND1,MT-ND2,GSN,DBN1,ACTB,ITM2B,B2M,FGA
7.	DOID:14566	Disease of cellular proliferation	0.3	H3-3B,BARD1,EHBP1,YWHAE,CEP70,RASA1,NPTN,ALB,RAB8A,CTNNA1,CAMTA1,DAB2,SUZ12,EZH2,KRT7,RAB11B,FIP1L1,SIRT6,TTC33,PARK7,TRIM24,GFI1B,RAC1,H3C12,CALD1,KRT19,GNAS,CD99,KRT18,SQSTM1,PRKAR1A,GAPDH,ARHGEF12,ANKRD28,MITF,TSC22D1,RHOA,TNRC6B,MTRNR2L8,KRT8,TXNIP,DDX6,SEPTIN2,TPM4,ACTB,TRIM66,B2M,TPM3,DEK

#	#term ID	Term Description (Disease-Gene association)	Strength	matching proteins in your network (labels)
8.	DOID:655	Inherited metabolic disorder	0.32	PYGL,H3-3B,ARG2,NDUFB11,APP,ALB,DAB2,PHKB,CLU,HADHB,NDUFA4,NDUFV3,H3C12,FUT8,MT-CO1,MT-CYB,MT-ATP6,MT-ND6,MT-ND1,MT-ND4L,MT-ND5,MT-CO2,MT-ND4,MT-CO3,MT-ND2,MT-ND3,GNAS,NDUFA1,CTSA,GSN,MTFR1L,UQCRQ,TMEM165,ASAH1,NDUFA11,UQCRB,CALU,ETFA,DNAJC3,ACTB,ALDOA,ITM2B,B2M,FGA
9.	DOID:3687	MELAS syndrome	1.66	MT-ND6,MT-ND1,MT-ND5,MT-ND4
10.	DOID:5656	Cranial nerve disease	0.72	MT-CO1,MT-CYB,MT-ATP6,MT-ND6,MT-ND1,MT-ND4L,MT-ND5,MT-ND4,MT-CO3,MT-ND2,CD99
11.	DOID:0014667	Disease of metabolism	0.28	PYGL,H3-3B,ARG2,NDUFB11,APP,ALB,DAB2,PHKB,CLU,HADHB,NDUFA4,NDUFV3,H3C12,FUT8,MT-CO1,MT-CYB,MT-ATP6,MT-ND6,MT-ND1,MT-ND4L,MT-ND5,MT-CO2,MT-ND4,MT-CO3,MT-ND2,MT-ND3,GNAS,NDUFA1,CTSA,GSN,MTFR1L,UQCRQ,TMEM165,ASAH1,DBN1,NDUFA11,UQCRB,CALU,ETFA,DNAJC3,ACTB,ALDOA,ITM2B,B2M,FGA
12.	DOID:1247	Blood coagulation disease	0.71	PF4V1,HRG,F13A1,FCER1G,PF4,FGB,GFI1B,GP1BB,ANO6,FGA
13.	DOID:0050686	Organ system cancer	0.31	H3-3B,BARD1,EHBP1,YWHAE,CEP70,RASA1,NPTN,ALB,CTNNA1,CAMTA1,SUZ12,EZH2,KRT7,RAB11B,FIP1L1,TTC33,RAC1,CALD1,KRT19,GNAS,CD99,KRT18,SQSTM1,PRKAR1A,GAPDH,ANKRD28,MITF,TSC22D1,MTRNR2L8,KRT8,SEPTIN2,ACTB,TRIM66,B2M
14.	DOID:176	Cardiovascular cancer	1.05	CAMTA1,CALD1,CD99,PRKAR1A,MITF

5. PPI Network Module Analysis & Hub Genes Selection

The **CytoHubba** plugin was employed to calculate connectivity scores and determine the common genes among the top 25 genes with a combination of four algorithms (Maximal Clique Centrality - MCC, Degree, Stress, and Radiality), (Chin et al., 2014b). Table 10, Figure 11.

Table 10: The Top 25 Hub Genes Rank in CytoHubba by 4 Different Methods.

MCC	Degree	Radiality	Stress
UQCR11	ACTB	TMSB4X	CD74
H3-3B	NDUFA6	DIAPH1	H3-3B
H2AC6	H2BC11	ACTB	RAB11A
SMARCA5	RHOA	PTK2	APP
MT-ND6	CD44	CD44	ALB
H2BC21	ITGB1	ARHGAP10	RAB8A
UQCRH	H2AC6	RDX	CTNNA1
MT-CO3	H2BC21	H3-3B	PTK2
MT-CO1	MT-ATP8	CFL1	H3C12
SUZ12	MT-ND3	GAPDH	H2BC21
MT-ND2	MT-ND2	H2BC21	CTTN
MT-ND4L	MT-CO3	ITGB1	SQSTM1
NDUFA6	MT-ND4	ILK	YWHAZ
MT-ND4	MT-CO2	CAPZB	ITGB1
MT-CO2	MT-ND5	ARHGEF12	GAPDH
MT-ND1	MT-ND4L	ARPC4	CD44
MT-CYB	MT-ND1	RHOA	RHOA
MT-ND5	MT-ND6	MYL12B	CAPZB
MT-ND3	MT-ATP6	MYL9	ASAP1
MT-ATP8	MT-CYB	ITGA4	BRK1
EZH2	MT-CO1	CTNNA1	CFL1
MT-ATP6	H3C12	ARPC1B	H2BC11
H2BC11	H2BC12	H3C12	RSRC1
H3C12	UQCRH	MYL6	ACTB
H2BC12	H3-3B	ACTR3B	RDX

All 4 methods identified 3 common central hub genes among the top 25 hub genes: H3-3B, H2BC21, H3C12. On the other hand, 5 genes (ACTB, RHOA, CD44, ITGB1, H2BC11) were identified by 3 of the 4 algorithms, whereas there are 6 common elements between "Stress" and "Radiality" (CTNNA1, PTK2, GAPDH, CAPZB, CFL1, RDX), while there are 17 common elements in "MCC" and "Degree": (H2AC6, MT-ND6, UQCRH, MT-CO3, MT-CO1, MT-ND2, MT-ND4L, NDUFA6, MT-ND4, MT-CO2, MT-ND1, MT-CYB, MT-ND5, MT-ND3, MT-ATP8, MT-ATP6, H2BC12) and only 1 common element in "Degree" and "Radiality" (ARPC1B) (Figure 12).

A total of 5 significant clusters were defined from the PPI network using the plugin **MCODE** with a criterion of selection as follows: degree cut-off = 2, node score cut-off = 0.2, k-score = 2, and Max depth = 100 (Table 11, figure 10).

Cluster	Score (Density*#Nodes)	Nodes	Edges	Node IDs
1	13.385	14	87	UQCRH, MT-ND3, MT-ND5, MT-ND1, MT-CYB, MT-CO2, MT-ND6, MT-ND4, MT-ND4L, MT-ND2, MT-CO1, MT-CO3, MT-ATP6, MT-ATP8
2	6.286	8	22	SMARCA5, SUZ12, H2BC12, H3-3B, BARD1, H2BC11, H3C12, EZH2
3	5	5	10	YWHAE, YWHAH, YWHAZ, CTNNA1, YWHAQ
4	4	4	6	H2BC9, H2BC21, H2AC6, H2BC5
5	4	4	6	ALDOA, TALDO1, GAPDH, PKM

Table 11: The Top 5 Clusters Identified by MCODE

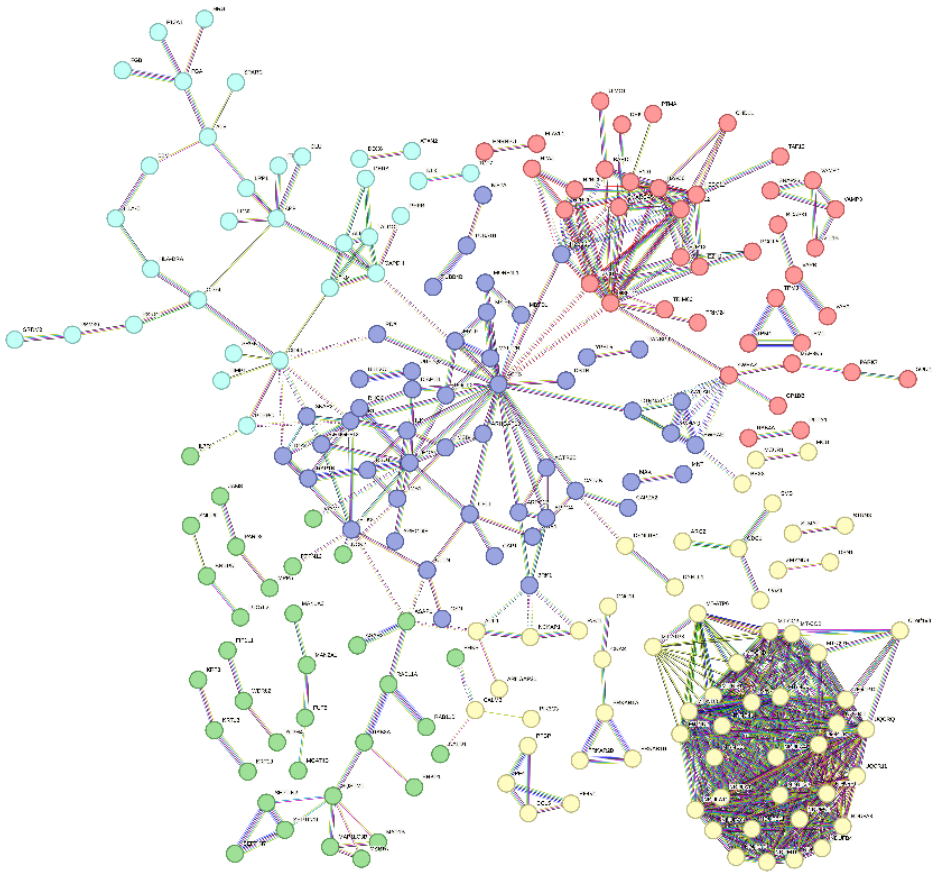

Figure 10: Top 5 Clusters (PPI) Network by STRING Database. using kmean absolute clustering technique.

A: STRING network_Stress_top25_and_expanded

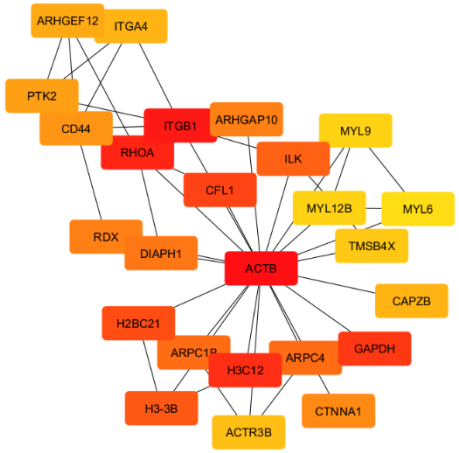

B: STRING network_Radiality_top25_and_expanded

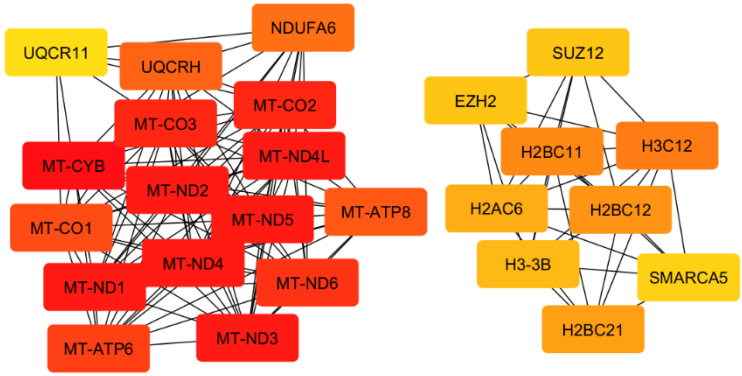

C: STRING network_MCC_top25_and_expanded

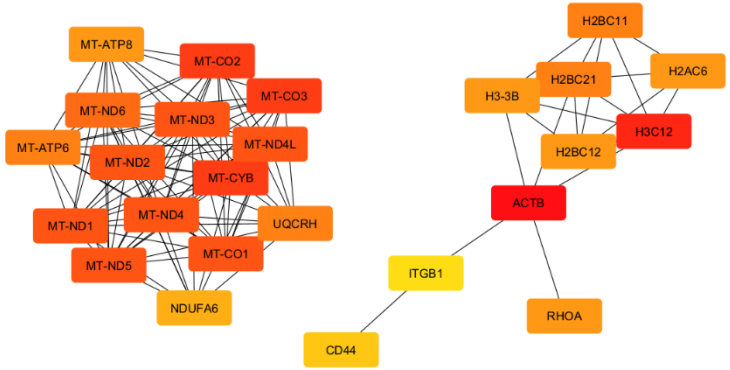

D: STRING network_Degree_top25_and_expanded

Figure 11: Hub Gene Networks Identified from the PPI Network Using.
(A) Stress Algorithm; (B) Radiality Algorithm; (C) MCC Algorithm; and (D) Degree Algorithm of the Cytoscape Plug-in CytoHubba

In order to confirm the representation of designated hub genes within the most highly significant modules, a thorough overlap analysis was performed. This comparison- conducted using Venny (2.1) - revealed the presence of eleven key genes. Thus, when crossing between hub genes identified between “CytoHubba” and “MCODE” 11 common elements: CTNNA1, EZH2, H2AC6, H2BC11, H2BC12, H2BC21, H3-3B, H3C12, SMARCA5, SUZ12, YWHAZ, constituting total of 14.1% (11 genes) Figure 13.

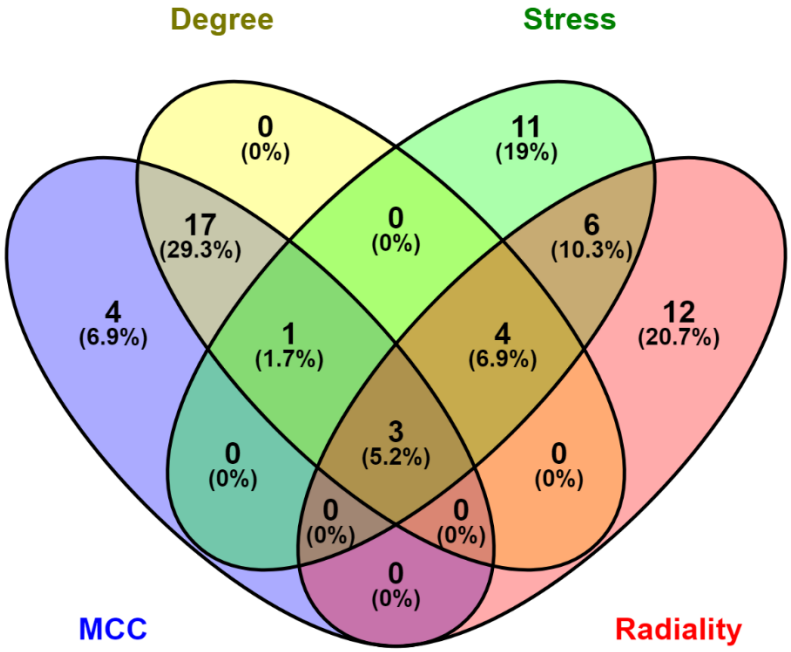

Figure 12: Venn Diagram of the Top 25 Genes in 4 Classification Methods of CytoHubba

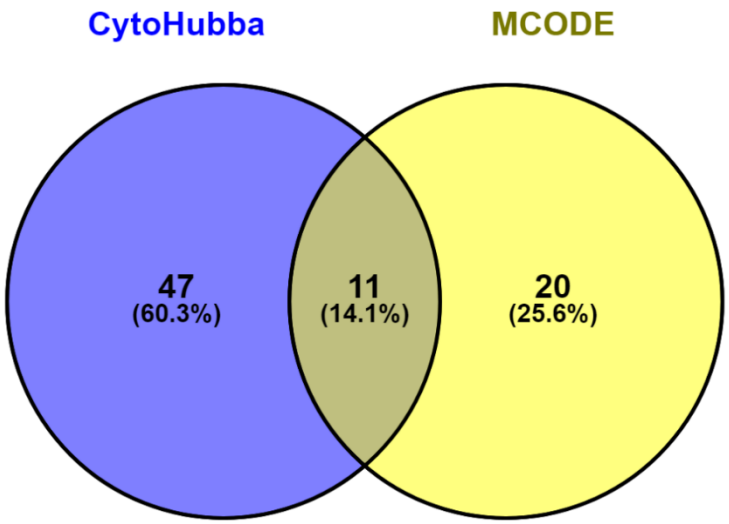

Figure 13: Top 3 clusters of the Hub Genes Identified through CytoHubba and MCODE.

6. Candidate Genes Enrichment and Pathway:

On the basis of the GO study and gene enrichment analysis with the KEGG pathway, it is clear that these hub genes regulate the different bioactivities as shown in **Table 8**. These bioactivities are concerned with different molecular functions (MF), biological processes (BP), as well as cellular components (CC). KEGG analysis revealed the involvement of the hub genes in different signaling pathways such as Lysine Degradation, ATP Dependent Chromatin remodeling, Polycomb repressive complex, Information based on the bioactivities and signaling pathways, the possible role of these hub genes in cancer regulation processes is shown in Figure 14.

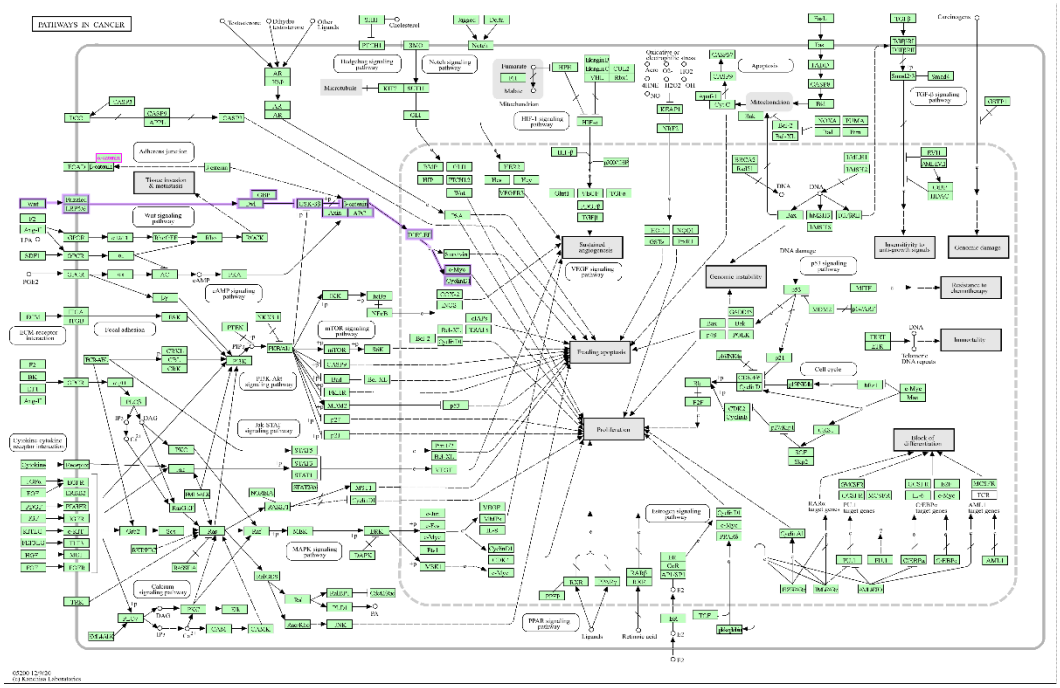

A: CTNNA1 Gene pathway

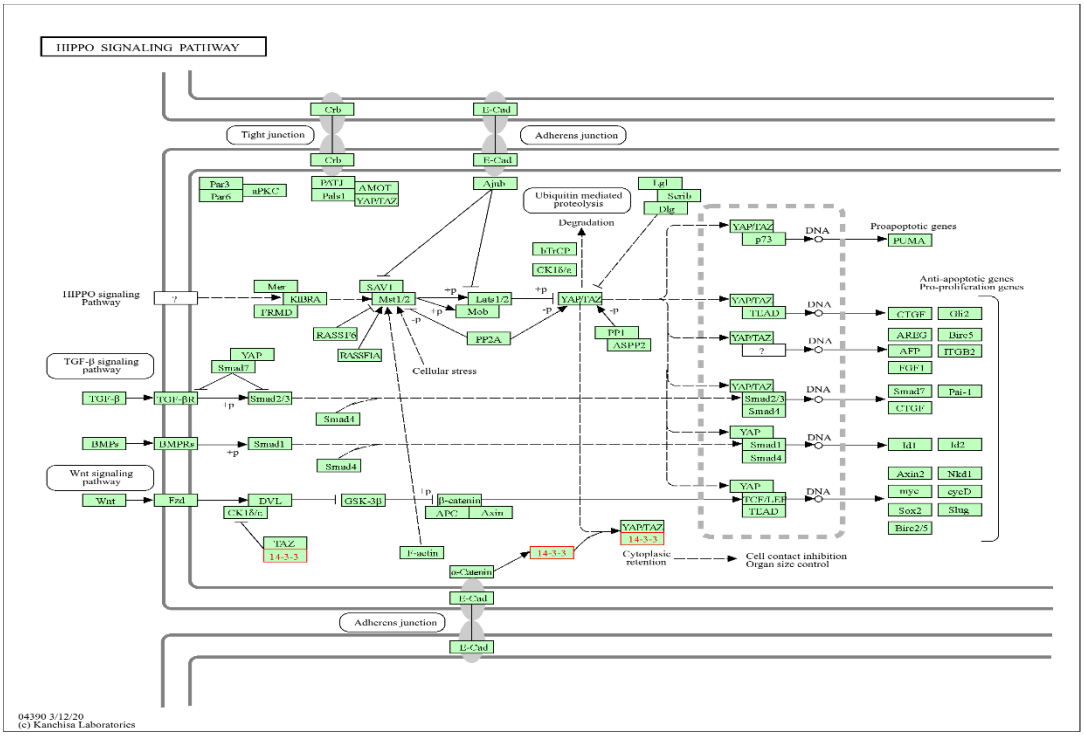

B: YWHAZ & CTNNA1 Gene pathway – HIPPO Signaling Pathway

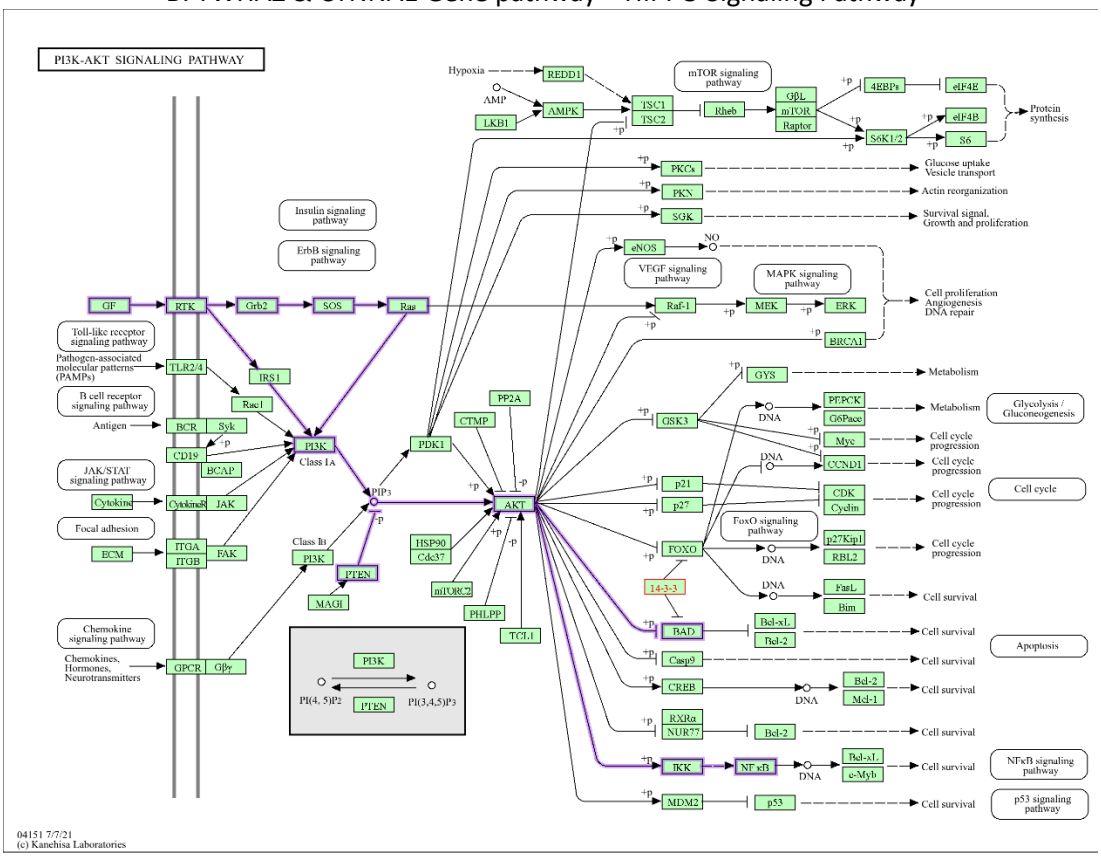

B: YWHAZ Gene pathway - PI3K-AKT signaling pathway

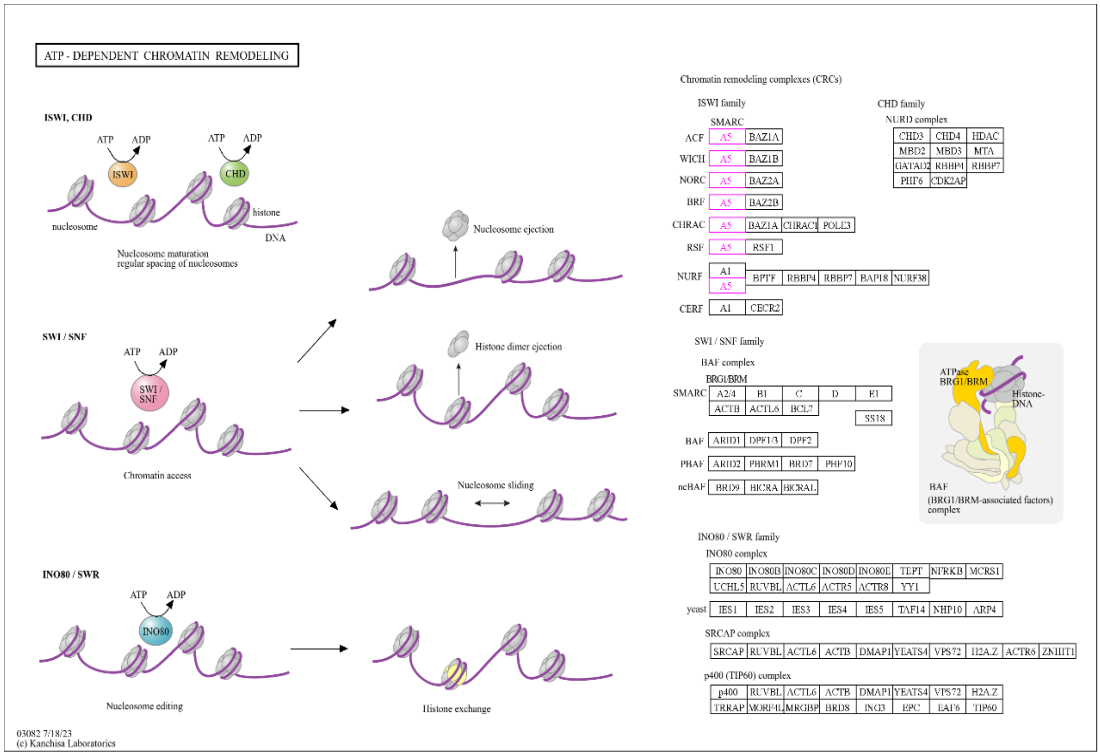

C: SMARCA5 & H2AC6 (H2AZ) Gene pathway

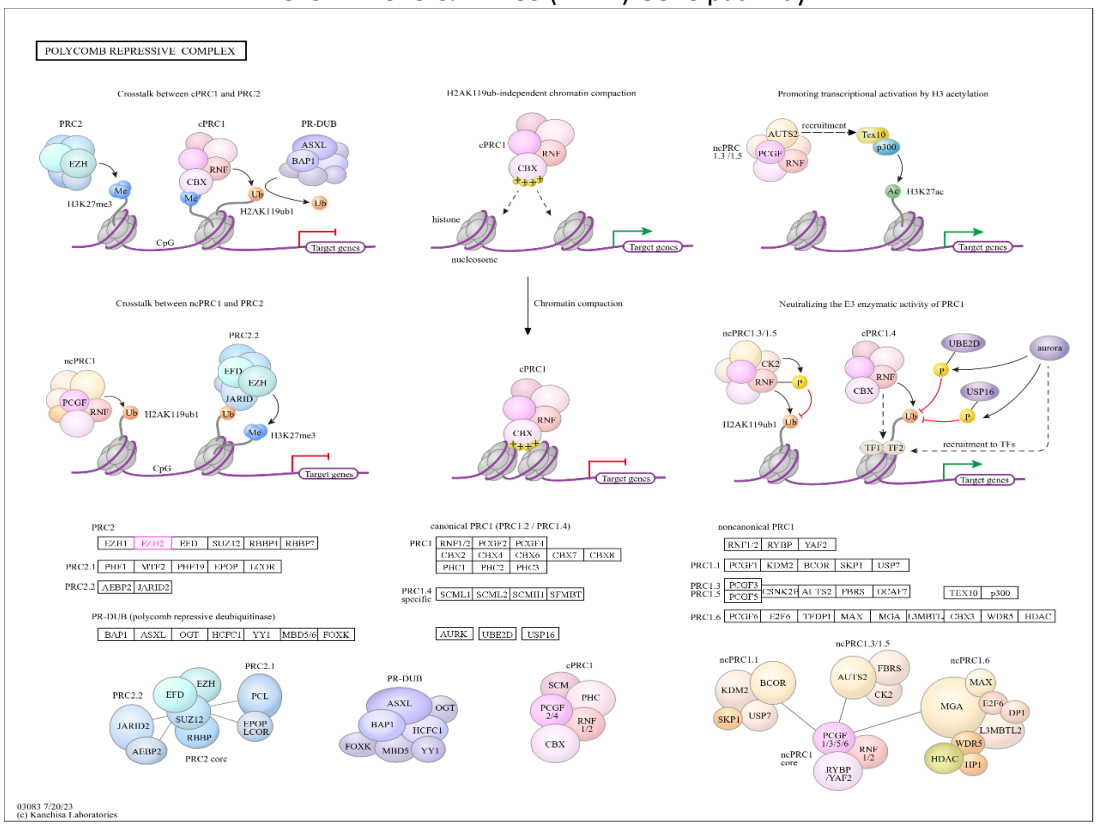

D: EZH2 Gene pathway

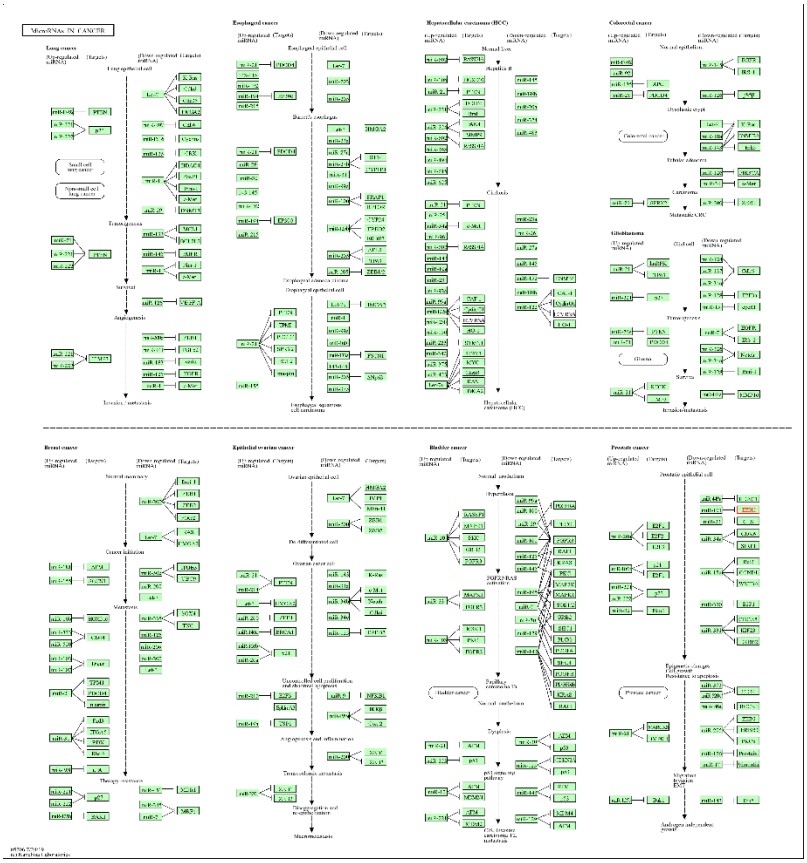

E: EZH2 Gene pathway

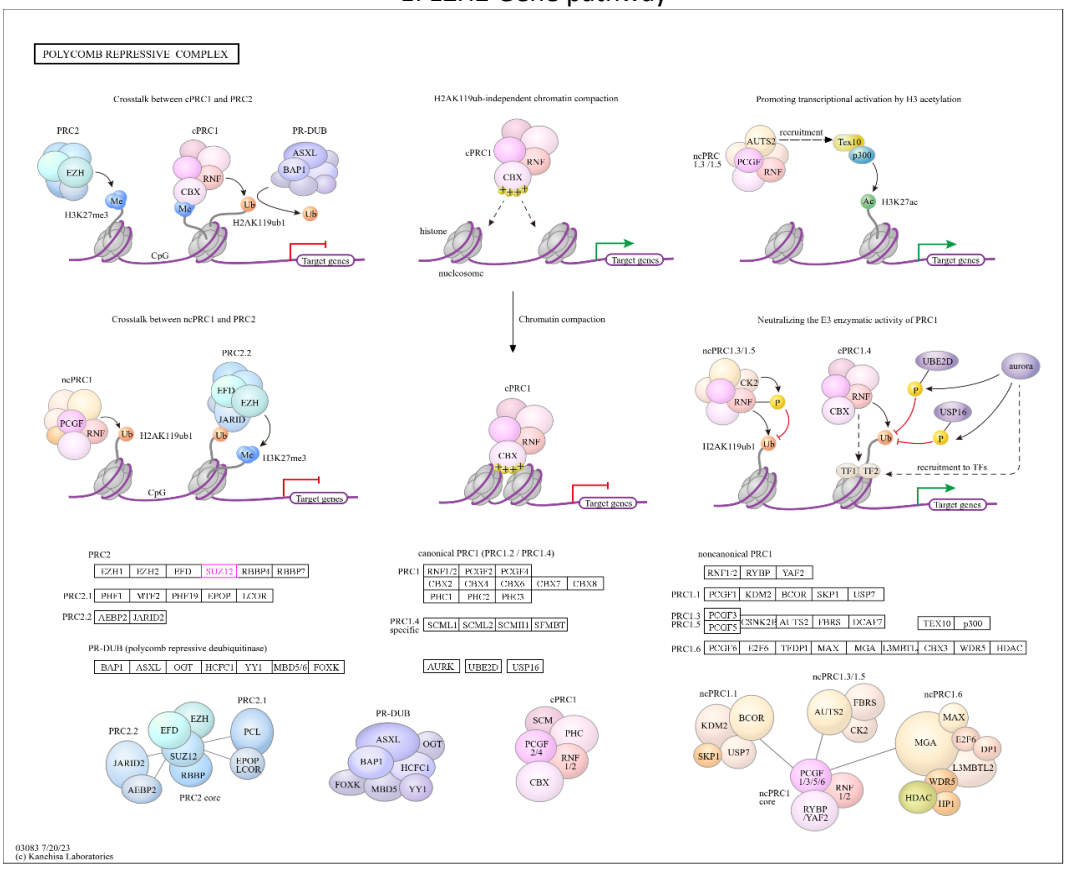

F: SUZ12 Gene pathway

Figure 14: The possible role of hub gene in the regulation of PDAC pathways (https://www.genome.jp/kegg).

Regarding SUZ12: Polycomb protein SUZ12; Polycomb group (PcG) protein. Component of the PRC2/EED-EZH2 complex, which methylates 'Lys-9' (H3K9me) and 'Lys-27' (H3K27me) of histone H3, leading to transcriptional repression of the affected target gene. The PRC2/EED-EZH2 complex may also serve as a recruiting platform for DNA methyltransferases, thereby linking two epigenetic repression systems. Genes repressed by the PRC2/EED-EZH2 complex include HOXC8, HOXA9, MYT1 and CDKN2A. Figure 14.F

On the other hand, CTNNA1 is Catenin alpha-1; Associates with the cytoplasmic domain of a variety of cadherins. The association of catenins to cadherins produces a complex which is linked to the actin filament network, and which seems to be of primary importance for cadherins cell-adhesion properties. Can associate with both E- and N-cadherins. Originally believed to be a stable component of E-cadherin/catenin adhesion complexes and to mediate the linkage of cadherins to the actin cytoskeleton at adherens junctions. Figure 14.A.

Regarding EZH2: Histone-lysine N-methyltransferase EZH2; Polycomb group (PcG) protein. Catalytic subunit of the PRC2/EED-EZH2 complex, which methylates 'Lys-9' (H3K9me) and 'Lys-27' (H3K27me) of histone H3, leading to transcriptional repression of the affected target gene. Able to mono-, di- and trimethylate 'Lys-27' of histone H3 to form H3K27me1, H3K27me2 and H3K27me3, respectively. Displays a preference for substrates with less methylation, loses activity when progressively more methyl groups are incorporated into H3K27, H3K27me0 > H3K27me1 > H3K27me2. Figure 14.E.D & Figure 14.E.

In the meanwhile, SMARCA5: SWI/SNF-related matrix-associated actin-dependent regulator of chromatin subfamily A member 5; Helicase that possesses intrinsic ATP-dependent nucleosome- remodeling activity. Complexes containing SMARCA5 are capable of forming ordered nucleosome arrays on chromatin; this may require intact histone H4 tails. Also required for replication of pericentric heterochromatin in S-phase specifically in conjunction with BAZ1A. Probably plays a role in repression of polI dependent transcription of the rDNA locus, through the recruitment of the SIN3/HDAC1 corepressor complex to the rDNA promoter. Figure 14.E.C

With regard to YWHAZ: Hippo signaling is an evolutionarily conserved signaling pathway that controls organ size from flies to humans. In humans and mice, the pathway consists of the MST1 and MST2 kinases, their cofactor Salvador and LATS1 and LATS2. In response to high cell densities, activated LATS1/2 phosphorylates the transcriptional coactivators YAP and TAZ, promoting its cytoplasmic localization, leading to cell apoptosis and restricting organ size overgrowth. When the Hippo pathway is inactivated at low cell density, YAP/TAZ translocates into the nucleus to bind to the transcription enhancer factor (TEAD/TEF) family of transcriptional factors to promote cell growth and proliferation. YAP/TAZ also interacts with other transcriptional factors or signaling molecules, by which Hippo pathway-mediated processes are interconnected with those of other key signaling cascades, such as those mediated by TGF-beta and Wnt growth factors. Figure 14.E.B

7. Verification and Survivability Assessment of Hub Genes:

An overall survival study of hub genes was carried out to describe the identification of prognostic variables in selected five hub genes for PDAC. The Kaplan–Meier plotter (Győrffy, 2024) and GEPIA2 analysis revealed highly significantly ($p > 0.05$) higher expressions of hub genes CTNNA1 and YWHAZ in patients with PDAC of early stages. On the hand, the SMARCA5 hub gene displayed significantly ($p < 0.05$) lower expression, as confirmed during GEPIA2 and Kaplan–Meier Plotter analysis, in patients suffering with PDAC (Fig. 4).

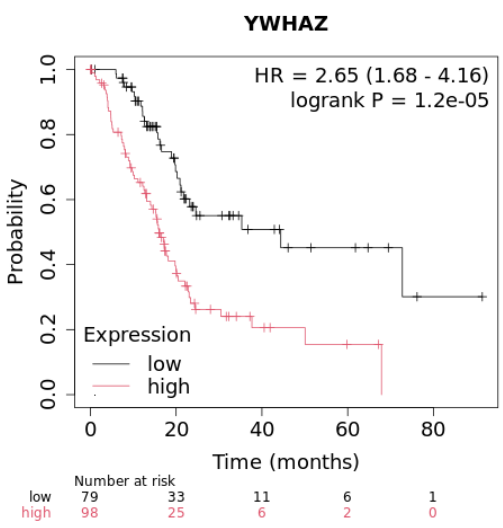

A1

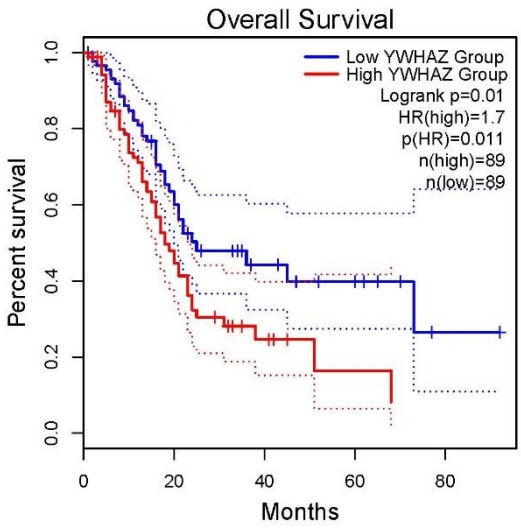

A2

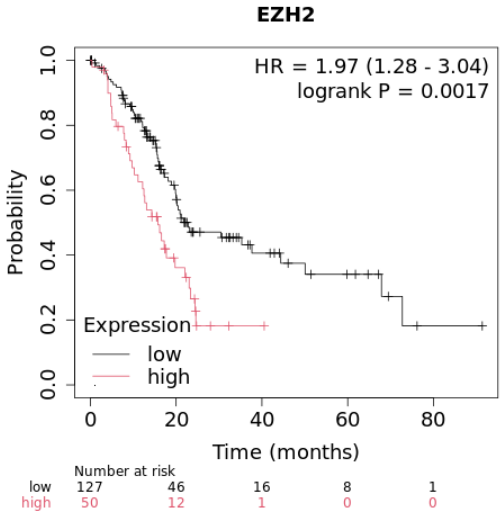

B1

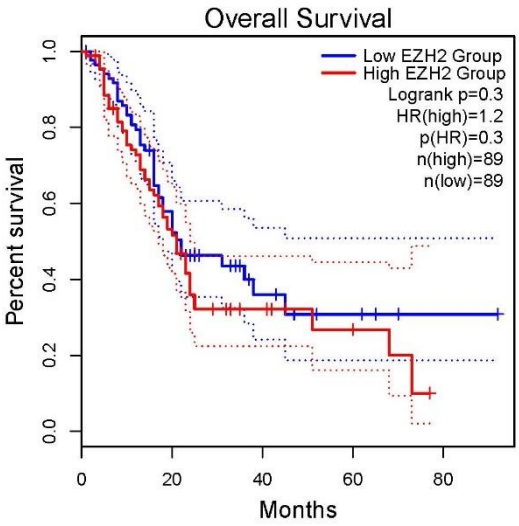

B2

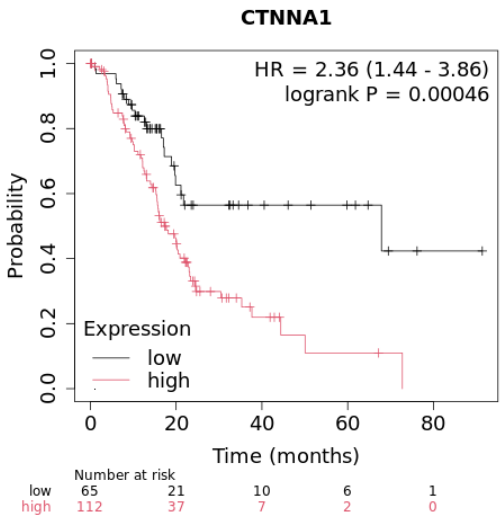

C1

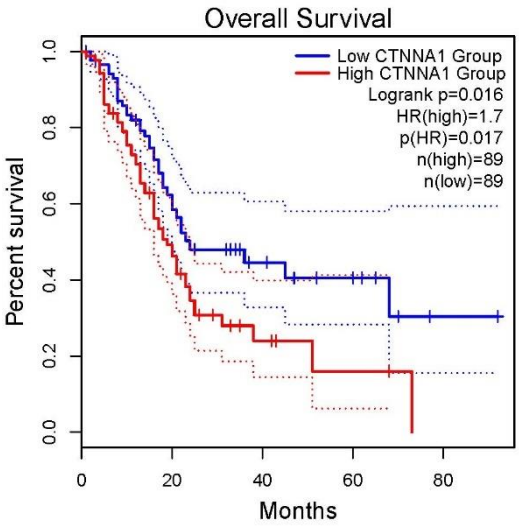

C2

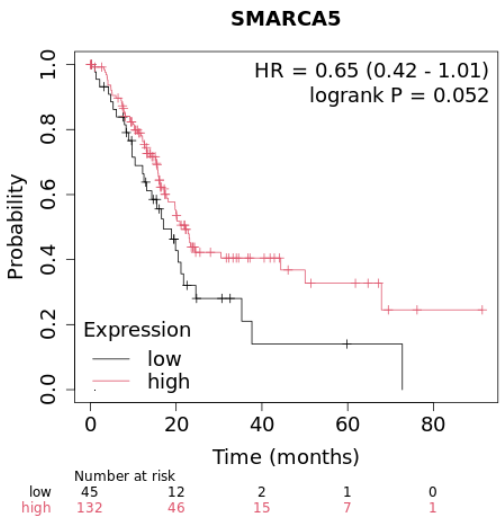

D1

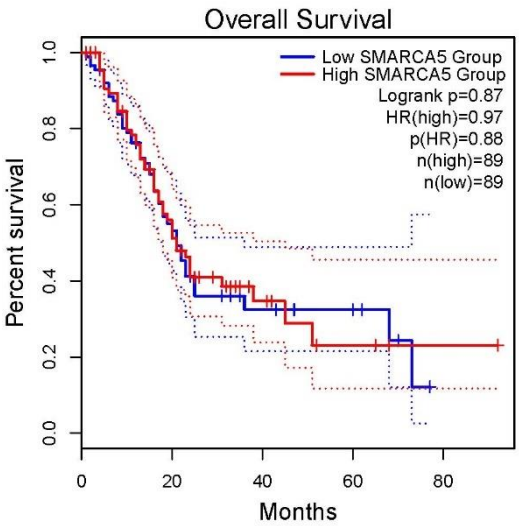

D2

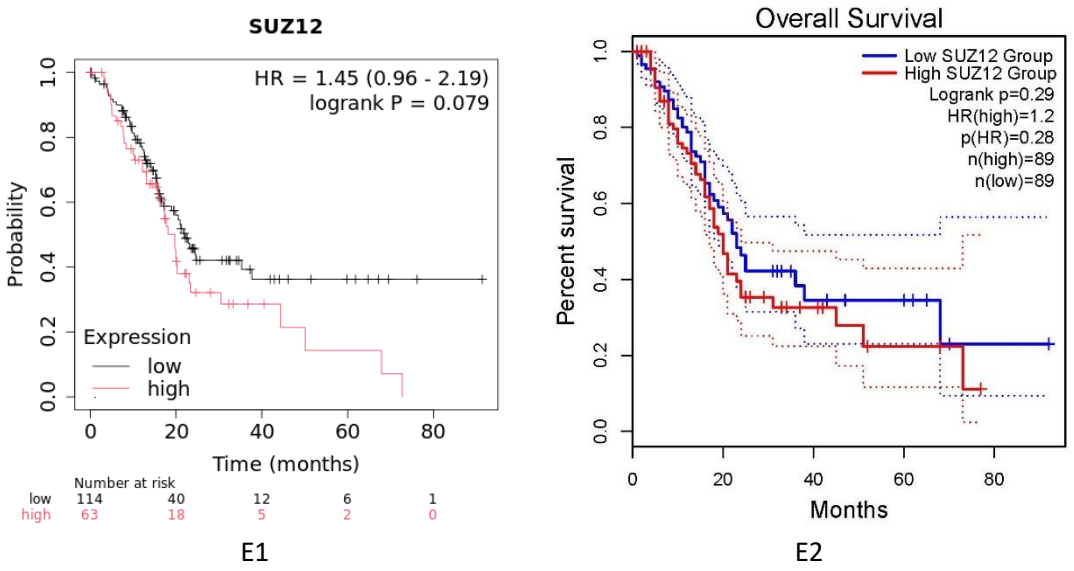

Figure 15: The overall survival of patients with PDAC in accordance to hub genes by Kaplan–Meier plots. (https://kmplot.com/analysis).

8. Verification of hub gene mRNA and protein expression

The GEPIA2 database was used to validate the mRNA expression levels of selected five hub genes in normal and PDAC samples (Fig. 16 A–E). All hub genes showed higher level of mRNA expression in PDAC patients in comparison with those normal, in particular the *YWHAZ* gene mRNA expression was significantly higher in PDAC than in normal hepatic tissues (Figure. 16E).

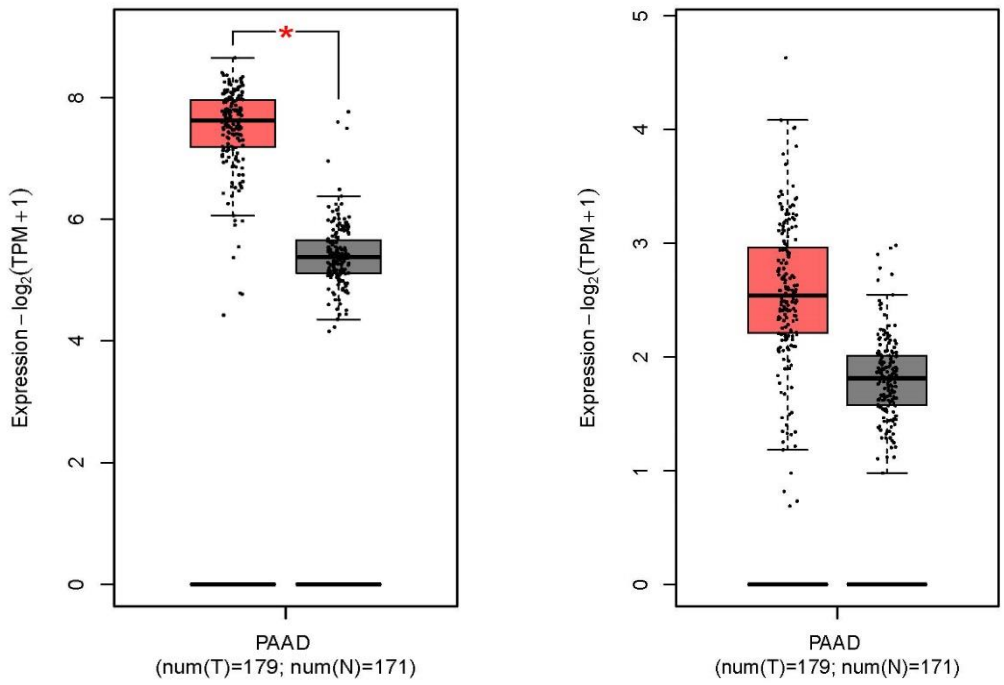

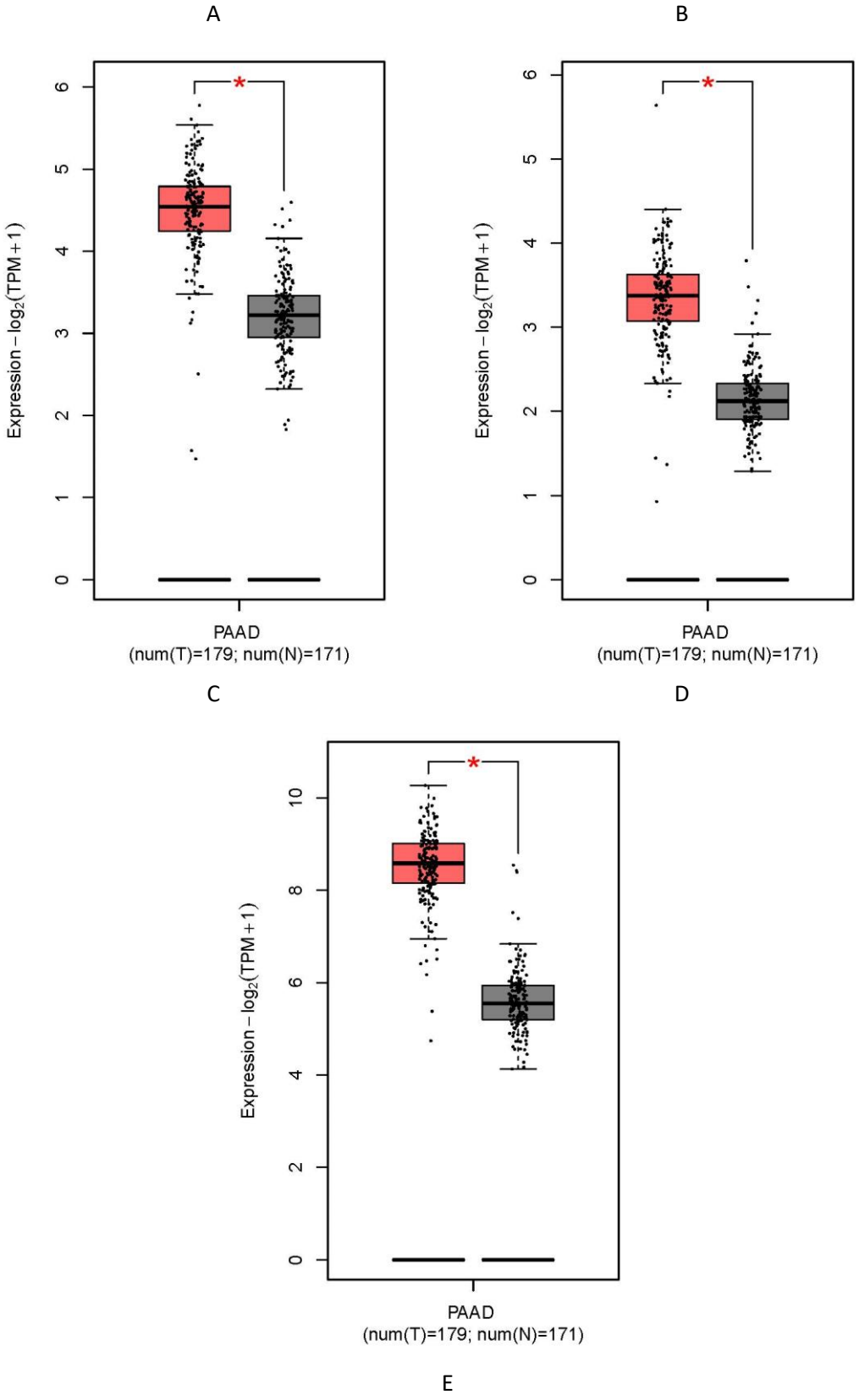

Figure 16: The mRNA expression of Hub Genes.
*the (A) CTNNA1, (B) EZH2, (C) SMARCA5, (D) SUZ12 and (E) YWHAZ in normal liver tissues and PDAC tissues from the GEPIA2 (http://gepia2.cancer-pku.cn/#index). The gray bars in box plots represent normal samples; the red bars in box plots represent tumor samples (*p < 0.01).*

Histochemistry of Genes expression as proteins using Protein Atlas web tool (https://www.proteinatlas.org/) (Sjöstedt et al., 2020). The images below (Figure 17) show the localization of gene target protein expression (shown in green) among the staining of other components of the cell, as the nucleus is stained with blue, endoplasmic reticulum (ER) with yellow, and microtubules with red. The staining indicates that the protein expression of CTNNA1 gene is localized in Cell junction, vesicles and plasma membrane, playing significant role in cell communication and intercellular signaling pathways. While, EZH2 protein expression is localized in nucleoplasm, and SUZ12 along with SMARCA5 are localized to the nucleoplasm, nucleoli, nuclear bodies & nucleoli rim contributing to nuclear activities, furthermore, YWHAZ localized in the intercellular area.

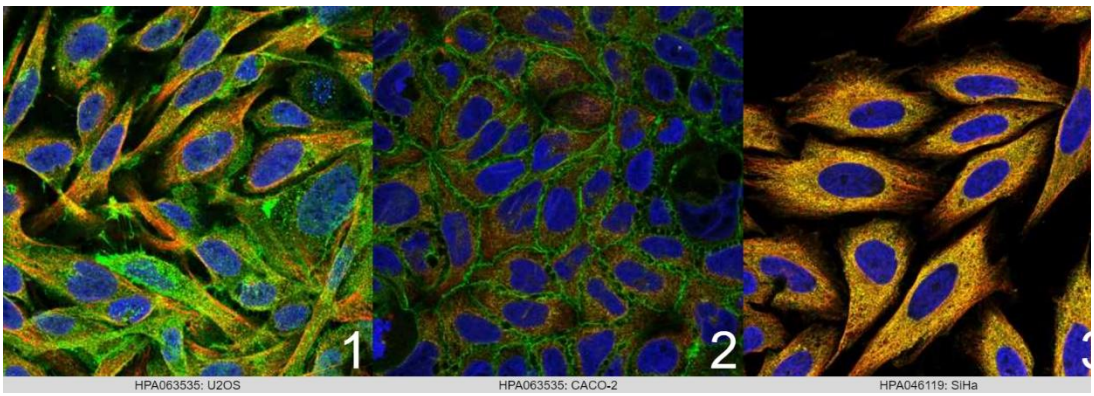

A: CTNNA1 protein expression localization in Cell Junction, Vesicles, and plasma membrane

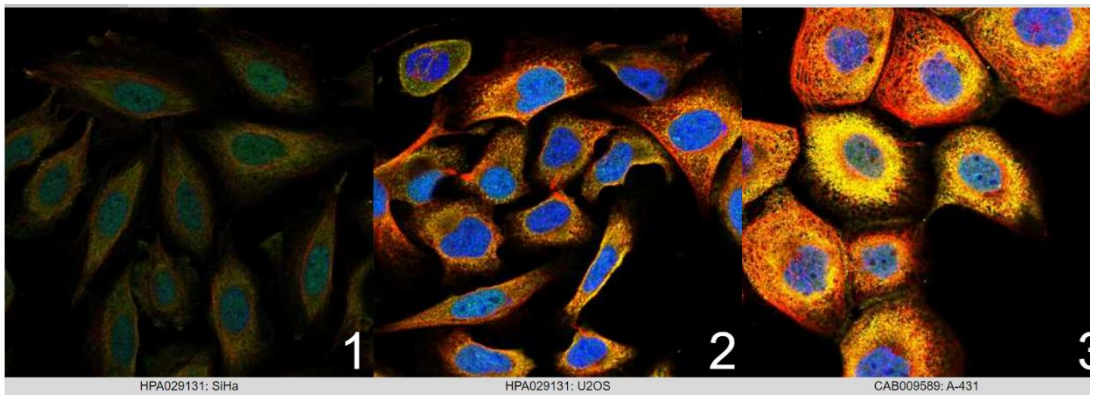

B: EZH2 protein expression localization in Nucleoplasm.

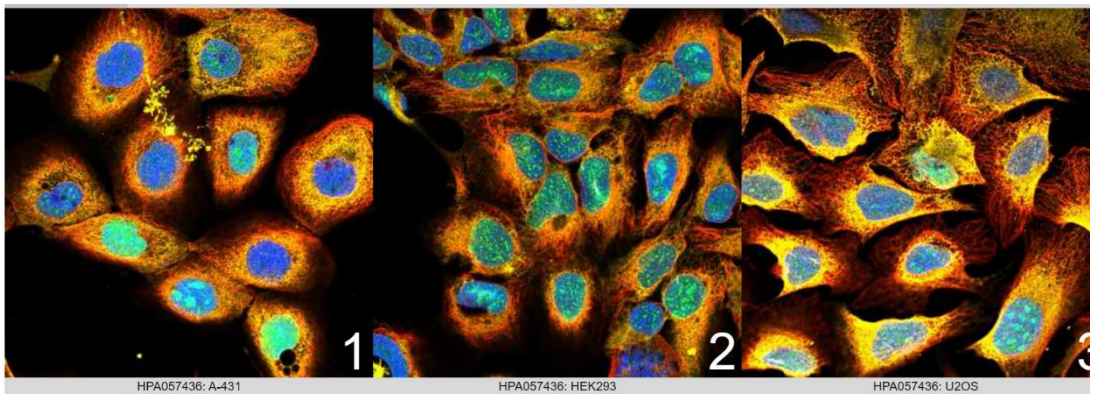

C: SUZ12 Localized to the nucleoplasm, nucleoli, nuclear bodies & nucleoli rim.

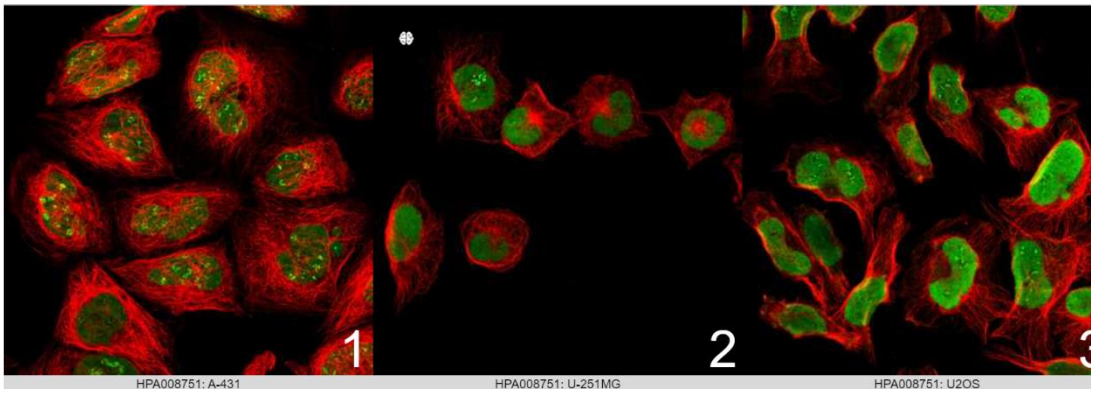

D: SMARCA5 Localized to the nucleoplasm

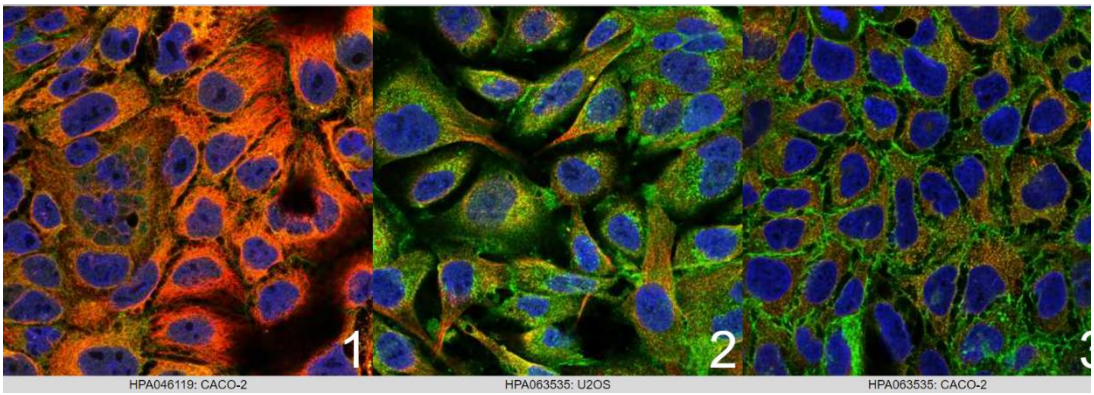

E: YWHAZ Localized to the intercellular area

Figure 17: The immunohistochemistry of the hub genes PDAC tissues from HPT database (https://www.proteinatlas.org/). target protein is stained with green, while nucleus is stained with blue, ER with Yellow, and Microtubules with Red

Thus, the mRNA expressions of genes as well as protein expression of the selected five hub genes were regulated in patients suffering with PDAC in comparison to normal liver tissue.

The UALCAN database (The University of ALabama at Birmingham CANcer data analysis Portal) (Chandrashekar et al., 2022) and (Chandrashekar et al., 2017), was used for the expression correlation analysis of selected five hub genes linked with PDAC. The results of the correlation revealed the significant expression of the selected genes at different stages of PDAC (Figure. 18 A–E). Based on the findings, hub genes SUZ12, EZH2, YWHAZ,

CTNNA1, and SMARCA5 were compactly regulated with the risk of PDAC development and its progression chronically

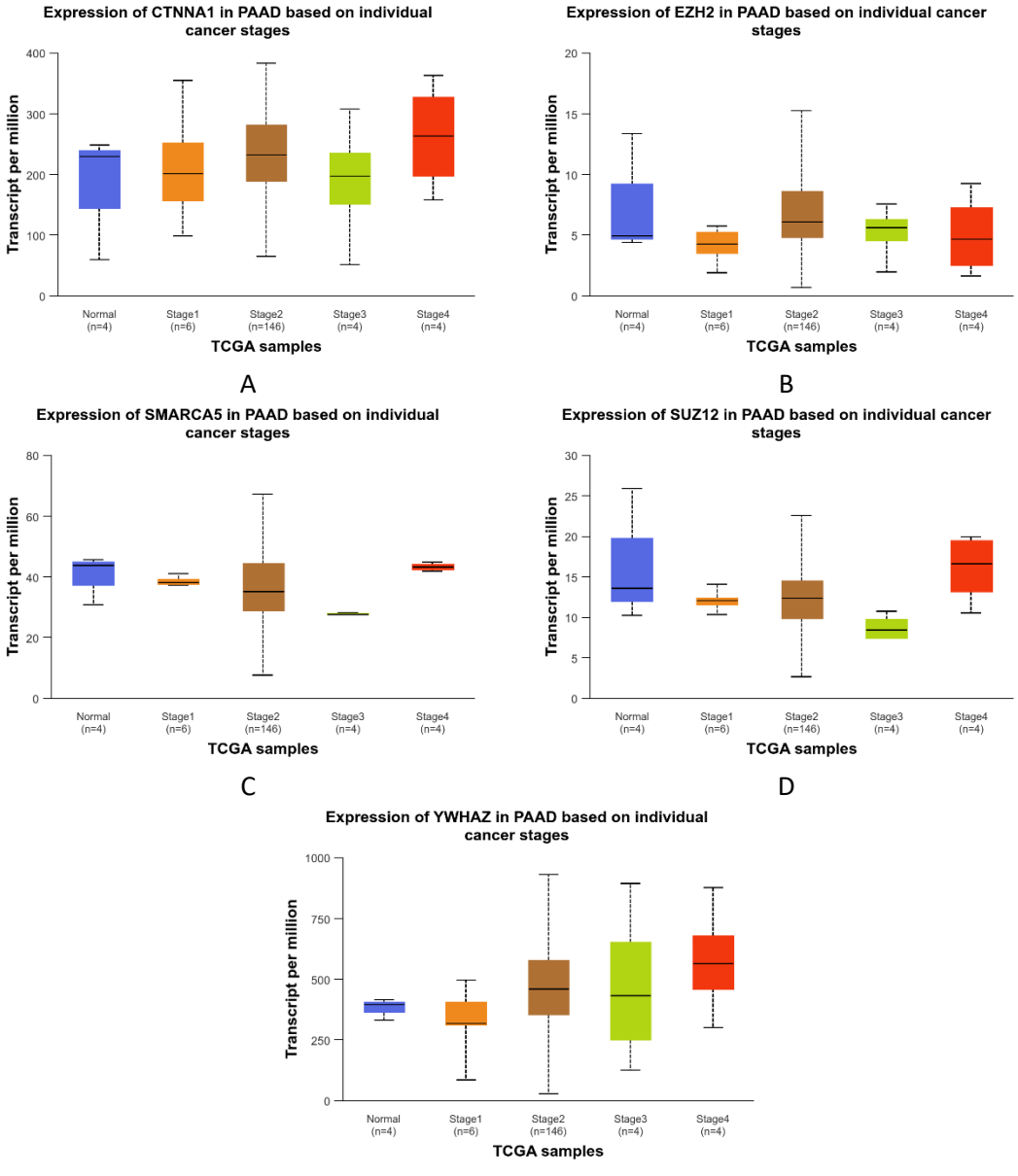

*Figure 18: The mRNA expression of hub genes CTNNA1 (A), EZH2 (B), SMARCA5 (C), SUZ12(D) and YWHAZ (E) in individual Cancer (*p < 0.05, ***p < 0.001) (http://ualcan.path.uab.edu).*

cBioPortal: **CBioPortal for Cancer Genomics** (Cerami et al., 2012), (De Bruijn et al., 2023), and (Gao et al., 2013):

Querying 983 samples/patients in combined studies and they are (Biankin et al., 2012), (Bailey et al., 2016), (Witkiewicz et al., 2015), (Cao et al., 2021), and 10 other studies used in TCGA database and they are (Hoadley et al., 2018), (Hoadley et al., 2018), (Taylor et al., 2018), (Liu et al., 2018),

(Sanchez-Vega et al., 2018), (Q. Gao et al., 2018), (Bhandari et al., 2019), (Poore et al., 2020), (Ding et al., 2018), and (Bonneville et al., 2017). The resulting analysis (Figure: 18) shows a summary of hub genes across the aforementioned studies:

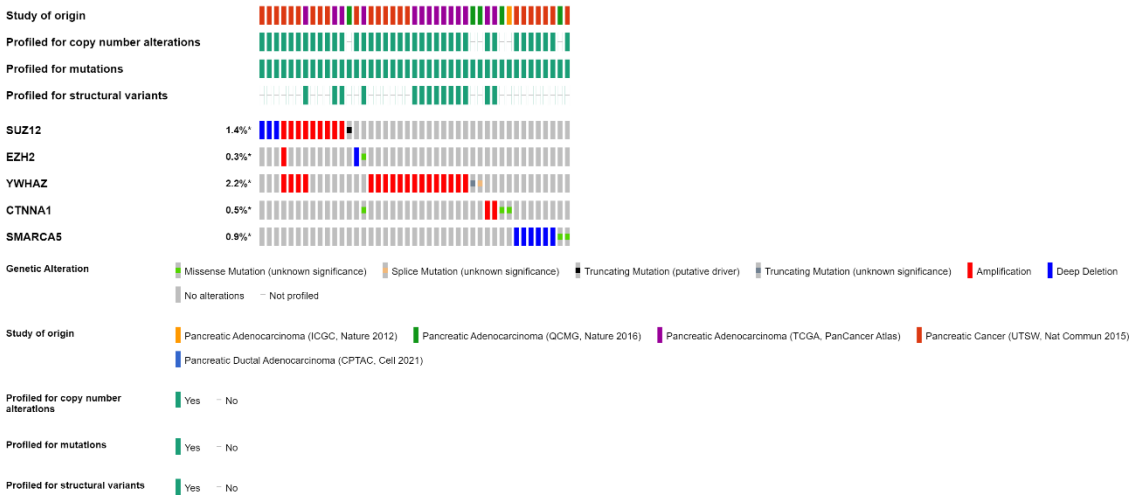

Figure 19: Text analysis of Hub Genes in previous PDAC studies using cBioPortal

The hub genes are altered in 5.3% of 983 samples as follows: CTNNA1 0.5% of samples, SUZ12 in 1.4%, the lowest percentage of alteration is in EZH2 with 0.3%, SMARCA5 0.9%, meanwhile the highest percentage of alteration is in WYHAZ with 2.2% of samples. However, the main genetic alteration among those genes were amplification, Deep deletion, Splice mutation, and Missense mutation. On the other hand, the following table (Table 12) states the mutual exclusivity analysis performed on the aforementioned genes.

Table 12: Mutual Exclusivity Analysis of Hub Genes by cBioPortal

A	B	Neither	A Not B	B Not A	Both	Log2 Odds Ratio	p-Value	q-Value	Tendency
SUZ12	YWHAZ	881	9	16	4	>3	<0.001	0.001	Co-occurrence
EZH2	CTNNA1	903	2	4	1	>3	0.016	0.082	Co-occurrence
SUZ12	EZH2	895	12	2	1	>3	0.042	0.141	Co-occurrence
EZH2	YWHAZ	888	2	19	1	>3	0.065	0.161	Co-occurrence
EZH2	SMARCA5	882	2	25	1	>3	0.083	0.167	Co-occurrence

A	B	Neither	A Not B	B Not A	Both	Log2 Odds Ratio	p-Value	q-Value	Tendency
CTNNA1	SMARCA5	880	4	25	1	>3	0.135	0.225	Co-occurrence
SUZ12	SMARCA5	872	12	25	1	1.539	0.316	0.451	Co-occurrence
YWHAZ	SMARCA5	865	19	25	1	0.865	0.443	0.554	Co-occurrence
SUZ12	CTNNA1	892	13	5	0	<-3	1	1	Mutual exclusivity
YWHAZ	CTNNA1	885	20	5	0	<-3	1	1	Mutual exclusivity

9. Hub gene expression in various immune cells

The TIMER database (*TIMER2.0*, n.d.) results revealed that the SUZ12, SMARCA5, YWHAZ, CTNNA1 and EZH2 genes have little significant correlation with the tumor purity parameter. The expression of hub gene EZH2 was down regulated and correlated against tumor-infiltrating levels negatively into PDAC; in contrast, up regulated hub genes (SUZ12, SMARCA5, YWHAZ, CTNNA1 and EZH2) expression was correlated against all subsets positively into PDAC (Figure 18). CTNNA1 gene expression was significantly correlated with all five TIICs. The infiltration of B cells and macrophages in SUZ12 gene expression was significantly observed. EZH2 gene expression was greatly significant against CD4+ T cells infiltration levels and insignificant against CD8+ T cell infiltration levels. In comparison to neutrophils, and CD8+ T cells, the hub genes YWHAZ and SMARCA5 were significantly more expressed in macrophages, CD4+ T cells, and B cells. Results suggested that neutrophils have a preferential corner in the immune infiltration study in PDAC with reference to selected five hub genes.

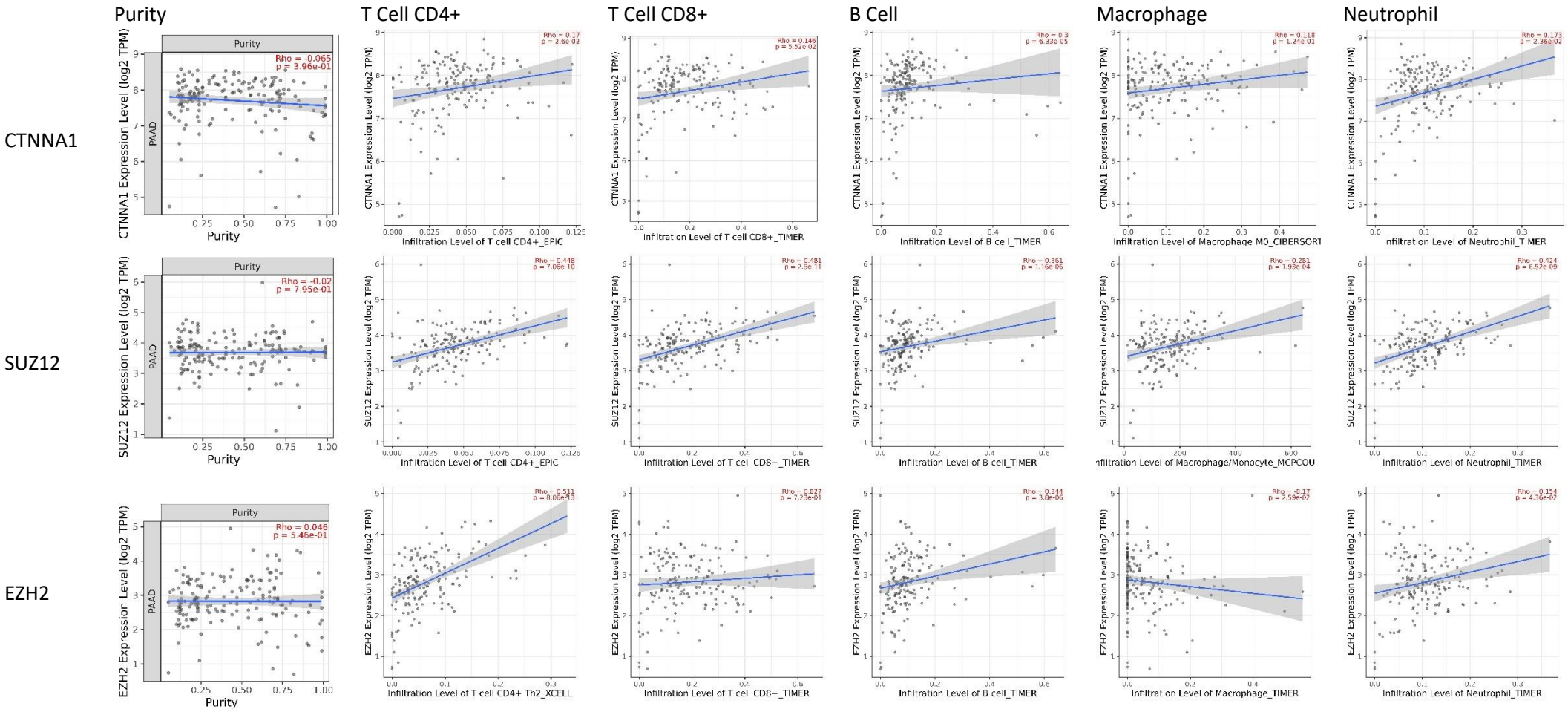
Purity
T Cell CD4+
T Cell CD8+
B Cell
Macrophage
Neutrophil
CTNNA1
SUZ12
EZH2
PAAD
Rho = -0.065
p = 3.96e-01
Rho = -0.02
p = 7.95e-01
Rho = 0.046
p = 5.46e-01
CTNNA1 Expression Level (log2 TPM)
SUZ12 Expression Level (log2 TPM)
EZH2 Expression Level (log2 TPM)
Infiltration Level of T cell CD4+_EPIC
Infiltration Level of T cell CD8+_TIMER
Infiltration Level of B cell_TIMER
Infiltration Level of Macrophage M0_CIBERSORT
Infiltration Level of Neutrophil_TIMER
Infiltration Level of Macrophage/Monocyte_MCPCOU
Infiltration Level of T cell CD4+ Th2_XCELL
Infiltration Level of Macrophage_TIMER

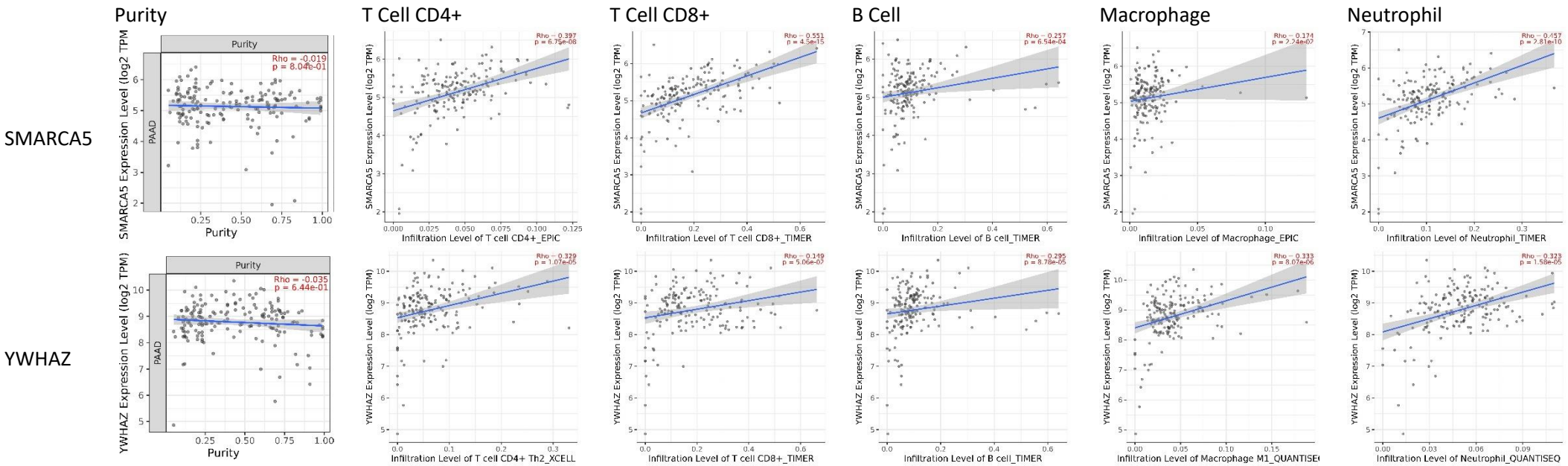

Figure 20: Analysis of hub gene expression in various immune cells in PDAC. (http://timer.cistrome. org)

10.Hub Genes Functional Enrichment Analysis

The functional enrichment analysis by Metascape showed that the key genes mainly contribute to PRC2 methylates histones and DNA (H3-3B,H2BC5,EZH2,H10,H2BC12,H3C12,H2BC21,H2AC6,H2AJ,H2BC11,H2BC9, ZC3H4,WDR82,EZH2,SIRT6,HNRNPU), FBXL 10 enhancement of MAP ERK signaling in diffuse large B cell (YWHAH,MPP5,SMAD2,YWHAE,CTNNA1,TCF7,PARD3,YWHAQ,YWHAZ,ACTB,BEX3,RHOA), and heterochromatin organization (H3-3B,H2BC5,EZH2,H1-0,H2BC12,H3C12,H2BC21, H2AC6,H2AJ,H2BC11, H2BC9,RAB4A,CHD1L,GNAS,KATNAL1,ATP8A1,RAB37,KIF2A,RAB6C,CHD9,RHOA), Figure 21:

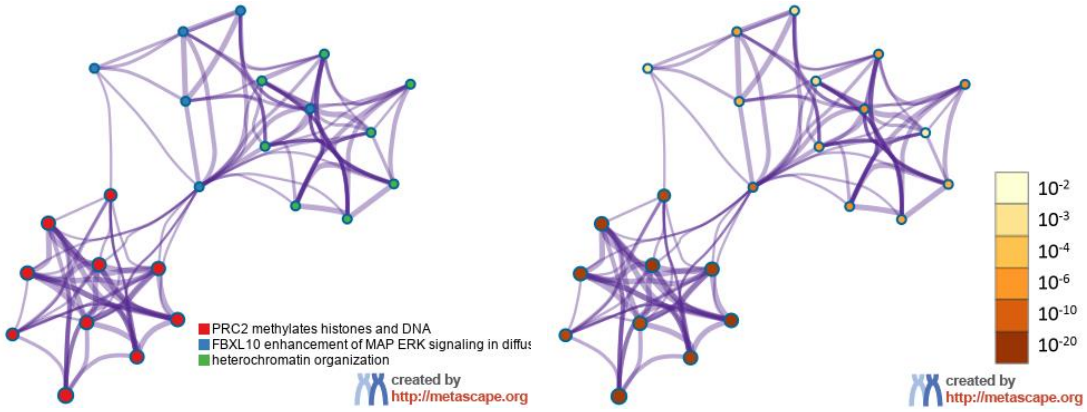

Figure 21: Network of Enriched Pathways and Biological Processes of the 11 Hub Genes: (A) Colored by Cluster ID, Where Nodes That Share the Same Cluster ID Are Typically Close To Each Other; (B) Colored by p-value, Where Terms Containing More Genes Tend to Have a More Significant P-Value

Figure 22 and Figure 23 show graphical representation of Enriched Pathways Biological process (consecutively) of the 11 hub genes identified by Metascape colored by P-Value. As the highest pathway of R-HAS-2123000 regarding PRC2 methylates histones and DNA score more than $\log_{10}$(P) of 17.5, followed by MAP ERK signaling $\log_{10}$(P) of 9.5, and heterochromatin organization $\log_{10}$(P) of 7. Whereas, cellular process plotted with p-value of $\log_{10}$(P) of 10.8.

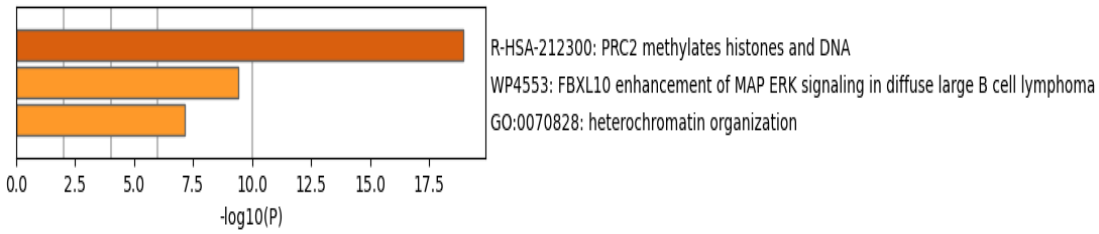

Figure 22: Bar Graph of Enriched Pathways of the 11 Hub Genes Identified by Metascape, Colored by P-values

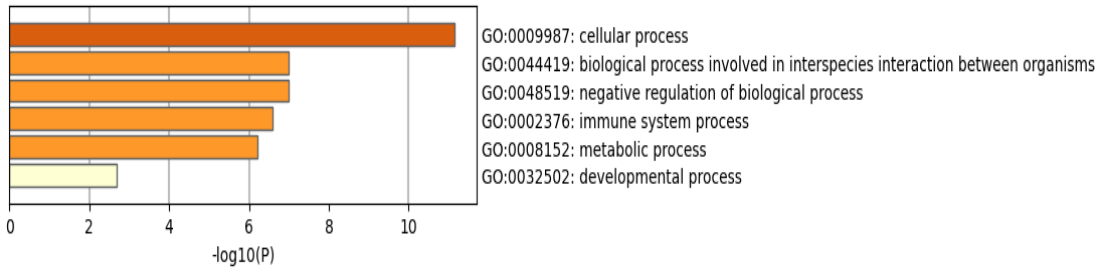

Figure 23: Bar Graph of Biological Processes of the 11 Hub Genes Identified by Metascape, Colored by P-values

11.Identification and validation of hub genes lncRNAs:

When intersecting those five hub genes previously identified in the dataset of interest with LNCipedia database version 5.2, the resulting output identified only four of the five hub genes to have long non coding transcripts, and they are; YWHAZ, SUZ12, EZH2, and SMARCA5. However, each of those genes has several Gene IDs with the same root gene yet varying in their corresponding transcript ID, Table: 13, Table: 14 Table: 15, and Table: 16 show list of Hub Gene IDs and their transcript ID along with their location, DNA strand, and transcript size.

Table 13: List of lncRNAs belongs to YWHAZ gene

#	Transcript ID	Gene ID	Location (hg38)	strand	transcript size
1.	lnc-YWHAZ-1:1	lnc-YWHAZ-1	chr8:100913247-100914388	-	1142
2.	lnc-YWHAZ-1:2	lnc-YWHAZ-1	chr8:100912760-100913774	-	534
3.	lnc-YWHAZ-2:1	lnc-YWHAZ-2	chr8:100916525-100918069	-	1545
4.	lnc-YWHAZ-3:1	lnc-YWHAZ-3	chr8:100951956-100953388	-	681
5.	lnc-YWHAZ-4:1	lnc-YWHAZ-4	chr8:101003516-101006239	-	2724
6.	lnc-YWHAZ-4:2	lnc-YWHAZ-4	chr8:100991844-101003711	-	757
7.	lnc-YWHAZ-4:3	lnc-YWHAZ-4	chr8:101002991-101003711	-	721
8.	lnc-YWHAZ-4:4	lnc-YWHAZ-4	chr8:100981044-101003711	-	2423
9.	lnc-YWHAZ-5:1	lnc-YWHAZ-5	chr8:101180858-101183176	-	2319
10.	lnc-YWHAZ-6:1	lnc-YWHAZ-6	chr8:101198924-101200288	-	615

#	Transcript ID	Gene ID	Location (hg38)	strand	transcript size
11.	lnc-YWHAZ-7:1	lnc-YWHAZ-7	chr8:101201220-101205507	-	597

Table 14: List of lncRNAs belongs to SUZ12 gene

#	Transcript ID	Gene ID	Location (hg38)	strand	transcript size
1.	lnc-SUZ12-1:1	lnc-SUZ12-1	chr17:31873926-31886666	+	488
2.	lnc-SUZ12-2:1	lnc-SUZ12-2	chr17:31830731-31831750	+	397
3.	lnc-SUZ12-3:1	lnc-SUZ12-3	chr17:31762440-31769048	+	505
4.	lnc-SUZ12-5:1	lnc-SUZ12-5	chr17:32031779-32033671	+	1893
5.	lnc-SUZ12-7:1	lnc-SUZ12-7	chr17:32039974-32040694	+	721
6.	lnc-SUZ12-8:1	lnc-SUZ12-8	chr17:31759795-31761385	+	1591

Table 15: List of lncRNA belongs to SMARCA5 gene

#	Transcript ID	Gene ID	Location (hg38)	strand	transcript size
1.	SMARCA5-AS1:1	SMARCA5-AS1	chr4:143513472-143514837	-	1147
2.	SMARCA5-AS1:2	SMARCA5-AS1	chr4:143513472-143514635	-	945
3.	SMARCA5-AS1:3	SMARCA5-AS1	chr4:143513472-143514654	-	964
4.	lnc-SMARCA5-4:1	lnc-SMARCA5-4	chr4:143559472-143568160	+	748
5.	lnc-SMARCA5-4:10	lnc-SMARCA5-4	chr4:143912331-143982454	+	1303
6.	lnc-SMARCA5-4:11	lnc-SMARCA5-4	chr4:143912331-143982452	+	1301
7.	lnc-SMARCA5-4:12	lnc-SMARCA5-4	chr4:143912331-144104040	+	992

#	Transcript ID	Gene ID	Location (hg38)	strand	transcript size
8.	lnc-SMARCA5-4:13	lnc-SMARCA5-4	chr4:143937867-143981916	+	410
9.	lnc-SMARCA5-4:14	lnc-SMARCA5-4	chr4:143953635-144126359	+	832
10.	lnc-SMARCA5-4:15	lnc-SMARCA5-4	chr4:143977232-143981916	+	796
11.	lnc-SMARCA5-4:16	lnc-SMARCA5-4	chr4:144089901-144188367	+	5037
12.	lnc-SMARCA5-4:2	lnc-SMARCA5-4	chr4:143559472-143561460	+	1989
13.	lnc-SMARCA5-4:3	lnc-SMARCA5-4	chr4:143559487-143560064	+	578
14.	lnc-SMARCA5-4:4	lnc-SMARCA5-4	chr4:143559695-143572724	+	766
15.	lnc-SMARCA5-4:5	lnc-SMARCA5-4	chr4:143560127-143649305	+	342
16.	lnc-SMARCA5-4:6	lnc-SMARCA5-4	chr4:143572413-143573674	+	473
17.	lnc-SMARCA5-4:7	lnc-SMARCA5-4	chr4:143559457-143913947	+	2723
18.	lnc-SMARCA5-4:8	lnc-SMARCA5-4	chr4:143700734-143982274	+	1292
19.	lnc-SMARCA5-4:9	lnc-SMARCA5-4	chr4:143859026-143982607	+	1368
20.	lnc-SMARCA5-5:1	lnc-SMARCA5-5	chr4:143601398-143615169	+	1175
21.	lnc-SMARCA5-7:1	lnc-SMARCA5-7	chr4:143381948-143395720	+	1176

#	Transcript ID	Gene ID	Location (hg38)	strand	transcript size
22.	lnc-SMARCA5-8:1	lnc-SMARCA5-8	chr4:143773356-143773723	+	368

Table 16: List of lncRNA belongs to EZH2 gene

#	Transcript ID	Gene ID	Location (hg38)	strand	transcript size
1.	lnc-EZH2-1:1	lnc-EZH2-1	chr7:148624699-148625450	-	229
2.	lnc-EZH2-1:2	lnc-EZH2-1	chr7:148624698-148625450	-	231
3.	lnc-EZH2-1:3	lnc-EZH2-1	chr7:148624698-148624856	-	231
4.	lnc-EZH2-2:1	lnc-EZH2-2	chr7:148543549-148568248	-	1081
5.	lnc-EZH2-2:2	lnc-EZH2-2	chr7:148543677-148572177	-	1227
6.	lnc-EZH2-3:1	lnc-EZH2-3	chr7:148441000-148497357	-	2011
7.	lnc-EZH2-3:2	lnc-EZH2-3	chr7:148473599-148503458	-	1501
8.	lnc-EZH2-4:1	lnc-EZH2-4	chr7:147080934-147097609	-	2145
9.	lnc-EZH2-4:2	lnc-EZH2-4	chr7:147080938-147097609	-	2141
10.	lnc-EZH2-5:1	lnc-EZH2-5	chr7:148918342-148918612	-	271
11.	lnc-EZH2-5:2	lnc-EZH2-5	chr7:148917877-148941187	-	23311
12.	lnc-EZH2-5:3	lnc-EZH2-5	chr7:148917877-148941187	-	23020
13.	lnc-EZH2-5:4	lnc-EZH2-5	chr7:148939888-148941187	-	1300
14.	lnc-EZH2-5:5	lnc-EZH2-5	chr7:148940472-148941187	-	378
15.	lnc-EZH2-5:6	lnc-EZH2-5	chr7:148919995-148920299	-	305
16.	lnc-EZH2-7:1	lnc-EZH2-7	chr7:148697334-148698764	-	1431
17.	lnc-EZH2-7:2	lnc-EZH2-7	chr7:148696467-148698664	-	2198

#	Transcript ID	Gene ID	Location (hg38)	strand	transcript size
18.	lnc-EZH2-7:3	lnc-EZH2-7	chr7:148697550-148698664	-	1115
19.	lnc-EZH2-7:4	lnc-EZH2-7	chr7:148696102-148697913	-	1812
20.	lnc-EZH2-7:5	lnc-EZH2-7	chr7:148696081-148698788	-	2708
21.	lnc-EZH2-7:6	lnc-EZH2-7	chr7:148694739-148698800	-	4062
22.	lnc-EZH2-7:7	lnc-EZH2-7	chr7:148697276-148698800	-	1525
23.	lnc-EZH2-7:8	lnc-EZH2-7	chr7:148696467-148698667	-	2201
24.	lnc-EZH2-8:1	lnc-EZH2-8	chr7:148449856-148450165	-	310
25.	lnc-EZH2-9:1	lnc-EZH2-9	chr7:147704294-147704575	-	282

Then, the resulting outputs were further analyzed by uploading to lncATLAS for localization of both hub genes mRNA and lncRNA. Figure 24 demonstrate the nuclear/cytoplasmic localization for hub genes transcripts (lncRNA & miRNA), along with their subcytoplasim and subnuclear localization.

Figure 24 introduces that genes YWHAZ, H2AC6, and H2BC21 are strictly localized in the cytoplasm of the cell as their Relative Concentration Index (RCI) & expression values are positive, while genes EZH2 and H3-3B are completely nuclear localized with negative RCI & expression values, whereas, genes SUZ12, CTNNA1, SMARCA5, H2BC11, H2BC12, and H3C12 have mixed localization in the cell with different ranges of RCI & expression values depending on tissue/cell line.

On the other hand, all genes are expressed in various tissue/cell lines with genes H2BC11 & H2BC12, and H3C12 having the lowest expression in tissues with (9, 8, 4 tissue/cell line – consecutively).

Furthermore, subcytoplasmic and subnuclear localization of hub genes' miRNAs and lncRNAs were studied in K562 cell line, all exhibited localization in the chromatin area except for CTNNA1, H2AC6, H2BC11, H2BC21, and H3-3B (no data available by lncATLAS).

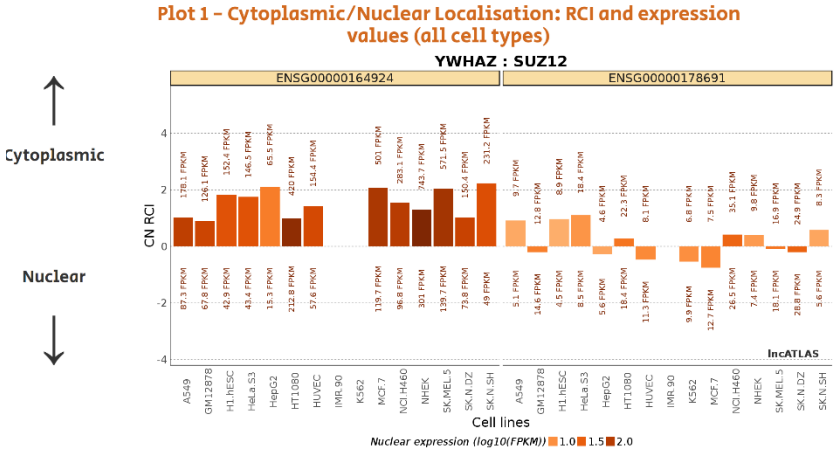

A: Genes YWHAZ & SUZ12 Cytoplasmic/nuclear localization

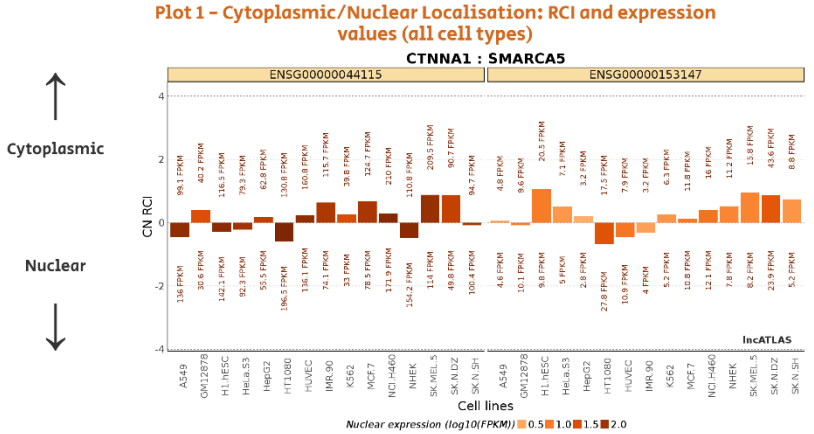

B: Genes CTNNA1 & SMARCA5 Cytoplasmic/nuclear localization

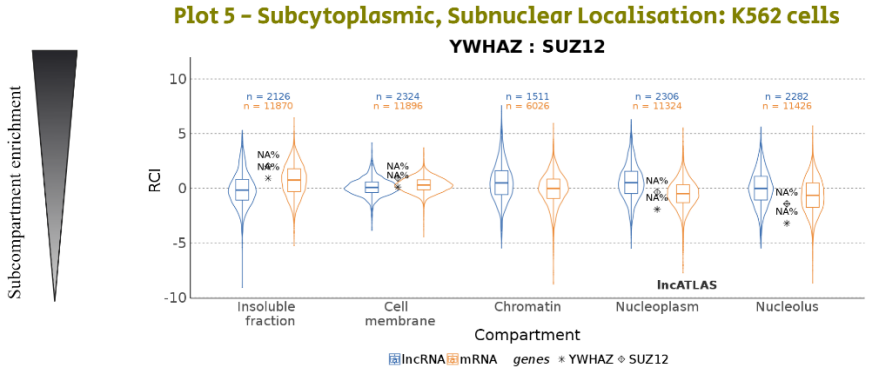

C: Genes YWHAZ & SUZ12 Subcytoplasmic & subnuclear localization

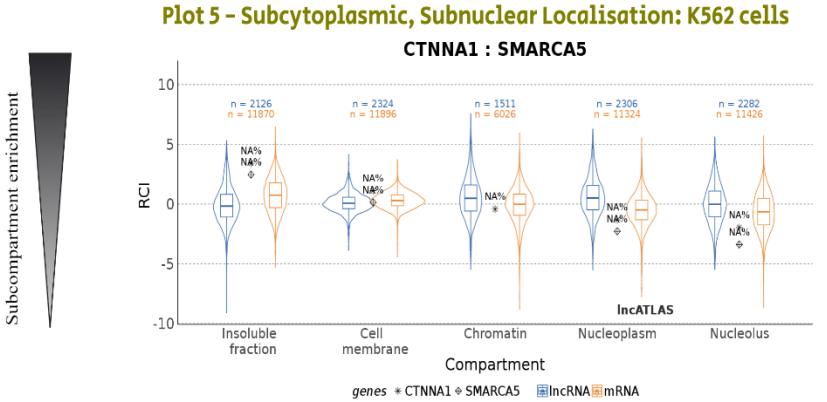

D: Genes CTNNA1 & SMARCA5 subcytoplasmic & subnuclear localization

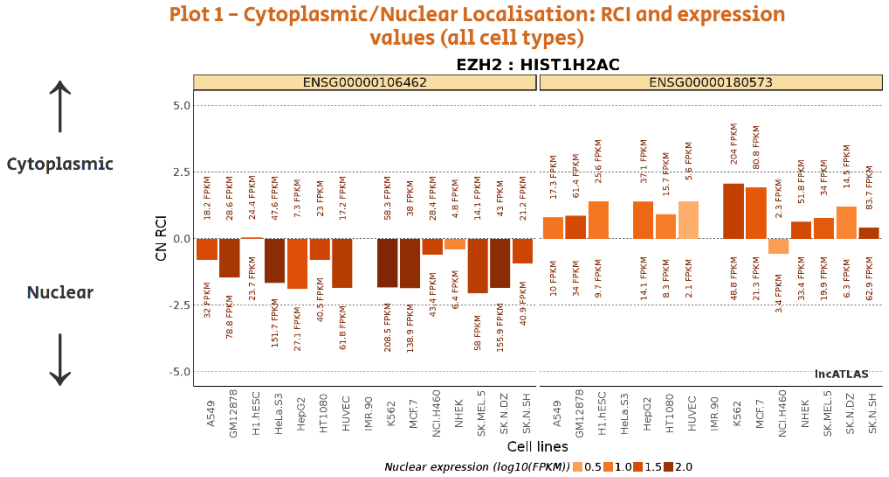

E: Genes EZH2 & H2AC6 Cytoplasmic/nuclear localization

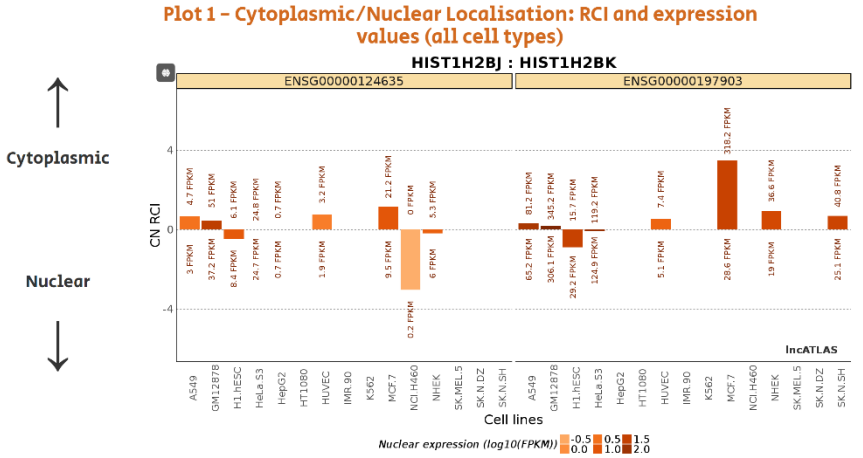

F: Genes H2BC11 & H2BC12 Cytoplasmic/nuclear localization

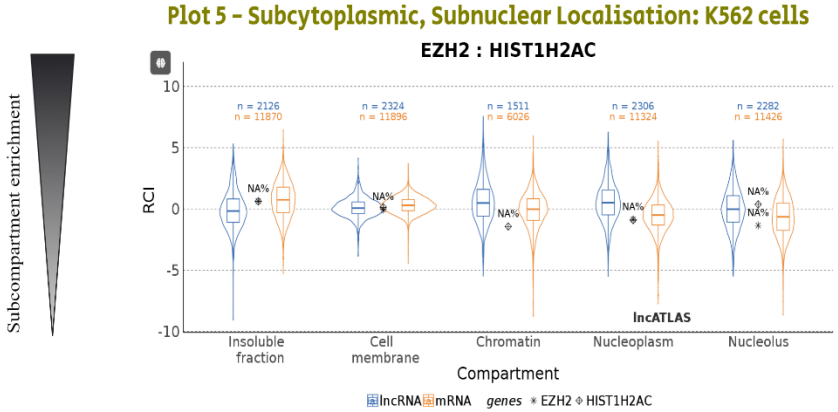

G: Gene EZH2 & H2AC6 Subcytoplasmic & Subnuclear localization

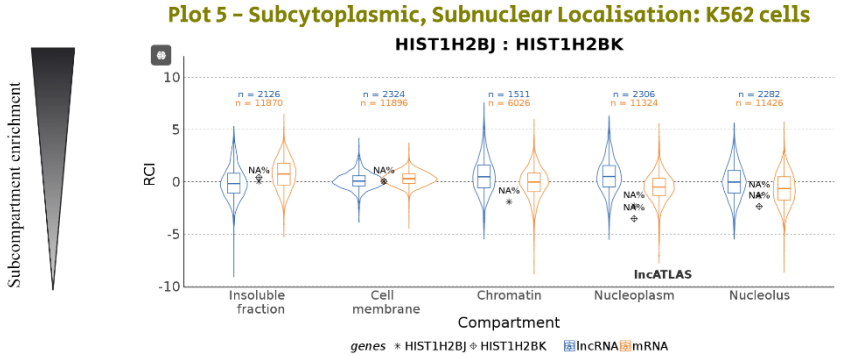

H: Gene H2BC11 & H2BC12 Subcytoplasmic & Subnuclear localization

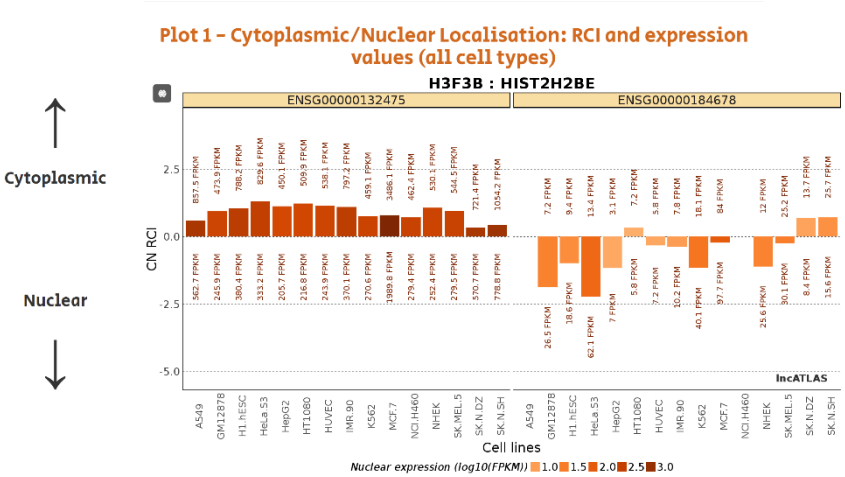

I: Genes H2BC21 & H3-3B Cytoplasmic/nuclear localization

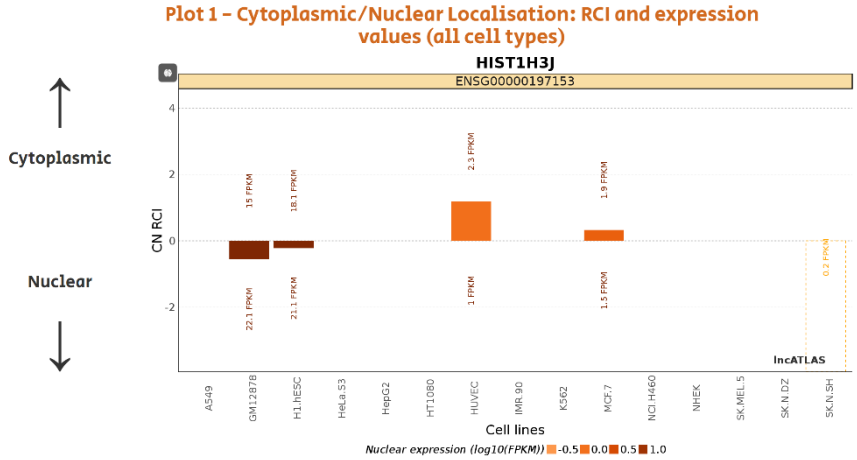

J: Genes H3C12 Cytoplasmic/nuclear localization

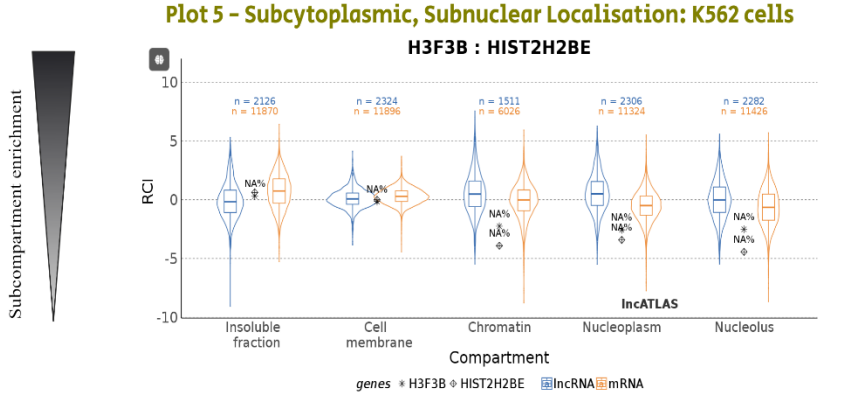

K: Genes H2BC21 & H3-3B subcytoplasmic & subnuclear localization

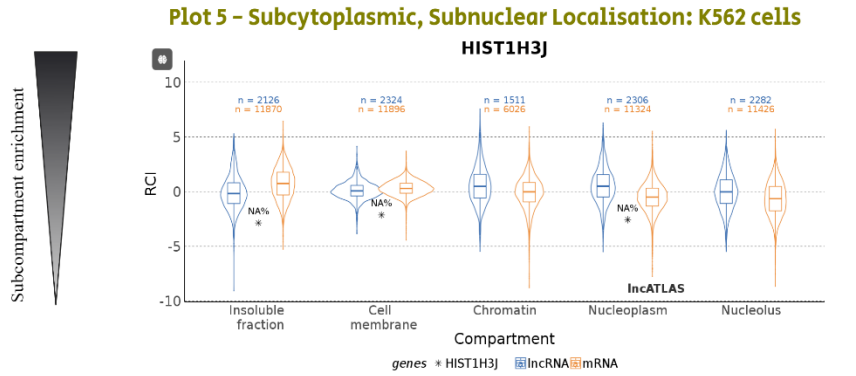

L: Genes H3C12 subcytoplasmic & subnuclear localization

Figure 24: Hub genes transcripts localization using lncATLAS

12. Prediction and Validation of Target miRNA

The hub genes were uploaded into **miRNet** and a total of 1266 miRNAs were obtained with 2156 edges (Figure 25), which shows all the hub genes of interest (Red stars) along with their corresponding miRNAs (Blue stars), in addition, target transcription factors (Green stars). Furthermore, when selecting the interaction of those genes, five modules were detected (Figure 26).

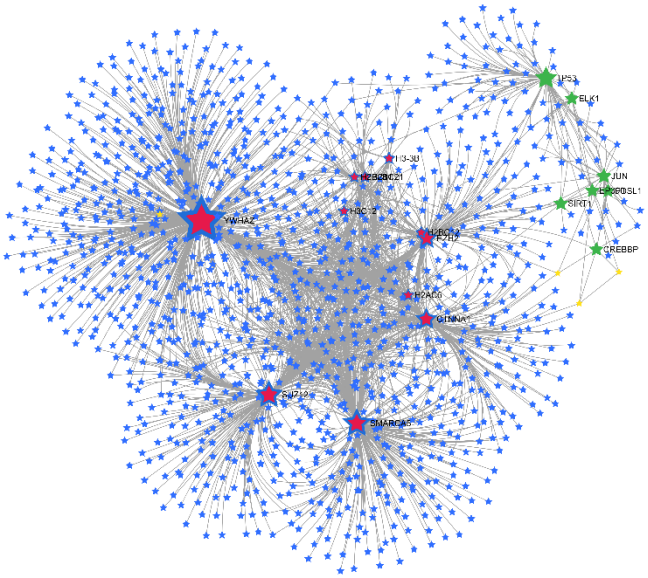

Figure 25: miRNA-Hub Gene Regulatory Network Extracted from miRNet
Where Red stars represent hub genes while blue ones represent miRNAs, and green for target transcription factors

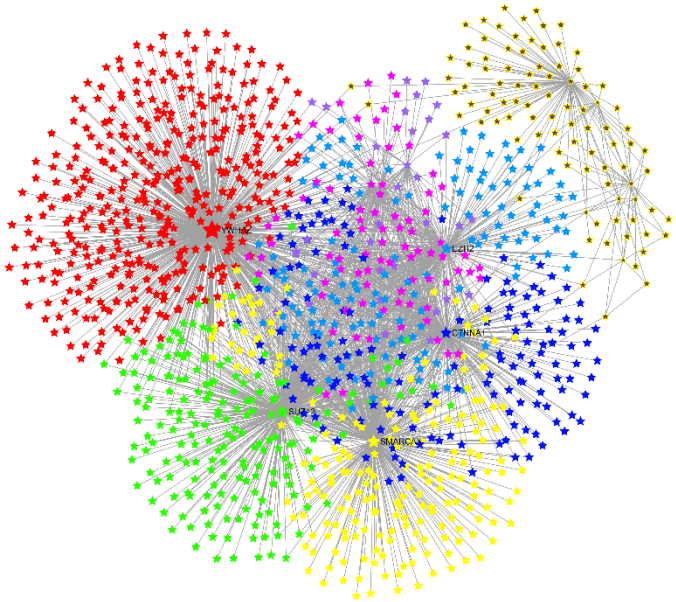

Figure 26: Modules selection of genes interactions groups

With gene YWHAZ being the highest with a score of 388 miRNA (shown in red), followed by SMARCA5 (shown in yellow), SUZ12 (shown in green), CTNNA1 (shown in light blue), and EZH2 (shown in dark blue) with scores of 199, 189, 155, 145 consecutively. The analysis also revealed the interaction of TP53 and JUN gens with the hub genes through 111 and 29 miRNAs consecutively. The results also states the interaction between EZH2 gene and several transcription factors such as TP53, JUN, SIRT1, ELK1, EP300, FOSL1 and CREBBP.

The resulting list of miRNAs was then submitted to DIANA tools for establishment of lncRNA-miRNA interaction confirmation through cross referencing with already published articles, the database retrieved 25 miRNAs targeted by 6 lncRNAs of hub genes of interest, the resulting list can be seen in Table 17. Results refer that only 3 out of 5 genes matched with DIANA lncRNA tool, with SMARCA5 gene having 3 transcripts (SMARCA5-AS1:2, lnc-SMARCA5-4:10, and lnc-SMARCA5-4:12) targeting 19 miRNAs, whereas, there is 1 transcript (lnc-YWHAZ-1:1) with 4 miRNAs, and 2 transcripts (lnc-EZH2-2:2, lnc-EZH2-4:1) with 2 different miRNAs.

Table 17: Hub gene transcripts and their corresponding miRNA using DIANA tools

#	Lncipedia Transcript ID	Ensembl Transcript ID	Class	Sequence Ontology term	miRNA name	Ensemble Gene ID	Tissue	Cell line	miRNA Conf.	Ref
1.	lnc-YWHAZ-1:1	ENST00000564694	Intergenic	lincRNA	hsa-miR-106b-5p	ENSG00000260368	Prostate	PC3	high	(Hamilton et al., 2016)
2.	lnc-YWHAZ-1:1	ENST00000564694	Intergenic	lincRNA	hsa-miR-128-3p	ENSG00000260368	Ovary	HEY	High	(Shahab et al., 2011)
3.	lnc-YWHAZ-1:1	ENST00000564694	Intergenic	lincRNA	hsa-miR-340-5p	ENSG00000260368	Prostate	PC3	High	(Hamilton et al., 2016)
4.	lnc-YWHAZ-1:1	ENST00000564694	Intergenic	lincRNA	hsa-miR-877-5p	ENSG00000260368	Prostate	PC3	High	(Hamilton et al., 2016)
5.	SMARCA5-AS1:2	ENST00000500800	antisense	antisense_lncRNA	hsa-miR-19b-1-5p	ENSG00000245112	Kidney	HEK293	High	(Memczak et al., 2013)
6.	SMARCA5-AS1:2	ENST00000500800	antisense	antisense_lncRNA	hsa-miR-25-3p	ENSG00000245112	Kidney	HEK293	High	(Memczak et al., 2013)
7.	SMARCA5-AS1:2	ENST00000500800	antisense	antisense_lncRNA	hsa-miR-29b-3p	ENSG00000245112	Kidney	HEK293	High	(Memczak et al., 2013)
8.	SMARCA5-AS1:2	ENST00000500800	antisense	antisense_lncRNA	hsa-miR-32-5p	ENSG00000245112	Embryo	ESC	High	(Lipchina et al., 2011)
9.	SMARCA5-AS1:2	ENST00000500800	antisense	antisense_lncRNA	hsa-miR-92a-3p	ENSG00000245112	Kidney	HEK293	High	(Memczak et al., 2013)

#	Lncipedia Transcript ID	Ensembl Transcript ID	Class	Sequence Ontology term	miRNA name	Ensemble Gene ID	Tissue	Cell line	miRNA Conf.	Ref
10	SMARCA5-AS1:2	ENST00000500800	antisense	antisense_lncRNA	hsa-miR-92b-3p	ENSG00000245112	Embryo	ESC	High	(Lipchina et al., 2011)
11	SMARCA5-AS1:2	ENST00000500800	antisense	antisense_lncRNA	hsa-miR-151b	ENSG00000245112	Embryo	ESC	Low	(Lipchina et al., 2011)
12	SMARCA5-AS1:2	ENST00000500800	antisense	antisense_lncRNA	hsa-miR-5581-5p	ENSG00000245112	Kidney	HEK293	Low	(Karginov & Hannon, 2013)
13	lnc-SMARCA5-4:10	ENST00000509873	Intergenic	lincRNA	hsa-miR-485-3p	ENSG00000251600	Brain	NA	High	(Boudreau et al., 2014)
14	lnc-SMARCA5-4:12	ENST00000641741	antisense	antisense_lncRNA	hsa-let-7a-5p	ENSG00000251600	Brain	NA	High	(Boudreau et al., 2014)
15	lnc-SMARCA5-4:12	ENST00000641741	antisense	antisense_lncRNA	hsa-let-7b-5p	ENSG00000251600	Brain	NA	High	(Boudreau et al., 2014)
16	lnc-SMARCA5-4:12	ENST00000641741	antisense	antisense_lncRNA	hsa-let-7c-5p	ENSG00000251600	Brain	NA	High	(Boudreau et al., 2014)
17	lnc-SMARCA5-4:12	ENST00000641741	antisense	antisense_lncRNA	hsa-let-7d-5p	ENSG00000251600	Brain	NA	High	(Boudreau et al., 2014)
18	lnc-SMARCA5-4:12	ENST00000641741	antisense	antisense_lncRNA	hsa-let-7e-5p	ENSG00000251600	Brain	NA	High	(Boudreau et al., 2014)

#	Lncipedia Transcript ID	Ensembl Transcript ID	Class	Sequence Ontology term	miRNA name	Ensemble Gene ID	Tissue	Cell line	miRNA Conf.	Ref
19	lnc-SMARCA5-4:12	ENST00000641741	antisense	antisense_lncRNA	hsa-let-7f-5p	ENSG00000251600	Brain	NA	High	(Boudreau et al., 2014)
20	lnc-SMARCA5-4:12	ENST00000641741	antisense	antisense_lncRNA	hsa-let-7g-5p	ENSG00000251600	Brain	NA	High	(Boudreau et al., 2014)
21	lnc-SMARCA5-4:12	ENST00000641741	antisense	antisense_lncRNA	hsa-let-7i-5p	ENSG00000251600	Brain	NA	High	(Boudreau et al., 2014)
22	lnc-SMARCA5-4:12	ENST00000641741	antisense	antisense_lncRNA	hsa-miR-124-3p	ENSG00000251600	Brain	NA	High	(Boudreau et al., 2014)
23	lnc-SMARCA5-4:12	ENST00000641741	antisense	antisense_lncRNA	hsa-miR-1301-3p	ENSG00000251600	Brain	NA	High	(Boudreau et al., 2014)
24	lnc-EZH2-2:2	ENST00000637240	Intergenic	lincRNA	hsa-miR-221-3p	ENSG00000283648	Brain	NA	High	(Boudreau et al., 2014)
25	lnc-EZH2-4:1	ENST00000434887	Antisense	antisense_lncRNA	hsa-miR-139-5p	ENSG00000236795	Kidney	293S	High	(Karginov FV et al. 2013)

Discussion:

Pancreatic ductal adenocarcinoma (PDAC) is recognized as an exceptionally aggressive malignancy exhibiting a 5-year survival rate of merely 10% (A. K. Beutel & Halbrook, 2023). The sole curative approach for this condition is surgical intervention. Regrettably, a limited number of individuals meet the criteria for surgery owing to delayed diagnosis. Consequently, there exists a necessity to identify methodologies for early disease detection, wherein reliable screening biomarkers could prove to be invaluable. Prior investigations have scrutinized circulating analytes within prospective research endeavors aimed at discerning initial signals of PDAC. Among these, long non-coding RNAs (lncRNAs) constitute a noteworthy category. LncRNAs, surpassing 200 nucleotides in length, function as post-transcriptional modulators through interactions with messenger RNAs (mRNAs). The functionality of a lncRNA can be elucidated via target prediction, facilitating the identification of potential targets, subsequently complemented by an enrichment analysis of the predicted targets. Challenges associated with this methodology include the generation of numerous false positives, in addition to the observation that lncRNAs may execute their role in a manner specific to either tissue or disease. Metabolites and proteins represent alternative classes of analytes previously examined within prospective PDAC cohorts.

Hence, the principal aim of this ongoing investigation revolves around the identification of noteworthy contributors and plausible molecular pathways linked to PDAC, alongside an exploration of innovative targets within PDAC pharmacotherapy, an endeavor accomplished through the utilization of bioinformatics analysis.

Initially, a normalized RNA-seq dataset of PDAC patients was retrieved from the **GEO** database. The analysis started by employing **GEO2R** which revealed that out of the total gene pool, 500 genes exhibited differential expression patterns in response to PDAC. Among these genes, 451 were up-regulated, indicating increased expression, while 49 were down-regulated, suggesting decreased expression, when comparing the PDAC group to the control group.

The DEGs were subjected to functional annotation and **KEGG** pathway enrichment analysis using the **DAVID** database. The annotation analysis involved categorizing the genes into three groups based on **Gene Ontology** (GO), which includes **Biological Processes** (BP), **Cell Component** (CC), and **Molecular Function** (MF).

The results of the analysis revealed that the majority of DEGs are mainly abandoned in the nucleus and cytoplasm, participating in many biological processes related to DNA methylation, unfolding, and replication. In addition to mRNA maturation and transcription, additionally, the genes were found to have functional roles in binding processes of many biomolecules, particularly proteins and RNAs, DNA and NADH dehydrogenase (ubiquinone) activity.

Furthermore, the DEGs were involved in a variety of essential pathways in cell cycle, cancer, apoptosis, inflammation, and immune response including signaling pathway.

These initial findings went along with several previous studies that suggested the strong link between PDAC and immune response alteration including high production of pro-inflammatory cytokines and TNF-a in PDAC patients compared to healthy individuals (Gola et al., 2013).

On the other hand, a reduced level of apoptotic markers in the serum of subjects with pancreatic cancer was detected (Bernard et al., 2019) and abnormal apoptosis in specific lung, liver, and Brest regions (Gao et al., 2019). These findings suggest that dysfunction in apoptosis may contribute to the observed inflammation pattern commonly seen in individuals with PDAC (Bernard et al., 2019).

The DEGs were analyzed using the **STRING** database to assess their interaction relationships where interactions with a confidence score greater than 0.9 were considered significant. The constructed network exhibited a higher number of interactions than expected which indicates that these proteins are biologically connected as a group, at least to some extent.

Cytoscape was employed to visually explore the interactive networks, with a cut-off criterion of a confidence score greater than 0.4 to determine the significance of the interactions. While **CytoHubba** was used to calculate the connectivity score of the genes based on a four-fold

algorithm. By intersecting the results, a total of 3 genes were identified as common among the four algorithms, with 11 of these genes (CTNNA1, EZH2, H2AC6, H2BC11, H2BC12, H2BC21, H3-3B, H3C12, SMARCA5, SUZ12, YWHAZ) appearing in the three most significant modules identified by **MCODE**.

The 5 candidate hub genes were checked in KEGG database for biological activity pathways resulting in preliminary verification of those hub genes activities with regard to Lysine Degradation, ATP Dependent Chromatin remodeling, Polycomb repressive complex cross-referenced with data from previous studies (Blackledge & Klose, 2021) and (Piunti & Shilatifard, 2021).

KEGG analysis found SUZ12's role in PRC2/EED-EZH2 complex, methylating histone H3 for gene repression. PRC2/EED-EZH2 complex represses genes like HOXC8, HOXA9, MYT1, and CDKN2A. On the other hand, CTNNA1 associates with cadherins, aids in cell-adhesion properties by linking to actin network. Whereas, EZH2 is a catalytic subunit of PRC2/EED-EZH2 complex methylating histone H3 for gene repression, preferring substrates with less methylation. In the meanwhile, SMARCA5 is a helicase with ATP-dependent nucleosome-remodeling activity, involved in chromatin organization and transcriptional regulation. Moreover, YWHAZ is part of the Hippo signaling pathway controlling organ size by regulating YAP and TAZ localization and activity. (Cao et al., 2021).

Hub genes were chosen for their high degree of connectivity. Hub gene mRNA and protein expression verification, overall survival, as well as immune infiltration were analyzed. According to the **DAVID** database, compromised genes were significantly associated with various signaling pathways that were linked with PDAC. The **GEPIA2** database was used to validate that *YWHAZ* and *CTNNA1* mRNA expression were significantly higher, which confirms the finding of other researchers (Heredia-Soto et al., 2021), (Huang, L et al., 2023). And the results also suggested that neutrophils have a preferential corner in the immune infiltration study in PDAC with reference to selected five hub genes.

On the other hand, several hub genes are linked to neuronal function and survival. For example, YWHAZ has been associated with the regulation of neuronal activity and synaptic plasticity. Recent research indicates that a lack of YWHAZ can result in a disruption of the normal functioning of

dopamine and serotonin in Zebrafish (Antón-Galindo et al., 2022) and (Wan et al., 2023).

In an attempt to investigate the ability of hub genes to mutate, a meta-analysis was performed on over 900 patients (addressed in figure 19), found that all hub genes are highly conserved except for WYHAZ gene which has 2.2% mutation ability. Moreover, the hub gene functional enrichment analysis performed by **Metascape** also confirmed the previous results obtained through **DAVID** and **KEGG** tools. Thus, results are consistent and dependable.

The previous step confirmed that final identified hub genes in the current study are SUZ12, EZH2, YWHAZ, CTNNA1, and SMARCA5 were of great significance in PDAC in consideration to healthy individuals as they are both upregulated and conserved through cell proliferation.

When intersecting hub genes with **LNCipedia** database, several transcripts were found to be linked to four of hub genes YWHAZ, SUZ12, EZH2, and SMARCA5, with total of 64 transcripts (11 ,6 ,25, 22 consecutively). Also, when uploaded to **lncATLAS** to further identify their localization within the cell, hub genes' miRNAs and lncRNAs varied in their localization between cytoplasmic and nuclear section with main positioning in the chromatin.

Then, through **miRNet** a total of 1266 miRNAs were obtained with 2156 edges with YWHAZ scoring 388 miRNAs followed SMARCA5, SUZ12, CTNNA1, and EZH2 consecutively, which supports the significant role these genes play in chromatin organization, RNA and DNA methylation and signaling pathways identified by previous studies of (Zeng et al., 2022), and (Rad & Tee, 2016) as they pointed out the role of EZH2 and SUZ2 in cancer development and potential targeting for drug discovery.

Another important finding was the interaction of hub genes with two of the most crucial and highly significant genes (TP53 and JUN). As TP53 acts as a tumor suppressor, the JUN gene is involved in both translocations and deletions in human malignancies.

A previous study (Eissa et al., 2019) could define five key biomarkers that differentiate individuals with pancreatic cancer from the healthy control group: as the researcher found that promoter methylation of ADAMTS1 and BNC1 as potential biomarkers for early detection of pancreatic cancer in blood. On the other hand, recent study (Chirravuri-Venkata et al., 2023)

stated that MUC16 and TP53 family co-regulate tumor-stromal heterogeneity in pancreatic adenocarcinoma. Furthermore, another lncRNA study (Tian et al., 2019) suggests that lncRNAs MIR600HG and TSPOAP1-AS1 may potentially act as biomarkers for predicting pancreatic cancer.

The resulting miRNAs were further validated through **DIANA tool** resulting the 25 miRNAs to be targeted by 6 lncRNAs (**ENST00000641741, ENST00000637240, ENST00000434887, ENST00000500800, ENST00000509873, ENST00000564694**) that are validated by previous studies (Karginov FV et al. 2013) (Boudreau et al., 2014) (Karginov & Hannon, 2013) (Lipchina et al., 2011) (Memczak et al., 2013) (Shahab et al., 2011) (Hamilton et al., 2016).

Conclusion

In conclusion, this research employed an integrative bioinformatics approach to analyze a normalized RNA-seq dataset of PDAC patients. The analysis identified total 500 DEGs (451 upregulated and 49 down regulated) and constructed PPI networks, leading to the identification of 11 hub genes using a four-fold algorithm method. These hub genes were found to be involved in key pathways associated with PDAC, such as cytokine signaling in the immune system, cell cycle regulation, and apoptosis-related processes. Additionally, the study predicted and confirmed 6 lncRNAs transcripts to regulate 25 miRNAs and 7 key TFs that were previously established to regulate the majority of the hub genes associated with PDAC. Separate networks were constructed for the interactions between miRNAs and hub genes, as well as between key TFs and hub genes. Therefore, these lncRNAs were validated as PDAC biomarkers and hold a potential for therapeutic targets for PDAC.

This investigation carries significant implications for enhancing our comprehension of the molecular basis of PDAC and pinpointing possible targets for therapeutic interventions. Through elucidation of the molecular processes and identification of biomarkers, this study aids in the advancement of enhanced diagnostic instruments and individualized treatment strategies. In conclusion, it is paramount to underscore that the outcomes of this bioinformatics investigation necessitate further validation and experimentation in laboratory settings. The execution of additional laboratory experiments is indispensable in verifying the

dependability and precision of the findings, thereby offering a more all-encompassing insight into the pathogenesis of PDAC and ensuring the robustness of the identified biomarkers and therapeutic targets.

Research Limitations

Limited access to recent publications in the Syrian Arab Republic is due to sanctions, leading to the use of less informative alternatives in unfunded research. Additionally, time constraints hindered the completion of this paper according to program guidelines.

Conversely, the large amount of data available online complicates reducing dimensionality through free websites. This includes methods like principal component analysis, Hierarchical clustering, and heatmap generation.

The outdated database for Pancreatic Ductal Adenocarcinoma (PDAC) hinders access to important, accurate information. Lack of experimental validation is a limitation in confirming identified hub genes and biomarkers. Prioritizing experimental validation, particularly through RT-qPCR, is recommended for future research to enhance reliability.

References

- Antón-Galindo, E., Vecchia, E. D., Orlandi, J. G., Castro, G., Gualda, E. J., Young, A. M. J., Guasch-Piqueras, M., Arenas, C., Herrera-Úbeda, C., Garcia-Fernàndez, J., Aguado, F., Loza-Alvarez, P., Cormand, B., Norton, W. H. J., & Fernàndez-Castillo, N. (2022). Deficiency of the ywhaz gene, involved in neurodevelopmental disorders, alters brain activity and behaviour in zebrafish. Molecular Psychiatry, 27(9), 3739–3748. https://doi.org/10.1038/s41380-022-01577-9
- Aprile, M., Costa, V., Cimmino, A., & Calin, G. A. (2022). Emerging role of oncogenic long noncoding RNA as cancer biomarkers. International Journal of Cancer, 152(5), 822–834. https://doi.org/10.1002/ijc.34282
- Aprile, M., Katopodi, V., Leucci, E., & Costa, V. (2020). LncRNAs in Cancer: From garbage to Junk. Cancers, 12(11), 3220. https://doi.org/10.3390/cancers12113220

- Aurilia, C., Donati, S., Palmini, G., Miglietta, F., Falsetti, I., Iantomasi, T., & Brandi, M. L. (2021). Are Non-Coding RNAs useful biomarkers in parathyroid tumorigenesis? International Journal of Molecular Sciences, 22(19), 10465. https://doi.org/10.3390/ijms221910465
- Bailey, P., Chang, D. K., Nones, K., Johns, A. L., Patch, A., Gingras, M., Miller, D. K., Christ, A. N., Bruxner, T. J. C., Quinn, M. C., Nourse, C., Murtaugh, L. C., Harliwong, I., Idrisoglu, S., Manning, S., Nourbakhsh, E., Wani, S., Fink, L., Holmes, O., . . . Grimmond, S. M. (2016). Genomic analyses identify molecular subtypes of pancreatic cancer. Nature, 531(7592), 47–52. https://doi.org/10.1038/nature16965
- Barshir, R., Fishilevich, S., Iny-Stein, T., Zelig, O., Mazor, Y., Guan-Golan, Y., Safran, M., & Lancet, D. (2021). GeNECARNA: a comprehensive gene-centric database of human non-coding RNAs in the GeneCards Suite. Journal of Molecular Biology/Journal of Molecular Biology, 433(11), 166913. https://doi.org/10.1016/j.jmb.2021.166913
- Bernard, V., Kim, D. U., Lucas, F. a. S., Castillo, J., Allenson, K., Mulu, F. C., Stephens, B. M., Huang, J., Semaan, A., Guerrero, P. A., Kamyabi, N., Zhao, J., Hurd, M. W., Koay, E. J., Taniguchi, C. M., Herman, J. M., Javle, M., Wolff, R., Katz, M., . . . Alvarez, H. A. (2019). Circulating nucleic acids are associated with outcomes of patients with pancreatic cancer. Gastroenterology, 156(1), 108-118.e4. https://doi.org/10.1053/j.gastro.2018.09.022
- Beutel, A., & Halbrook, C. J. (2023). Barriers and opportunities for gemcitabine in pancreatic cancer therapy. American Journal of Physiology. Cell Physiology, 324(2), C540–C552. https://doi.org/10.1152/ajpcell.00331.2022
- Bhandari, V., Hoey, C., Liu, L. Y., Lalonde, E., Ray, J., Livingstone, J., Lesurf, R., Shiah, Y., Vujcic, T., Huang, X., Espiritu, S. M. G., Heisler, L. E., Yousif, F., Huang, V., Yamaguchi, T. N., Yao, C. Q., Sabelnykova, V. Y., Fraser, M., Chua, M. L. K., . . . Bristow, R. G. (2019b). Molecular landmarks of tumor hypoxia across cancer types. Nature Genetics, 51(2), 308–318. https://doi.org/10.1038/s41588-018-0318-2
- Biankin, A. V., Waddell, N., Kassahn, K. S., Gingras, M., Muthuswamy, L. B., Johns, A. L., Miller, D. K., Wilson, P. J., Patch, A., Wu, J., Chang, D. K., Cowley, M. J., Gardiner, B. B., Song, S., Harliwong, I., Idrisoglu, S., Nourse, C., Nourbakhsh, E., Manning, S., . . . Grimmond, S. M. (2012). Pancreatic cancer genomes reveal aberrations in axon guidance

pathway genes. Nature, 491(7424), 399–405. https://doi.org/10.1038/nature11547

- Blackledge, N. P., & Klose, R. J. (2021). The molecular principles of gene regulation by Polycomb repressive complexes. Nature Reviews Molecular Cell Biology, 22(12), 815–833. https://doi.org/10.1038/s41580-021-00398-y
- Bolha, L., Ravnik-Glavač, M., & Glavač, D. (2017). Long noncoding RNAs as biomarkers in cancer. Disease Markers, 2017, 1–14. https://doi.org/10.1155/2017/7243968
- Bonneville, R., Krook, M. A., Kautto, E. A., Miya, J., Wing, M. R., Chen, H., Reeser, J. W., Yu, L., & Roychowdhury, S. (2017). Landscape of microsatellite instability across 39 cancer types. JCO Precision Oncology, 1, 1–15. https://doi.org/10.1200/po.17.00073
- Boudreau, R. L., Jiang, P., Gilmore, B. L., Spengler, R. M., Tirabassi, R., Nelson, J. A., Ross, C. A., Xing, Y., & Davidson, B. L. (2014). Transcriptome-wide discovery of microRNA binding sites in human brain. Neuron, 81(2), 294–305. https://doi.org/10.1016/j.neuron.2013.10.062
- Bridges, M. C., Daulagala, A. C., & Kourtidis, A. (2021). LNCcation: lncRNA localization and function. the Journal of Cell Biology/ the Journal of Cell Biology, 220(2). https://doi.org/10.1083/jcb.202009045
- C, W., Zy, T., Hy, C., J, Z., & C, Z. (2019). High-expression of lncRNA CEBPA-AS1 promotes liver cancer progression. PubMed, 23(19), 8295–8302. https://doi.org/10.26355/eurrev_201910_19140
- Cao, L., Huang, C., Zhou, D. C., Hu, Y., Lih, T. M., Savage, S. R., Krug, K., Clark, D. J., Schnaubelt, M., Chen, L., Da Veiga Leprevost, F., Eguez, R. V., Yang, W., Pan, J., Wen, B., Dou, Y., Jiang, W., Liao, Y., Shi, Z., . . . Zhao, G. (2021). Proteogenomic characterization of pancreatic ductal adenocarcinoma. Cell, 184(19), 5031-5052.e26. https://doi.org/10.1016/j.cell.2021.08.023
- Carlevaro-Fita, J., Lanzós, A., Feuerbach, L., Hong, C., Mas-Ponte, D., Pedersen, J. S., Abascal, F., Amin, S. B., Bader, G. D., Barenboim, J., Beroukhim, R., Bertl, J., Boroevich, K. A., Brunak, S., Campbell, P. J., Carlevaro-Fita, J., Chakravarty, D., Chan, C. W. Y., Chen, K., . . . Von Mering, C. (2022). Author Correction: Cancer LncRNA Census reveals evidence for deep functional conservation of long noncoding RNAs in

tumorigenesis. Communications Biology, 5(1). https://doi.org/10.1038/s42003-022-03769-z

- Castells, A., Puig, P., Móra, J., Boadas, J., Boix, L., Urgell, E., Solé, M., Capellà, G., Lluís, F., Fernández-Cruz, L., Navarro, S., & Farré, A. (1999). K-RAS mutations in DNA extracted from the plasma of patients with pancreatic carcinoma: diagnostic utility and prognostic significance. Journal of Clinical Oncology, 17(2), 578. https://doi.org/10.1200/jco.1999.17.2.578
- *CBioPortal for Cancer Genomics*. (n.d.). https://www.cbioportal.org/
- Cerami, E., Gao, J., Dogrusoz, U., Gross, B. E., Sumer, S. O., Aksoy, B. A., Jacobsen, A., Byrne, C. J., Heuer, M. L., Larsson, E., Antipin, Y., Reva, B., Goldberg, A. P., Sander, C., & Schultz, N. (2012). The CBIO Cancer Genomics Portal: an open platform for exploring multidimensional cancer genomics data. Cancer Discovery, 2(5), 401–404. https://doi.org/10.1158/2159-8290.cd-12-0095
- Chandrashekar, D. S., Bashel, B., Balasubramanya, S. a. H., Creighton, C. J., Ponce-Rodriguez, I., Chakravarthi, B. V., & Varambally, S. (2017). UALCAN: a portal for facilitating tumor subgroup gene expression and survival analyses. Neoplasia, 19(8), 649–658. https://doi.org/10.1016/j.neo.2017.05.002
- Chandrashekar, D. S., Karthikeyan, S. K., Korla, P. K., Patel, H., Shovon, A. R., Athar, M., Netto, G. J., Qin, Z. S., Kumar, S., Manne, U., Crieghton, C. J., & Varambally, S. (2022). UALCAN: An update to the integrated cancer data analysis platform. Neoplasia, 25, 18–27. https://doi.org/10.1016/j.neo.2022.01.001
- Chang, L., Zhou, G., Soufan, O., & Xia, J. (2020). miRNet 2.0: network-based visual analytics for miRNA functional analysis and systems biology. Nucleic Acids Research, 48(W1), W244–W251. https://doi.org/10.1093/nar/gkaa467
- Chang, L., Zhou, G., Soufan, O., & Xia, J. (2020b). miRNet 2.0: network-based visual analytics for miRNA functional analysis and systems biology. Nucleic Acids Research, 48(W1), W244–W251. https://doi.org/10.1093/nar/gkaa467
- Chin, C., Chen, S., Wu, H., Ho, C., Ko, M., & Lin, C. (2014). cytoHubba: identifying hub objects and sub-networks from complex interactome. BMC Systems Biology, 8(S4). https://doi.org/10.1186/1752-0509-8-s4-s11

- Chirravuri-Venkata, R., Dam, V., Nimmakayala, R. K., Alsafwani, Z. W., Bhyravbhatla, N., Lakshmanan, I., Ponnusamy, M. P., Kumar, S., Jain, M., Ghersi, D., & Batra, S. K. (2023). MUC16 and TP53 family co-regulate tumor-stromal heterogeneity in pancreatic adenocarcinoma. Frontiers in Oncology, 13. https://doi.org/10.3389/fonc.2023.1073820
- Collazos, J. C. O. (n.d.-b). Venny 2.1.0. https://bioinfogp.cnb.csic.es/tools/venny/index.html
- De Bruijn, I., Kundra, R., Mastrogiacomo, B., Tran, T. N., Sikina, L., Mazor, T., Li, X., Ochoa, A., Zhao, G., Lai, B., Abeshouse, A., Baiceanu, D., Ciftci, E., Dogrusoz, U., Dufilie, A., Erkoc, Z., Lara, E. G., Fu, Z., Gross, B., . . . Schultz, N. (2023). Analysis and Visualization of Longitudinal Genomic and Clinical Data from the AACR Project GENIE Biopharma Collaborative in cBioPortal. Cancer Research, 83(23), 3861–3867. https://doi.org/10.1158/0008-5472.can-23-0816
- Ding, L., Bailey, M. H., Porta-Pardo, E., Thorsson, V., Colaprico, A., Bertrand, D., Gibbs, D. L., Weerasinghe, A., Huang, K., Tokheim, C., Cortés-Ciriano, I., Jayasinghe, R., Chen, F., Yu, L., Sun, S., Olsen, C., Kim, J., Taylor, A. M., Cherniack, A. D., . . . Mariamidze, A. (2018b). Perspective on oncogenic processes at the end of the beginning of cancer genomics. Cell, 173(2), 305-320.e10. https://doi.org/10.1016/j.cell.2018.03.033
- Donati, S., Aurilia, C., Palmini, G., Falsetti, I., Iantomasi, T., & Brandi, M. L. (2022). Autophagy-Related NCRNAs in pancreatic cancer. Pharmaceuticals, 15(12), 1547. https://doi.org/10.3390/ph15121547
- Eissa, M. A., Lerner, L., Abdelfatah, E., Shankar, N., Canner, J. K., Hasan, N. M., Yaghoobi, V., Huang, B., Kerner, Z., Takaesu, F., Wolfgang, C., Kwak, R., Ruiz, M., Tam, M., Pisanic, T. R., Iacobuzio-Donahue, C. A., Hruban, R. H., He, J., Wang, T. H., . . . Ahuja, N. (2019c). Promoter methylation of ADAMTS1 and BNC1 as potential biomarkers for early detection of pancreatic cancer in blood. Clinical Epigenetics, 11(1). https://doi.org/10.1186/s13148-019-0650-0
- Ellrott, K., Bailey, M. H., Saksena, G., Covington, K. R., Kandoth, C., Stewart, C., Hess, J., Ma, S., Chiotti, K. E., McLellan, M., Sofia, H. J., Hutter, C., Getz, G., Wheeler, D., Ding, L., Caesar-Johnson, S. J., Demchok, J. A., Felau, I., Kasapi, M., . . . Mariamidze, A. (2018). Scalable open science approach for mutation calling of tumor exomes using

multiple genomic pipelines. Cell Systems, 6(3), 271-281.e7. https://doi.org/10.1016/j.cels.2018.03.002

- Fabbri, M., Girnita, L., Varani, G., & Calin, G. A. (2019). Decrypting noncoding RNA interactions, structures, and functional networks. Genome Research, 29(9), 1377–1388. https://doi.org/10.1101/gr.247239.118
- Feng, Y., Gao, L., Cui, G., & Cao, Y. (2020). LncRNA NEAT1 facilitates pancreatic cancer growth and metastasis through stabilizing ELF3 mRNA. American journal of cancer research, 10(1), 237–248. PMID: 32064164
- Fuchs, S. B., Lieder, I., Stelzer, G., Mazor, Y., Buzhor, E., Kaplan, S., Bogoch, Y., Plaschkes, I., Shitrit, A., Rappaport, N., Kohn, A., Edgar, R., Shenhav, L., Safran, M., Lancet, D., Guan-Golan, Y., Warshawsky, D., & Shtrichman, R. (2016). GeneAnalytics: an integrative gene set analysis tool for next generation sequencing, RNASEq and microarray data. Omics, 20(3), 139–151. https://doi.org/10.1089/omi.2015.0168
- Gao, H., Yin, Y., Qian, A., Guo, R., & Qi, J. (2019). LNCRNA LINC00974 upregulates CDK6 to promote cell cycle progression in gastric carcinoma. Cancer Biotherapy and Radiopharmaceuticals, 34(10), 666–670. https://doi.org/10.1089/cbr.2019.2904
- Gao, J., Aksoy, B. A., Dogrusoz, U., Dresdner, G., Gross, B., Sumer, S. O., Sun, Y., Jacobsen, A., Sinha, R., Larsson, E., Cerami, E., Sander, C., & Schultz, N. (2013). Integrative analysis of complex cancer genomics and clinical profiles using the CBioPortal. Science Signaling, 6(269). https://doi.org/10.1126/scisignal.2004088
- Gao, Q., Liang, W., Foltz, S. M., Mutharasu, G., Jayasinghe, R. G., Cao, S., Liao, W., Reynolds, S. M., Wyczalkowski, M. A., Yao, L., Yu, L., Sun, S. Q., Chen, K., Lazar, A. J., Fields, R. C., Wendl, M. C., Van Tine, B. A., Vij, R., Chen, F., . . . Mariamidze, A. (2018b). Driver fusions and their implications in the development and treatment of human cancers. Cell Reports, 23(1), 227-238.e3. https://doi.org/10.1016/j.celrep.2018.03.050
- Gao, Y., Li, X., Zhi, H., Zhang, Y., Wang, P., Wang, Y., Shang, S., Fang, Y., Shen, W., Ning, S., Chen, S. X., & Li, X. (2019). Comprehensive characterization of somatic mutations impacting LNCRNA expression for Pan-Cancer. Molecular Therapy. Nucleic Acids, 18, 66–79. https://doi.org/10.1016/j.omtn.2019.08.004

- Gola, H., Engler, H., Sommershof, A., Adenauer, H., Kolassa, S., Schedlowski, M., Groettrup, M., Elbert, T., & Kolassa, I. (2013). Posttraumatic stress disorder is associated with an enhanced spontaneous production of pro-inflammatory cytokines by peripheral blood mononuclear cells. BMC Psychiatry, 13(1). https://doi.org/10.1186/1471-244x-13-40
- Győrffy, B. (2024). Integrated analysis of public datasets for the discovery and validation of survival-associated genes in solid tumors. the Innovation, 5(3), 100625. https://doi.org/10.1016/j.xinn.2024.100625
- Hamilton, M. P., Rajapakshe, K. I., Bader, D. A., Cerne, J. Z., Smith, E. A., Coarfa, C., Hartig, S. M., & McGuire, S. E. (2016). The landscape of microRNA targeting in prostate cancer defined by AGO-PAR-CLIP. Neoplasia, 18(6), 356–370. https://doi.org/10.1016/j.neo.2016.04.008
- Henriksen, S. D., Madsen, P. H., Larsen, A. C., Johansen, M. B., Drewes, A. M., Pedersen, I. S., Krarup, H., & Thorlacius-Ussing, O. (2016). Cell-free DNA promoter hypermethylation in plasma as a diagnostic marker for pancreatic adenocarcinoma. Clinical Epigenetics, 8(1). https://doi.org/10.1186/s13148-016-0286-2
- Heredia-Soto, V., Rodríguez-Salas, N., & Feliu, J. (2021). Liquid biopsy in pancreatic cancer: Are we ready to apply it in the clinical practice? Cancers, 13(8), 1986. https://doi.org/10.3390/cancers13081986
- Hoadley, K. A., Yau, C., Hinoue, T., Wolf, D. M., Lazar, A. J., Drill, E., Shen, R., Taylor, A. M., Cherniack, A. D., Thorsson, V., Akbani, R., Bowlby, R., Wong, C. K., Wiznerowicz, M., Sanchez-Vega, F., Robertson, A. G., Schneider, B. G., Lawrence, M. S., Noushmehr, H., . . . Mariamidze, A. (2018b). Cell-of-Origin Patterns Dominate the Molecular Classification of 10,000 Tumors from 33 Types of Cancer. Cell, 173(2), 291-304.e6. https://doi.org/10.1016/j.cell.2018.03.022
- http://geneanalytics.genecards.org/, GeneAnalytics analysis tool offered by Gene
- https://www.genecards.org/
- https://www.genecards.org/genecarna
- Hu, X., Wu, J., & Xu, J. (2023). UCA1 executes an oncogenic role in pancreatic cancer by regulating miR-582-5p/BRCC3. Frontiers in Oncology, 13. https://doi.org/10.3389/fonc.2023.1133200

- Huang, B., Liu, C., Wu, Q., Zhang, J., Min, Q., Sheng, T., Wang, X., & Zou, Y. (2017). Long non-coding RNA NEAT1 facilitates pancreatic cancer progression through negative modulation of miR-506-3p. Biochemical and Biophysical Research Communications, 482(4), 828–834. https://doi.org/10.1016/j.bbrc.2016.11.120
- Huang, D. W., Sherman, B. T., & Lempicki, R. A. (2008). Bioinformatics enrichment tools: paths toward the comprehensive functional analysis of large gene lists. Nucleic Acids Research, 37(1), 1–13. https://doi.org/10.1093/nar/gkn923
- Huang, D. W., Sherman, B. T., & Lempicki, R. A. (2008b). Systematic and integrative analysis of large gene lists using DAVID bioinformatics resources. Nature Protocols, 4(1), 44–57. https://doi.org/10.1038/nprot.2008.211
- Huang, J., Zhou, Y., Zhang, H., & Wu, Y. (2023). A neural network model to screen feature genes for pancreatic cancer. BMC Bioinformatics, 24(1). https://doi.org/10.1186/s12859-023-05322-z
- Huang, L., Yuan, X., Zhao, L., Han, Q., Yan, H., Yuan, J., Guan, S., Xu, X., Dai, G., Wang, J., & Shi, Y. (2023). Gene signature developed for predicting early relapse and survival in early-stage pancreatic cancer. BJS Open, 7(3). https://doi.org/10.1093/bjsopen/zrad031
- Huarte, M. (2015). The emerging role of lncRNAs in cancer. Nature Medicine, 21(11), 1253–1261. https://doi.org/10.1038/nm.3981
- Hussain, M. S., Gupta, G., Afzal, M., Alqahtani, S. M., Samuel, V. P., Almalki, W. H., Kazmi, I., Alzarea, S. I., Saleem, S., Dureja, H., Singh, S. K., Dua, K., & Thangavelu, L. (2023). Exploring the role of lncrna neat1 knockdown in regulating apoptosis across multiple cancer types: A review. Pathology, Research and Practice, 252, 154908. https://doi.org/10.1016/j.prp.2023.154908
- Huynh, N. P. T., Anderson, B. A., Guilak, F., & McAlinden, A. (2016). Emerging roles for long noncoding RNAs in skeletal biology and disease. Connective Tissue Research, 58(1), 116–141. https://doi.org/10.1080/03008207.2016.1194406
- Iyer, M. K., Niknafs, Y. S., Malik, R., Singhal, U., Sahu, A., Hosono, Y., Barrette, T. R., Prensner, J. R., Evans, J. R., Zhao, S., Poliakov, A., Cao, X., Dhanasekaran, S. M., Wu, Y., Robinson, D. R., Beer, D. G., Feng, F. Y., Iyer, H. K., & Chinnaiyan, A. M. (2015). The landscape of long noncoding

RNAs in the human transcriptome. Nature Genetics, 47(3), 199–208. https://doi.org/10.1038/ng.3192

- Kamisawa, T., Wood, L. D., Itoi, T., & Takaori, K. (2016). Pancreatic cancer. Lancet, 388(10039), 73–85. https://doi.org/10.1016/s0140-6736(16)00141-0
- Karagkouni, D., Paraskevopoulou, M. D., Tastsoglou, S., Skoufos, G., Karavangeli, A., Pierros, V., Zacharopoulou, E., & Hatzigeorgiou, A. G. (2019). DIANA-LncBase v3: indexing experimentally supported miRNA targets on non-coding transcripts. Nucleic Acids Research. https://doi.org/10.1093/nar/gkz1036
- Karginov, F. V., & Hannon, G. J. (2013f). Remodeling of Ago2–mRNA interactions upon cellular stress reflects miRNA complementarity and correlates with altered translation rates. Genes & Development, 27(14), 1624–1632. https://doi.org/10.1101/gad.215939.113
- Kirchweger, P., Kupferthaler, A., Burghofer, J., Webersinke, G., Jukic, E., Schwendinger, S., Wundsam, H., Biebl, M., Petzer, A., & Rumpold, H. (2022). Prediction of response to systemic treatment by kinetics of circulating tumor DNA in metastatic pancreatic cancer. Frontiers in Oncology, 12. https://doi.org/10.3389/fonc.2022.902177
- Kishore, C., & Karunagaran, D. (2022). Non-coding RNAs as emerging regulators and biomarkers in colorectal cancer. Molecular and Cellular Biochemistry, 477(6), 1817–1828. https://doi.org/10.1007/s11010-022-04412-5
- Kumar, L.; Kumar, S.; Sandeep, K.; Patel, S.K.S. Therapeutic Approaches in Pancreatic Cancer: Recent Updates. Biomedicines 2023, 11, 1611. https://doi.org/10.3390/biomedicines11061611
- Kumar, P., Khadirnaikar, S., & Shukla, S. K. (2019). PILAR1, a novel prognostic LncRNA, reveals the presence of a unique subtype of lung adenocarcinoma patients with KEAP1 mutations. Gene, 691, 167–175. https://doi.org/10.1016/j.gene.2018.12.060
- Lee, B., Lipton, L., Cohen, J., Tie, J., Javed, A., Li, L., Goldstein, D., Burge, M., Cooray, P., Nagrial, A., Tebbutt, N., Thomson, B., Nikfarjam, M., Harris, M., Haydon, A., Lawrence, B., Tai, D., Simons, K., Lennon, A., . . . Gibbs, P. (2019). Circulating tumor DNA as a potential marker of adjuvant chemotherapy benefit following surgery for localized pancreatic cancer. Annals of Oncology, 30(9), 1472–1478. https://doi.org/10.1093/annonc/mdz200

- Lee, Y. J., Oh, H., Kim, E., Ahn, B., Lee, J. H., Lee, Y., Chae, Y. S., Kang, S. G., & Kim, C. H. (2019). Long noncoding RNA HOTTIP overexpression: A potential prognostic biomarker in prostate cancer. Pathology - Research and Practice, 215(11), 152649. https://doi.org/10.1016/j.prp.2019.152649
- Li, B., Severson, E., Pignon, J., Zhao, H., Li, T., Novak, J., Jiang, P., Shen, H., Aster, J. C., Rodig, S., Signoretti, S., Liu, J. S., & Liu, X. S. (2016). Comprehensive analyses of tumor immunity: implications for cancer immunotherapy. Genome Biology, 17(1). https://doi.org/10.1186/s13059-016-1028-7
- Li, J., Han, L., Roebuck, P., Diao, L., Liu, L., Yuan, Y., Weinstein, J. N., & Liang, H. (2015). TANRIC: an interactive open platform to explore the function of LNCRNAs in cancer. Cancer Research, 75(18), 3728–3737. https://doi.org/10.1158/0008-5472.can-15-0273
- Li, J., Xu, Q., Wang, W., & Sun, S. (2019). MIR100HG: a credible prognostic biomarker and an oncogenic lncRNA in gastric cancer. Bioscience Reports, 39(4). https://doi.org/10.1042/bsr20190171
- Li, T., Fan, J., Wang, B., Traugh, N., Chen, Q., Liu, J. S., Li, B., & Liu, X. S. (2017). TIMER: a web server for comprehensive analysis of Tumor-Infiltrating immune cells. Cancer Research, 77(21), e108–e110. https://doi.org/10.1158/0008-5472.can-17-0307
- Li, T., Fu, J., Zeng, Z., Cohen, D., Li, J., Chen, Q., Li, B., & Liu, X. S. (2020). TIMER2.0 for analysis of tumor-infiltrating immune cells. Nucleic Acids Research, 48(W1), W509–W514. https://doi.org/10.1093/nar/gkaa407
- Liang, S., Gong, X., Zhang, G., Huang, G., Lu, Y., & Li, Y. (2017). The lncRNA XIST interacts with miR-140/miR-124/iASPP axis to promote pancreatic carcinoma growth. Oncotarget, 8(69), 113701–113718. https://doi.org/10.18632/oncotarget.22555
- Liao, Y., Wang, Y., Cheng, M., Huang, C., & Fan, X. (2020). Weighted gene coexpression network analysis of features that control cancer stem cells reveals prognostic biomarkers in lung adenocarcinoma. Frontiers in Genetics, 11. https://doi.org/10.3389/fgene.2020.00311
- Ling, H., Girnita, L., Buda, O., & Calin, G. A. (2017). Non-coding RNAs: the cancer genome dark matter that matters! Clinical Chemistry and Laboratory Medicine, 55(5). https://doi.org/10.1515/cclm-2016-0740

- Lipchina, I., Elkabetz, Y., Hafner, M., Sheridan, R., Mihailovic, A., Tuschl, T., Sander, C., Studer, L., & Betel, D. (2011). Genome-wide identification of microRNA targets in human ES cells reveals a role for miR-302 in modulating BMP response. Genes & Development, 25(20), 2173–2186. https://doi.org/10.1101/gad.17221311
- Liu, C., Wang, J., Zhou, W., Chang, X., Zhang, M., Zhang, Y., & Yang, X. (2019). Long non-coding RNA LINC01207 silencing suppresses AGR2 expression to facilitate autophagy and apoptosis of pancreatic cancer cells by sponging miR-143-5p. Molecular and Cellular Endocrinology, 493, 110424. https://doi.org/10.1016/j.mce.2019.04.004
- Liu, J., Lichtenberg, T., Hoadley, K. A., Poisson, L. M., Lazar, A. J., Cherniack, A. D., Kovatich, A. J., Benz, C. C., Levine, D. A., Lee, A. V., Omberg, L., Wolf, D. M., Shriver, C. D., Thorsson, V., Hu, H., Caesar-Johnson, S. J., Demchok, J. A., Felau, I., Kasapi, M., . . . Mariamidze, A. (2018b). An integrated TCGA Pan-Cancer Clinical Data resource to drive High-Quality Survival Outcome Analytics. Cell, 173(2), 400-416.e11. https://doi.org/10.1016/j.cell.2018.02.052
- Liu, Y., Luo, D., Li, X., Li, Z., Yu, X., & Zhu, H. (2021). PVT1 knockdown inhibits autophagy and improves gemcitabine sensitivity by regulating the MIR-143/HIF-1A/VMP1 axis in pancreatic cancer. Pancreas, 50(2), 227–234. https://doi.org/10.1097/mpa.0000000000001747
- Mahmoudi, R., Saidijam, M., Nikzad, S., Tapak, L., Alvandi, M., & Afshar, S. (2021). Human exposure to low dose ionizing radiation affects miR-21 and miR-625 expression levels. Molecular Biology Reports, 49(2), 1321–1327. https://doi.org/10.1007/s11033-021-06960-3
- Mas-Ponte, D., Carlevaro-Fita, J., Palumbo, E., Pulido, T. H., Guigo, R., & Johnson, R. (2017c). LncATLAS database for subcellular localization of long noncoding RNAs. RNA, 23(7), 1080–1087. https://doi.org/10.1261/rna.060814.117
- Memczak, S., Jens, M., Elefsinioti, A., Torti, F., Krueger, J., Rybak, A., Maier, L., Mackowiak, S. D., Gregersen, L. H., Munschauer, M., Loewer, A., Ziebold, U., Landthaler, M., Kocks, C., Noble, F. L., & Rajewsky, N. (2013). Circular RNAs are a large class of animal RNAs with regulatory potency. Nature, 495(7441), 333–338. https://doi.org/10.1038/nature11928
- Mortezapour, M., Tapak, L., Bahreini, F., Najafi, R., & Afshar, S. (2023). Identification of key genes in colorectal cancer diagnosis by weighted

gene co-expression network analysis. Computers in Biology and Medicine, 157, 106779. https://doi.org/10.1016/j.compbiomed.2023.106779

- Nitschke, C., Markmann, B., Walter, P., Badbaran, A., Tölle, M., Kropidlowski, J., Belloum, Y., Goetz, M. R., Bardenhagen, J., Stern, L., Tintelnot, J., Schönlein, M., Sinn, M., Van Der Leest, P., Simon, R., Heumann, A., Izbicki, J. R., Pantel, K., Wikman, H., & Uzunoglu, F. G. (2023). Peripheral and Portal VenousKRASCTDNA detection as independent prognostic markers of early tumor recurrence in pancreatic ductal adenocarcinoma. Clinical Chemistry, 69(3), 295–307. https://doi.org/10.1093/clinchem/hvac214
- Paraskevopoulou, M. D., Karagkouni, D., Vlachos, I. S., Tastsoglou, S., & Hatzigeorgiou, A. G. (2018). microCLIP super learning framework uncovers functional transcriptome-wide miRNA interactions. Nature Communications, 9(1). https://doi.org/10.1038/s41467-018-06046-y
- Peng, Y., Wu, H., Fang, Q., Liu, J., & Gong, Z. (2016). Residual velocities of projectiles after normally perforating the thin ultra-high performance steel fiber reinforced concrete slabs. International Journal of Impact Engineering, 97, 1–9. https://doi.org/10.1016/j.ijimpeng.2016.06.006
- Piñero, J., Ramírez-Anguita, J. M., Saüch-Pitarch, J., Ronzano, F., Centeno, E., Sanz, F., & Furlong, L. I. (2019b). The DisGeNET knowledge platform for disease genomics: 2019 update. Nucleic Acids Research. https://doi.org/10.1093/nar/gkz1021
- Piunti, A., & Shilatifard, A. (2021). The roles of Polycomb repressive complexes in mammalian development and cancer. Nature Reviews Molecular Cell Biology, 22(5), 326–345. https://doi.org/10.1038/s41580-021-00341-1
- Poore, G. D., Kopylova, E., Zhu, Q., Carpenter, C., Fraraccio, S., Wandro, S., Kosciolek, T., Janssen, S., Metcalf, J., Song, S. J., Kanbar, J., Miller-Montgomery, S., Heaton, R., Mckay, R., Patel, S. P., Swafford, A. D., & Knight, R. (2020b). Microbiome analyses of blood and tissues suggest cancer diagnostic approach. Nature, 579(7800), 567–574. https://doi.org/10.1038/s41586-020-2095-1
- Rad, E., & Tee, A. R. (2016). Neurofibromatosis type 1: Fundamental insights into cell signalling and cancer. Seminars in Cell and

Developmental Biology, 52, 39–46. https://doi.org/10.1016/j.semcdb.2016.02.007

- Safran, M., Rosen, N., Twik, M., BarShir, R., Stein, T. I., Dahary, D., Fishilevich, S., & Lancet, D. (2021). The GeneCards Suite. In Practical Guide to Life Science Databases (pp. 27–56). https://doi.org/10.1007/978-981-16-5812-9_2
- Sanchez-Vega, F., Mina, M., Armenia, J., Chatila, W. K., Luna, A., La, K. C., Dimitriadoy, S., Liu, D. L., Kantheti, H. S., Saghafinia, S., Chakravarty, D., Daian, F., Gao, Q., Bailey, M. H., Liang, W., Foltz, S. M., Shmulevich, I., Ding, L., Heins, Z., . . . Mariamidze, A. (2018b). Oncogenic Signaling Pathways in the Cancer Genome Atlas. Cell, 173(2), 321-337.e10. https://doi.org/10.1016/j.cell.2018.03.035
- Shahab, S. W., Matyunina, L. V., Mezencev, R., Walker, L. D., Bowen, N. J., Benigno, B. B., & McDonald, J. F. (2011). Evidence for the Complexity of MicroRNA-Mediated Regulation in Ovarian Cancer: A Systems Approach. PLoS ONE, 6(7), e22508. https://doi.org/10.1371/journal.pone.0022508
- Sherman, B. T., Hao, M., Qiu, J., Jiao, X., Baseler, M. W., Lane, H. C., Imamichi, T., & Chang, W. (2022). DAVID: a web server for functional enrichment analysis and functional annotation of gene lists (2021 update). Nucleic Acids Research, 50(W1), W216–W221. https://doi.org/10.1093/nar/gkac194
- Silva, A., Bullock, M., & Calin, G. (2015). The clinical relevance of Long Non-Coding RNAs in cancer. Cancers, 7(4), 2169–2182. https://doi.org/10.3390/cancers7040884
- Sjöstedt, E., Zhong, W., Fagerberg, L., Karlsson, M., Mitsios, N., Adori, C., Oksvold, P., Edfors, F., Limiszewska, A., Hikmet, F., Huang, J., Du, Y., Lin, L., Dong, Z., Yang, L., Liu, X., Jiang, H., Xu, X., Wang, J., . . . Mulder, J. (2020). An atlas of the protein-coding genes in the human, pig, and mouse brain. Science, 367(6482). https://doi.org/10.1126/science.aay5947
- Smith, B. J., Silva-Costa, L. C., & Martins-De-Souza, D. (2021). Human disease biomarker panels through systems biology. Biophysical Reviews, 13(6), 1179–1190. https://doi.org/10.1007/s12551-021-00849-y
- Smolkova, B., Kataki, A., Earl, J., Ruz-Caracuel, I., Cihova, M., Urbanova, M., Buocikova, V., Tamargo, S., Rovite, V., Niedra, H., Schrader, J., &

Kohl, Y. (2022). Liquid biopsy and preclinical tools for advancing diagnosis and treatment of patients with pancreatic neuroendocrine neoplasms. Critical Reviews in Oncology/Hematology, 180, 103865. https://doi.org/10.1016/j.critrevonc.2022.103865

- Stelzer, G., Rosen, N., Plaschkes, I., Zimmerman, S., Twik, M., Fishilevich, S., Stein, T. I., Nudel, R., Lieder, I., Mazor, Y., Kaplan, S., Dahary, D., Warshawsky, D., Guan-Golan, Y., Kohn, A., Rappaport, N., Safran, M., & Lancet, D. (2016). The GeneCards suite: from gene data mining to disease genome sequence analyses. Current Protocols in Bioinformatics, 54(1). https://doi.org/10.1002/cpbi.5
- Sugimori, M., Sugimori, K., Tsuchiya, H., Suzuki, Y., Tsuyuki, S., Kaneta, Y., Hirotani, A., Sanga, K., Tozuka, Y., Komiyama, S., Sato, T., Tezuka, S., Goda, Y., Irie, K., Miwa, H., Miura, Y., Ishii, T., Kaneko, T., Nagahama, M., . . . Maeda, S. (2019). Quantitative monitoring of circulating tumor DNA in patients with advanced pancreatic cancer undergoing chemotherapy. Cancer Science, 111(1), 266–278. https://doi.org/10.1111/cas.14245
- Szklarczyk, D., Kirsch, R., Koutrouli, M., Nastou, K., Mehryary, F., Hachilif, R., Gable, A. L., Fang, T., Doncheva, N. T., Pyysalo, S., Bork, P., Jensen, L. J., & Von Mering, C. (2022). The STRING database in 2023: protein–protein association networks and functional enrichment analyses for any sequenced genome of interest. Nucleic Acids Research, 51(D1), D638–D646. https://doi.org/10.1093/nar/gkac1000
- Takahashi, K., Taniue, K., Ono, Y., Fujiya, M., Mizukami, Y., & Okumura, T. (2021). Long Non-Coding RNAs in Epithelial-Mesenchymal transition of pancreatic Cancer. Frontiers in Molecular Biosciences, 8. https://doi.org/10.3389/fmolb.2021.717890
- Tamang, S., Acharya, V., Roy, D., Sharma, R., Aryaa, A., Sharma, U., Khandelwal, A., Prakash, H., Vasquez, K. M., & Jain, A. (2019). SNHG12: an LNCRNA as a potential therapeutic target and biomarker for human cancer. Frontiers in Oncology, 9. https://doi.org/10.3389/fonc.2019.00901
- Tang, Z., Kang, B., Li, C., Chen, T., & Zhang, Z. (2019). GEPIA2: an enhanced web server for large-scale expression profiling and interactive analysis. Nucleic Acids Research, 47(W1), W556–W560. https://doi.org/10.1093/nar/gkz430

- Taylor, A. M., Shih, J., Ha, G., Gao, G. F., Zhang, X., Berger, A. C., Schumacher, S. E., Wang, C., Hu, H., Liu, J., Lazar, A. J., Cherniack, A. D., Beroukhim, R., Meyerson, M., Caesar-Johnson, S. J., Demchok, J. A., Felau, I., Kasapi, M., Ferguson, M. L., . . . Mariamidze, A. (2018b). Genomic and functional approaches to understanding cancer aneuploidy. Cancer Cell, 33(4), 676-689.e3. https://doi.org/10.1016/j.ccell.2018.03.007
- Thomas, P., Seim, I., Jeffery, P., Gahete, M., Maugham, M., Crisp, G., Stacey, A., Shah, E., Walpole, C., Whiteside, E., Nelson, C., Herington, A., Luque, R., Veedu, R., & Chopin, L. (2019). The long non-coding RNA GHSROS facilitates breast cancer cell migration and orthotopic xenograft tumour growth. International Journal of Oncology. https://doi.org/10.3892/ijo.2019.4891
- TIMER2.0. (n.d.). http://timer.cistrome.org/
- Toledano-Fonseca, M., Cano, M. T., Inga, E., Rodríguez-Alonso, R., Gómez-España, M. A., Guil-Luna, S., Mena-Osuna, R., De La Haba-Rodríguez, J. R., Rodríguez-Ariza, A., & Aranda, E. (2020). Circulating Cell-Free DNA-Based liquid biopsy markers for the Non-Invasive prognosis and Monitoring of metastatic pancreatic Cancer. Cancers, 12(7), 1754. https://doi.org/10.3390/cancers12071754
- Uhlén, M., Fagerberg, L., Hallström, B. M., Lindskog, C., Oksvold, P., Mardinoglu, A., Sivertsson, Å., Kampf, C., Sjöstedt, E., Asplund, A., Olsson, I., Edlund, K., Lundberg, E., Navani, S., Szigyarto, C. A., Odeberg, J., Djureinovic, D., Takanen, J. O., Hober, S., . . . Pontén, F. (2015). Tissue-based map of the human proteome. Science, 347(6220). https://doi.org/10.1126/science.1260419
- V23.proteinatlas.org
- Van Heesch, S., Van Iterson, M., Jacobi, J., Boymans, S., Essers, P. B., De Bruijn, E., Hao, W., MacInnes, A. W., Cuppen, E., & Simonis, M. (2014). Extensive localization of long noncoding RNAs to the cytosol and mono- and polyribosomal complexes. GenomeBiology.com, 15(1), R6. https://doi.org/10.1186/gb-2014-15-1-r6
- Venny 2.1.0, https://bioinfogp.cnb.csic.es/tools/venny/
- Volders, P., Anckaert, J., Verheggen, K., Nuytens, J., Martens, L., Mestdagh, P., & Vandesompele, J. (2018). LNCipedia 5: towards a reference set of human long non-coding RNAs. Nucleic Acids Research, 47(D1), D135–D139. https://doi.org/10.1093/nar/gky1031

- Wan, R., Liu, Z., Huang, X., Kwan, P., Li, Y., Qu, X., Ye, X., Chen, F., Zhang, D., He, M., Wang, J., Mao, Y., & Qiao, J. (2022). YWHAZ variation causes intellectual disability and global developmental delay with brain malformation. Human Molecular Genetics, 32(3), 462–472. https://doi.org/10.1093/hmg/ddac210
- Wang, K., Wang, X., Pan, Q., & Zhao, B. (2023). Liquid biopsy techniques and pancreatic cancer: diagnosis, monitoring, and evaluation. Molecular Cancer, 22(1). https://doi.org/10.1186/s12943-023-01870-3
- Wang, R., Zhao, Y., Wang, Y., Zhao, Z., Chen, Q., Duan, Y., Xiong, S., Luan, Z., Wang, J., & Cheng, B. (2022). Diagnostic and prognostic values of KRAS mutations on EUS-FNA specimens and circulating tumor DNA in patients with pancreatic cancer. Clinical and Translational Gastroenterology, 13(5), e00487. https://doi.org/10.14309/ctg.0000000000000487
- Wanowska, E., Kubiak, M., Makałowska, I., & Szcześniak, M. W. (2021). A chromatin-associated splicing isoform of OIP5-AS1 acts in cis to regulate the OIP5 oncogene. RNA Biology, 18(11), 1834–1845. https://doi.org/10.1080/15476286.2021.1871816
- Watanabe, F., Suzuki, K., Tamaki, S., Abe, I., Endo, Y., Takayama, Y., Ishikawa, H., Kakizawa, N., Saito, M., Futsuhara, K., Noda, H., Konishi, F., & Rikiyama, T. (2019). Longitudinal monitoring of KRAS-mutated circulating tumor DNA enables the prediction of prognosis and therapeutic responses in patients with pancreatic cancer. PloS One, 14(12), e0227366. https://doi.org/10.1371/journal.pone.0227366
- Watanabe, K., Nakamura, T., Kimura, Y., Motoya, M., Kojima, S., Kuraya, T., Murakami, T., Kaneko, T., Shinohara, Y., Kitayama, Y., Fukuda, K., Hatanaka, K. C., Mitsuhashi, T., Pittella-Silva, F., Yamaguchi, T., Hirano, S., Nakamura, Y., & Low, S. (2022). Tumor-Informed Approach improved CTDNA detection rate in resected pancreatic cancer. International Journal of Molecular Sciences, 23(19), 11521. https://doi.org/10.3390/ijms231911521
- Witkiewicz, A. K., McMillan, E. A., Balaji, U., Baek, G., Lin, W., Mansour, J., Mollaee, M., Wagner, K., Koduru, P., Yopp, A., Choti, M. A., Yeo, C. J., McCue, P., White, M. A., & Knudsen, E. S. (2015). Whole-exome sequencing of pancreatic cancer defines genetic diversity and

therapeutic targets. Nature Communications, 6(1). https://doi.org/10.1038/ncomms7744

- Wu, P., Mo, Y., Peng, M., Tang, T., Zhong, Y., Deng, X., Xiong, F., Guo, C., Wu, X., Li, Y., Li, X., Li, G., Zeng, Z., & Xiong, W. (2020). Emerging role of tumor-related functional peptides encoded by lncRNA and circRNA. Molecular Cancer, 19(1). https://doi.org/10.1186/s12943-020-1147-3
- Xi, X., Li, T., Huang, Y., Sun, J., Zhu, Y., Yang, Y., & Lu, Z. J. (2017). RNA biomarkers: Frontier of precision medicine for cancer. Non-coding RNA, 3(1), 9. https://doi.org/10.3390/ncrna3010009
- Xing, S., Wang, Y., Hu, K., Wang, F., Sun, T., & Li, Q. (2020). WGCNA reveals key gene modules regulated by the combined treatment of colon cancer with PHY906 and CPT11. Bioscience Reports, 40(9). https://doi.org/10.1042/bsr20200935
- Yang, H., Liu, P., Zhang, J., Peng, X., Lu, Z., Yu, S., Meng, Y., Tong, W., & Chen, J. (2015). Long noncoding RNA MIR31HG exhibits oncogenic property in pancreatic ductal adenocarcinoma and is negatively regulated by miR-193b. Oncogene, 35(28), 3647–3657. https://doi.org/10.1038/onc.2015.430
- Yin, Q., Shen, X., Cui, X., & Ju, S. (2019). Elevated serum lncRNA TUG1 levels are a potential diagnostic biomarker of multiple myeloma. Experimental Hematology, 79, 47-55.e2. https://doi.org/10.1016/j.exphem.2019.10.002
- Yu, D. J., Zhong, M., & Wang, W. L. (2021). Long noncoding RNA CASC15 is upregulated in non-small cell lung cancer and facilitates cell proliferation and metastasis via targeting miR-130b-3p. European review for medical and pharmacological sciences, 25(4), 1765. https://doi.org/10.26355/eurrev_202102_25053
- Yu, S., Li, Y., Liao, Z., Wang, Z., Wang, Z., Li, Y., Qian, L., Zhao, J., Zong, H., Kang, B., Zou, W., Chen, K., He, X., Meng, Z., Chen, Z., Huang, S., & Wang, P. (2019). Plasma extracellular vesicle long RNA profiling identifies a diagnostic signature for the detection of pancreatic ductal adenocarcinoma. Gut, 69(3), 540–550. https://doi.org/10.1136/gutjnl-2019-318860
- Zandieh, M. A., Farahani, M. H., Rajabi, R., Avval, S. T., Karimi, K., Rahmanian, P., Razzazan, M., Javanshir, S., Mirzaei, S., Paskeh, M. D. A., Salimimoghadam, S., Hushmandi, K., Taheriazam, A., Pandey, V., & Hashemi, M. (2023). Epigenetic regulation of autophagy by non-coding

RNAs in gastrointestinal tumors: Biological functions and therapeutic perspectives. Pharmacological Research, 187, 106582. https://doi.org/10.1016/j.phrs.2022.106582

- Zeng, J., Zhang, J., Sun, Y., Wang, J., Ren, C., Banerjee, S., Ouyang, L., & Wang, Y. (2022). Targeting EZH2 for cancer therapy: From current progress to novel strategies. European Journal of Medicinal Chemistry, 238, 114419. https://doi.org/10.1016/j.ejmech.2022.114419
- Zhang, M., Dang, P., Liu, Y., Qiao, B., & Sun, Z. (2022). Noncoding RNAs in pyroptosis and cancer progression: Effect, mechanism, and clinical application. Frontiers in Immunology, 13. https://doi.org/10.3389/fimmu.2022.982040
- Zhang, W., Duan, X., Zhang, Z., Yang, Z., Zhao, C., Liang, C., Liu, Z., Cheng, S., & Zhang, K. (2021). Combination of CT and telomerase-positive circulating tumor cells improves diagnosis of small pulmonary nodules. JCI Insight. https://doi.org/10.1172/jci.insight.148182
- Zhang, X., Sun, X., Shen, B., & Zhang, H. (2019). Potential Applications of DNA, RNA and Protein Biomarkers in Diagnosis, Therapy and Prognosis for Colorectal Cancer: A Study from Databases to AI-Assisted Verification. Cancers, 11(2), 172. https://doi.org/10.3390/cancers11020172
- Zhang, X., Zhang, Q., Zhang, K., Wang, F., Qiao, X., & Cui, J. (2021). Circ SMARCA5 Inhibited Tumor Metastasis by Interacting with SND1 and Downregulating the YWHAB Gene in Cervical Cancer. Cell Transplantation, 30, 096368972098378. https://doi.org/10.1177/0963689720983786
- Zhong, J., Shi, S., Peng, W., Liu, B., Yang, B., Niu, W., Zhang, B., Qin, C., Zhong, D., Cui, H., Zhang, Z., & Sun, X. (2022). Weighted Gene Co-Expression Network Analysis (WGCNA) reveals the functions of Syndecan-1 to regulate immune infiltration by influenced T cells in glioma. Frontiers in Genetics, 13. https://doi.org/10.3389/fgene.2022.792443
- Zhou, B., Guo, W., Sun, C., Zhang, B., & Zheng, F. (2018). Linc00462 promotes pancreatic cancer invasiveness through the miR-665/TGFBR1-TGFBR2/SMAD2/3 pathway. Cell Death and Disease, 9(6). https://doi.org/10.1038/s41419-018-0724-5
- Zhou, Y., Zhou, B., Pache, L., Chang, M., Khodabakhshi, A. H., Tanaseichuk, O., Benner, C., & Chanda, S. K. (2019). Metascape

provides a biologist-oriented resource for the analysis of systems-level datasets. Nature Communications, 10(1). https://doi.org/10.1038/s41467-019-09234-6